Spring 2009

Effects of HZE Irradiation on Chemical Neurotransmission in Rodent Hippocampus

Mayumi Machida
Old Dominion University

EFFECTS OF HZE IRRADIATION ON CHEMICAL NEUROTRANSMISSION IN RODENT HIPPOCAMPUS

by

Mayumi Machida
B.A. March 1979, Aoyama Gakuin University
B.S. June 2004, Old Dominion University

A Dissertation Submitted to the Faculty of
Eastern Virginia Medical School in Partial Fulfillment of the
Requirement for the Degree of

DOCTOR OF PHILOSOPHY

BIOMEDICAL SCIENCES

EASTERN VIRGINIA MEDICAL SCHOOL
May 2009

Approved by:

György Lonart (Director)

Richard A. Britten (Member)

Laura K. Hanson (Member)

Larry D. Sanford (Member)

ABSTRACT

EFFECTS OF HZE IRRADIATION ON CHEMICAL NEUROTRANSMISSION IN RODENT HIPPOCAMPUS

Mayumi Machida
Eastern Virginia Medical School, 2009
Director: Dr. György Lonart

Space radiation represents a significant risk to the CNS (central nervous system) during space missions. Most harmful are the HZE (high mass, highly charged (Z), high energy) particles, e.g. ^{56}Fe, which possess high ionizing ability, dense energy deposition pattern, and high penetrance.

Accumulating evidence suggests that radiation has significant impact on cognitive functions. In ground-base experiments, HZE radiation induces pronounced deficits in hippocampus dependent learning and memory in rodents. However, the mechanisms underlying these impairments are mostly unknown.

Exposure to HZE radiation elevates the level of oxidation, resulting in cell loss, tissue damage and functional deficits through direct ionization and generation of reactive oxygen species (ROS). When hippocampal slices were exposed to ROS, neuronal excitability was reduced. My preliminary results showed enhanced radio-vulnerability of the hippocampus and reduction in basal and depolarization-evoked [^{3}H]-norepinephrine release after HZE exposure. These results raised the possibility that HZE radiation deteriorates cognitive function through radiation-induced impairments in hippocampal chemical neurotransmission, the hypothesis of this dissertation.

In Aim 1 I have focused on the effects of HZE radiation on release of major neurotransmitter systems in the hippocampus. I have further extended my research on the

levels of receptors of these systems in Aim 2. In Aim 3, I have studied the level of oxidation in membranes of my samples.

My research reveals that HZE radiation significantly reduces hyperosmotic sucrose evoked [^{3}H]-glutamate and [^{14}C]-GABA release both three and six months post irradiation. The same radiation regimen also significantly enhances oxidative stress as indicated by increased levels of lipid peroxidation in the hippocampus, suggesting that increased levels of lipid peroxidation may play a role in reduction of neurotransmitter release. HZE radiation also significantly reduces levels of neurotransmitter receptors critical to synaptic plasticity; glutamatergic NMDA (*N*-methyl *D*-aspartate) receptors and β1 adrenergic receptors, three months post irradiation. By six months post irradiation, the levels of these receptors are returned to normal, implying that partial repair may take place.

My findings demonstrate that a single dose of HZE radiation alters the neurochemical environment in the hippocampus, which may underlie radiation-induced cognitive dysfunction.

This dissertation is dedicated to my husband, Akira Machida. Without his unconditional love, and unselfish support, I would not have been here today. Nobody could ask for a better husband than you.

I also dedicate this dissertation to my parents, Zenjiro and Nobue Tanaka. Their love and commitment from the day I was born have enabled me to achieve this goal.

Last but not least, I would love to dedicate this to my beloved children, Kei, Yui, and Leigh, who have filled my life with joy and have given me the meaning for my existence.

ACKNOWLEDGMENTS

There are many people who have contributed to the successful completion of this dissertation. From the bottom of my heart, I would like to thank the current and former members of my dissertation committee, Dr. Britten, Dr. Hanson, Dr. Sanford, and Dr. White for their patience and hours of guidance on my research and editing of this manuscript. I would also like to extend many thanks to the members of my guidance committee, Dr. Aravich, Dr. Castora, and Dr. Duffy for getting me prepared for any forthcoming challenge in dissertation research. My special thanks go to Dr. Godfrey, who, as Director of the program, always gives the best advice to keep me on track throughout my doctoral training. I would like to thank my co-worker, Mr. Brian Parris, for his warm friendship which has always cheered me up in good times and bad times.

The untiring efforts of my mentor and a chair of my dissertation committee, Dr. György Lonart, deserve special recognition. His high expectation and trust on me have forced me to achieve higher than I could. During all these years, he has constantly supported, guided, and encouraged me, both academically and emotionally, as a mentor and as a friend.

This work was funded by NASA grant support NNJ06ZSA001N. This dissertation research would not have been here without Dr. Britten's financial support.

TABLE OF CONTENTS

Page

LIST OF TABLES vii

LIST OF FIGURES viii

Chapter

I. INTRODUCTION 1
- INTRODUCTION TO THE PRESENT STUDY 1
- INTRODUCTION TO SPACE RADIATION BIOLOGY 8
- PRELIMINARY RESULTS 19

II. EFFECTS OF HZE RADIATION ON NEUROTRANSMITTER RELEASE 23
- BACKGROUND 23
- MATERIALS AND METHODS 31
- RESULTS 36
- DISCUSSION 44

III. EFFECTS OF HZE RADIATION ON SELECTED SYNAPTIC PROTEIN LEVELS 50
- BACKGROUND 50
- MATERIALS AND METHODS 57
- RESULTS 60
- DISCUSSION 69

IV. HZE RADIATION INDUCED LIPID PEROXIDATION 74
- BACKGROUND 74
- MATERIALS AND METHODS 78
- RESULTS 79
- DISCUSSION 79

V. SUMMARY 82

REFERENCES 86

VITA 101

LIST OF TABLES

Table Page

1. Neurotransmitter Receptors (A) and Synaptic Proteins (B) Evaluated in Quantitative Western Blot Analysis 6

2. Optimized General Immunoblotting Parameters 59

3. Change of Levels in Selected Synaptic Proteins 3 and 6 Months Post 0.6 Gy ^{56}Fe Irradiation 63

LIST OF FIGURES

Figure		Page
1.	Direct and Indirect Actions of Ionizing Radiation	10
2.	Computer Simulation of Tracks of Representative Particulate Radiation	12
3.	"Bystander Effect"	14
4.	Binding Energy / Nucleon for the Most Stable Isotope of Each Naturally Occurring Element	16
5.	Dose Effects of Selected HZE Particles on Conditioned Taste Aversion (CTA) Production	17
6.	Over 2 Gy HZE Radiation Effects on [^{3}H]-catecholaminergic Release from Rat Brain Slices	21
7.	Thirteen Gy X-ray Effects on [^{3}H]-catecholaminergic Release from Rat Brain Slices	22
8.	Schematic Representation of Glutamatergic Neurotransmission	24
9.	Electron Micrograph of Rat Brain Synaptosome	26
10.	Readily Releasable Pool (RRP) in Synaptic Vesicle Cycle	29
11.	Dose Effects of ^{56}Fe Radiation (1 GeV/n) on Hyperosmotic Sucrose Evoked [^{3}H]-glutamate Efflux from Hippocampal Synaptosomes	37
12.	Effects of 0.6 Gy of ^{56}Fe Radiation (1 GeV/n) on [^{3}H]-glutamate Release from Hippocampal Synaptosomes	39
13.	Effects of 0.6 Gy of ^{56}Fe Radiation (1 GeV/n) on [^{3}H]-glutamate Release from Associative Cortical Synaptosomes	40
14.	Correlation between Evoked [^{3}H]-glutamate Release and [^{14}C]-GABA Release	42
15.	Effects of 0.6 Gy of ^{56}Fe Radiation (1 GeV/n) on [^{14}C]-GABA Release from Hippocampal Synaptosomes	43
16.	Effects of 0.6 Gy of ^{56}Fe Radiation (1 GeV/n) on [^{3}H]-norepinephrine (NE) Release from Hippocampal Synaptosomes	45

17. Three and Six Months Post Irradiation Effects of 0.6 Gy of ^{56}Fe Radiation (1 GeV/n) on Basal (A) and Evoked Release (B) 46

18. Effects of 0.6 Gy of ^{56}Fe Radiation (1 GeV/n) on VGlut1 and Synaptophysin Levels 62

19. Effects of 0.6 Gy of ^{56}Fe Radiation (1 GeV/n) on Selected Glutamatergic Receptor Levels 64

20. Effects of 0.6 Gy of ^{56}Fe Radiation (1 GeV/n) on PSD-95 Levels 66

21. Effects of 0.6 Gy of ^{56}Fe Radiation (1 GeV/n) on β1 Adrenergic Receptor Levels 68

22. Effects of 0.6 Gy of ^{56}Fe Radiation (1 GeV/n) on MAP2c Levels 70

23. Point six Gy of ^{56}Fe Radiation (1 GeV/n) Induced Changes in Products of Lipid Peroxidation in the Hippocampus 80

24. Classic Paradigm of Radiation-induced Cognitive Dysfunction 83

CHAPTER I

INTRODUCTION

INTRODUCTION TO THE PRESENT STUDY

In the 20-year Strategic Program Plan (SPP) for Space Radiation Health Research (SRHR), NASA has identified four major health concerns regarding exposure to **space HZE** (high mass, highly charged (Z), high energy) **radiation**; 1) acute radiation syndromes, 2) degenerative tissue effects, 3) carcinogenesis, and 4) **damage to the Central Nervous System (CNS)** (*1*). Currently, with the possible exception of cataracts, there are no direct human data available for space radiation risk assessment (*2*). The CNS risks are classified as acute and delayed radiation effects (*1*), and the late delayed effects of radiation are the major concern in estimating risks to crew members (*3, 4*). Currently, the following delayed risks are reported; 1) deterioration in motor function (*5*), 2) behavioral impairments mediated by the dopaminergic system (*6-8*) and 3) **cognitive dysfunction** (*9, 10*), with no proven mitigation strategies (*2*). These risks may be enhanced by synergistic effects such as bone loss, cardiovascular alterations, and impaired sensory-motor adaptation (*1, 11*). NASA plans to return humans to the Moon by 2019 and to Mars by 2030. They have placed high priority on investigating CNS risks (*1*), as CNS injury may cause severe interference with job performance during an extended space mission to Mars. Phase 1 of this plan (2006 ~ 2013) emphasizes the

---

The model journal for this dissertation is *Radiation Research.*

urgent needs to; 1) develop a new risk model to reduce uncertainties regarding radiation induced CNS damage, 2) develop experimental evidence for radiation induced CNS damage, and 3) validate permissible exposure limits for space radiation in terms of CNS functions (*12*).

Studies with conventional radiation, e.g., X-rays and γ-rays, in ground based settings have established deleterious effects of ionizing radiation on the human brain. Long-term studies with childhood cancer survivors revealed that cranial radiation therapy often results in progressive cognitive dysfunction (*13-16*). Young and adult patients of acute lymphoblastic leukemia and brain tumors who had received cranial radiation therapy display a delayed and progressive decline in cognitive performance including impairments in attention, visual perceptual skills, executive function, and memory (*13*). Ris and co-workers reported that brain tumor survivors had a 17.4 point decrease in full scale intelligence quotient (IQ) four years after radiation therapy even when moderate doses of radiation were applied (*14*). The neuronal mechanisms that underlie these effects remain mostly unknown. Possible causes include demyelination suggested by quantitative magnetic resonance imaging (MRI) studies that detected white matter necrosis (*15*). Since the damage correlated with decreased attention, lower IQ and academic achievement (*16*), this histopathological change has been hypothesized as a mechanistic base for radiation induced cognitive dysfunction (*13*). Rodents given a 25 Gy dose of X-ray radiation have been used extensively to investigate the histopathology of the radiation-induced damage, as this dose induces vascular lesions as well as radionecrosis that is associated with demyelination one year after irradiation (*17*).

Research on hippocampal neurogenesis has revealed that radiation may induce cognitive impairments even at doses that are well below the threshold for producing histopathological changes. Whole brain irradiation of mice subjected to a single mild dose (10 Gy) of X-rays showed reduced performance in a Barnes maze, a hippocampal-dependent spatial learning test (*18*). Since the same dose of radiation nearly abolishes the production of new neurons in rodents one or two months post irradiation (*19, 20*), it has been suggested that radiation-induced cognitive dysfunction may depend on adult neurogenesis in the hippocampus. However, there was no correlation between radiation induced suppression of adult neurogenesis and spatial learning tested in a different behavioral paradigm, e.g. Morris water maze (*21, 22*). In addition, when other techniques were used to suppress adult neurogenesis, they failed to establish an unambiguous link between adult neurogenesis and learning and memory (*23, 24*). Thus, a causative relationship between radiation induced suppression of neurogenesis and radiation induced cognitive impairment still awaits clarification (*24*).

An alternative neuronal mechanism of radiation-induced cognitive dysfunction is **perturbation of chemical neurotransmission**, a mechanism mostly independent of neurogenesis (*25*). Transduction of neuronal signal may be achieved by electrical coupling of pre- and postsynaptic elements at electrical synapses. However, the overwhelming majority is chemical synapses, which use chemical substances for transmission[a]. Exposure to radiation results in the generation of toxic free radicals (*26, 27*) which affects neurotransmission (*28-31*). When a hippocampal slice preparation was exposed to H_2O_2, an experimental model to assess effects of HZE radiation (*28*), the

---

[a] In the rest of the text, the term "neurotransmission" will refer to "chemical neurotransmission".

exposure altered neuronal excitability, the ability to generate action potentials (*29*), and reduced synaptic efficacy at both inhibitory and excitatory synapses (*30*). H_2O_2 also suppressed [K^+]-depolarization-evoked [^{3}H]-glutamate release from isolated cortical nerve terminals, suggesting that radiation induced reactive oxygen species (ROS) production may perturb the functional integrity of release machinery (*31*).

Currently neurochemical research on space HZE radiation effects has been mostly limited to nigrostriatal dopaminergic (DA) and cholinergic neurotransmission (*5, 32, 33*), a brain region mostly involved in movement coordination (*34*). Joseph et al found that 0.1 to 1.0 Gy of HZE radiation significantly reduced the enhancement of depolarization-evoked DA release by oxotremorine, muscarinic cholinergic receptor agonist (*5*). This effect was region-specific, as decrements were observed only in the striatum but not in the hippocampus (*35*).

Much less understood are the effects of space radiation on **hippocampal neurotransmission,** despite the well documented HZE radiation-induced impairments in hippocampus dependent behavior (*9, 10, 36*), and radio-sensitivity of the region (*28, 37*). In line with these previous reports, my preliminary results also demonstrated significantly enhanced radio-vulnerability of the hippocampus (Chapter I, Preliminary Results for a full detail). Thus, in this study, I have focused on **the effects of HZE radiation on chemical neurotransmission in the hippocampus.** My hypothesis is that HZE radiation disrupts functional integrity of hippocampal neurotransmission, which may be a component of radiation-induced cognitive dysfunction.

Since major events in synaptic neurotransmission are release of neurotransmitters and activation of neurotransmitter receptors, I addressed possible HZE effects on these in the following specific aims.

In Aim 1, I tested effects of HZE radiation on release of major hippocampal neurotransmitters. I assayed basal and hyperosmotic-shock evoked release from **glutamatergic, GABAergic** (γ-amino-butyric acid), and **noradrenergic** systems (Chapter II). Hyperosmotic sucrose evoked release has been used as a measure of the size of the readily releasable pool, which reflects release probability (*38*) and synaptic strength (*39*). Glutamate is the major excitatory transmitter in the CNS and the participation of glutamatergic NMDA receptors in long-term potentiation (LTP) and depression (LTD) provides a strong link between the glutamatergic systems and the mechanisms of learning and memory (*40*). GABA is the major inhibitory transmitter in the CNS, and behavioral/pharmacological studies have suggested that GABA receptor blockade can improve hippocampal dependent learning and memory (*41*). NE is also implicated in synaptic plasticity; α- and β-adrenergic receptor manipulations modulate LTP in hippocampal pathways (*42, 43*) and learning tasks (*44*). My working hypothesis was that HZE radiation perturbs release of these hippocampal neurotransmitters, which play critical roles in hippocampal dependent learning and memory.

In Aim 2, I tested the effects of HZE radiation on levels of neurotransmitter receptors (Table 1) by quantitative western blot analysis to elucidate biochemical correlates of possible changes in neurotransmission (Chapter III). My working hypothesis was that HZE radiation may affect these protein levels, and in turn these may lead to alterations in synaptic strength, giving rise to impaired learning and memory.

TABLE 1A

Neurotransmitter Receptors Evaluated in Quantitative Western Blot Analysis

	Receptor subtype:	Mw
Glutamatergic		
	NMDA NR1	120kDa
	NMDA NR2A	170 kDa
	NMDA NR2B	180kDa
	AMPA GluR1	106 kDa
GABAergic		
	$GABA_A$ α1	50 kDa
	$GABA_B$	130 kDa
Noradrenergic		
	α1	60 kDa
	α2A	45 kDa
	β1	64 kDa

TABLE 1B

Synaptic Proteins Evaluated in Quantitative Western Blot Analysis

Description	Proteins	Mw
Synaptic vesicular protein	Synaptophysin	38 kDa
Vesicular glutamate transporter	VGlut1	70-80kDa
Scaffold protein for glutamatergic re	PSD-95	95kDa
Microtubule associated protein	MAP2a/2b/2c	280kDa (2a, 2b), 70kDa (2c)
Loading control	Actin	42 kDa
Loading control	VCP	97 kDa

Aim 3 was designed to test HZE effects on **lipid peroxidation** in the hippocampus (Chapter IV). By definition, ionizing radiation generates ions, which increase the formation of free radicals and reactive oxygen species (ROS). Imbalance between the pro-oxidants and anti-oxidants may cause oxidative stress, e.g. oxidation of membranes. My working hypothesis was that lipid peroxidation of membranes may underlie impairments in hippocampal neurotransmission.

To investigate these specific aims, I exposed rats to single doses of 0.6, 1.4, 2.0 Gy of HZE (^{56}Fe, 1 GeV/n, 150 keV/μm) radiation, or sham radiation. The dose of 2.0 Gy was chosen based on my preliminary study where 2.0 Gy significantly inhibited basal and evoked [^{3}H]-norepinephrine release from rat hippocampal slices (Chapter I, Preliminary Results). One point four Gy was chosen to approximate doses that inhibit hippocampus dependent cognitive performance previously reported (*9, 10, 36*). I have chosen 0.6 Gy as the lowest test dose, since our behavior data displayed highly variable performance of 0.6 Gy irradiated animals in hippocampus dependent spatial learning test, which implies that the dose is capable to induce neurochemical change in hippocampus, but a degree of change depends on sensitivity to radiation within each individual (*45*).

As discussed earlier, it is the delayed effects that may lead to severe neurological consequences in the CNS (*46, 47*). In this study, animals were sacrificed three and six months post-irradiation to investigate the early and late delayed radiation effects.

I used **synaptosomal preparation** to evaluate effects of HZE irradiation on hippocampal neurotransmission and protein levels. Synaptosomes are isolated nerve terminals, and have been used as an experimental model system to study the structure and function of the synapse (*48*), and **synaptic plasticity** (*49*).

My findings indicate that a single treatment with 0.6 Gy of **^{56}Fe HZE particles**[b] (1 GeV/n, whole-brain irradiation) significantly disturbs functional integrity of the release machinery of rat hippocampal synaptosomes, and results in the reduction of evoked [^{3}H]-glutamate and [^{14}C]-GABA release three months post irradiation. A pronounced change has also been found at the 6 month time-point, indicating that the effects are persistent. Exposure to ^{56}Fe HZE radiation also significantly perturbs levels of glutamatergic NMDA receptors and β adrenergic receptors, while levels of marker proteins for glutamatergic nerve terminals, and glutamatergic synaptic vesicles are not significantly altered, thus it is unlikely that observed reduction in glutamatergic release is caused by radiation-induced depletion of glutamatergic store or apoptotic damage of nerve terminals. Increased level of lipid peroxidation after exposure may be a possible mechanism of disrupted neurotransmission in the hippocampus.

Considering critical roles of glutamatergic and GABAergic systems, and NMDA receptors and β adrenergic receptors in learning and memory, my findings provide experimental evidence which underlie radiation-induced cognitive dysfunction.

INTRODUCTION TO SPACE RADIATION BIOLOGY

Radiation is a process in which energy *radiates*, i.e. energy travels outward in straight lines to all directions from a source. When radiated energy hits atoms or molecules, it may lead to *excitation* or *ionization* of them. Excitation is where energy causes an electron in an atom or molecule move to a higher energy level without actual

---

[b] ^{56}Fe particles are discussed in Chapter I, Introduction to Space Radiation Biology.

ejection of the electron, while ionization is a process where the incident energy is sufficient to eject orbital electrons from the atom or molecule. Ejected electrons are capable of causing damage to biological materials by breaking a chemical bond and initiating a chain of events, or to induce free radical production. An important characteristic of potentially hazardous radiation is the ability to ionize, and such radiation is classified as **ionizing radiation**.

Ionizing radiation is categorized as either **electromagnetic** or **particulate**, depending on the source of energy. X-rays are a conventional example of electromagnetic radiation and are used in clinical practice. The source of particulate radiation could be electrons, protons, α-particles, neutrons and **heavy charged ions (HZE,** high mass, highly charged (Z), high energy**)**.

The biological effects of radiation are caused by either **direct** or **indirect action** of ionization. Direct action of radiation is where energy directly interacts with targets in cells and initiates a chain of events that leads to a biological change (Fig. 1, direct action). Alternatively, radiation may interact with other atoms or molecules in the cell, for example, **water,** to produce reactive oxygen species (ROS) that are able to diffuse to critical targets and inflict damage (Fig. 1, indirect action). A principal target for direct action is chromosomal DNA, as depicted in Figure 1.

Galactic cosmic radiation (GCR) is a major constituent of space radiation, which is composed of protons (85%), helium (14%) and heavier HZE particles (1%) (*2*). Although protons make up a large portion of the radiation spectrum, no significant effect of proton radiation at any dose on behavioral and neurochemical endpoints has been reported (*50*). In contrast, HZE particles have multiple biological effects (*8, 33, 51, 52*).

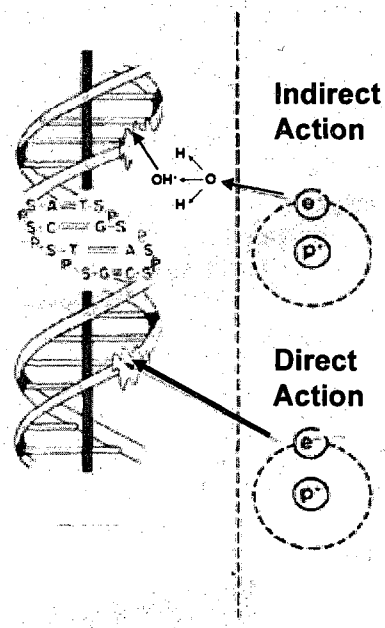

FIG. 1. Direct and indirect actions of ionizing radiation. In direct action, an emitted electron (e^-) interacts with a target, for example, DNA helix, to produce an insult. In indirect action, an electron interacts with, for example, a water molecule to produce ROS, here a hydroxyl radical ($OH^\bullet$), which in turn produces the damage to the DNA. (Modified from Hall, 2006; ref. *46*)

Thus, the general consensus is that HZE particles represent the most hazardous type of radiation in space. Human exposure to HZE in space was first described as an episode during the lunar missions of the 1970's, when astronauts "saw" light flashes with eyes closed in complete darkness. This phenomenon was caused by HZE particles crossing the retina. It has been estimated (*53*) that on a 3-year mission to Mars, 3% of cells in the body would be traversed by HZE (^{56}Fe) particles even behind aluminum shielding of 4 g/cm^3 (*4*).

HZE particles are nuclei of elements; e.g. carbon, neon, argon, or iron. They are positively charged because some or all of the planetary electrons have been stripped away (*46*). In ground based studies, HZE particles must be accelerated to energies of mega (10^6) to giga (10^9) electron volts, therefore, can be produced in only specialized facilities. HZE radiation has a characteristic pattern of energy deposition in a defined range along a linear track. Figure 2 shows computer simulations for track structures of proton (A) and three types of HZE particles (B, C, D) in liquid water to estimate energy distribution in biological matter (*54*). In contrast with a diffuse pattern of proton (A), HZE particle tracks take the appearance of a dense "bottle brush" pattern with a central "core". In the core, the local dose may be quite high, but may drop to zero just a few microns away. Thus, HZE particles are categorized as high LET (linear energy transfer) radiation per unit length of track.

Another important property of HZE particles is that they undergo nuclear fragmentation reactions to produce multiple secondary particles (*55*). These secondary particles, whose effects are similar to X-rays, create their own tracks (delta-ray) and may extend the range of effects beyond that of the primary particle. In Figure 2, lateral

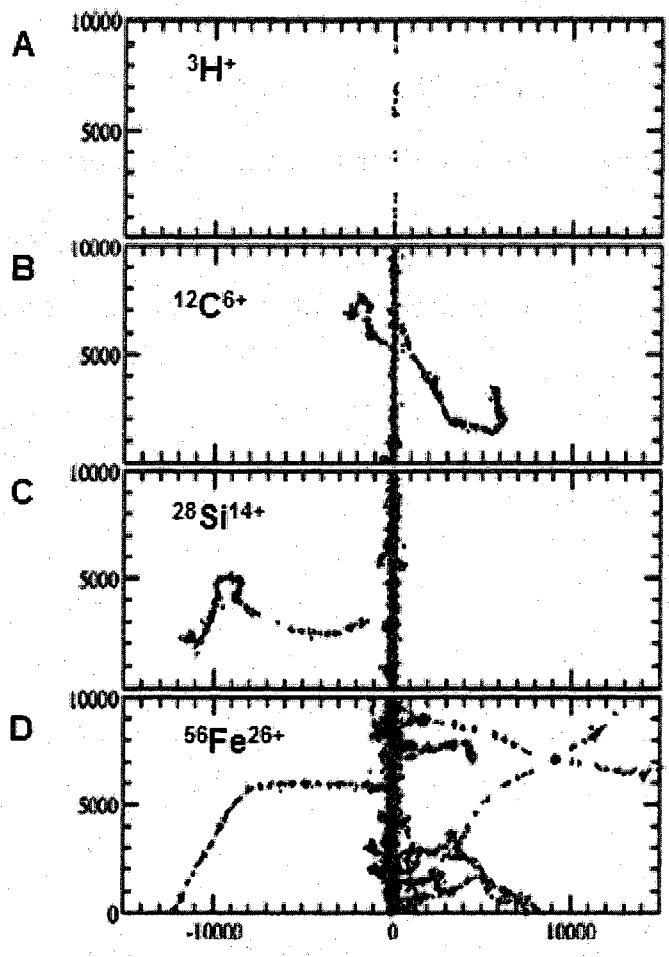

FIG. 2. Computer simulation of tracks of representative particulate radiation: proton (A), carbon (B), silicon (C), and iron (D) ion passing through a thin slab (1μm) of liquid water with initial energy 100 MeV/nucleon. The particles are started in positive Z-direction, and the coordinates are given in Angstrom (Å). Lateral tracks indicate delta-ray from secondary particles. (From Dingfelder, 2006; ref *54*)

delta-ray tracks are shown along the longitudinal primary trajectories.

Also, as the panels B, C, and D show, the greater the nuclear charge (Z), the higher the ionization density becomes, which leads to the increased probability of a direct interaction between the particle track and target molecule. A characteristic dense pronounced track of ^{56}Fe shows that heavy HZE particles could be more devastating.

Another important feature of HZE particles is so called "bystander effect", which is illustrated in Figure 3 (*55*). Bystander effect is when an isolated individual cell in a population is traversed by a particle, both the "hit" cell and many of its "un-hit" neighbors (bystanders) respond to radiation exposure (*56-58*). The effect is likely mediated by damage-inducing factor(s), as transfer of culture medium from an exposed culture to unexposed cells often exhibits the effect. Protection by ROS (reactive oxygen species) scavengers such as superoxide dismutase (SOD) or catalase blocks the bystander effect in some systems, while proteases block the effect in others, thus it is assumed that damage in a "hit" cell may lead to the spread of either radical products or signaling proteins to neighboring cells. This effect may persist for several years (*58*). Although currently bystander effects have been reported in preparations exposed at low dose, the existence of the effect provides evidence for damage amplification.

Considering the highly-layered and interconnected structure of the CNS, the possibility of HZE tracks to cause a "functional micro-lesion" via its characteristic dense energy deposition pattern or via bystander effect in the organ is extremely high (*55*), in contrast to isotropic tissues such as liver or connective tissue. Thus, the CNS has been suggested as a system of the body that might be particularly sensitive to HZE particles.

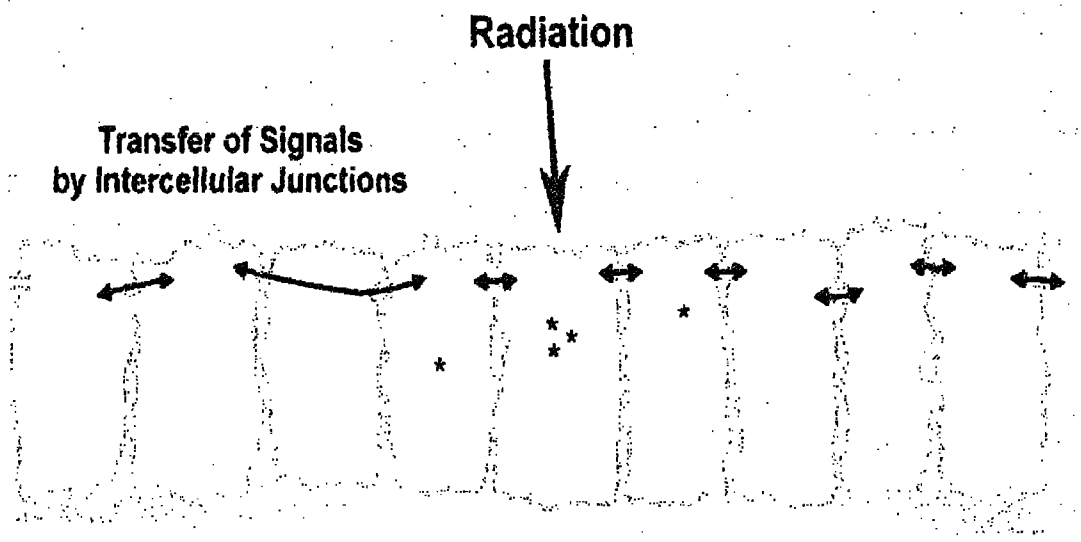

FIG. 3. "Bystander effect". Damage created in a cell struck by a single charged particle radiation leads to the spread of signals or toxic products to many neighboring cells via intercellular junctions, soluble molecules, or remodeling of the extracellular matrix. The "bystander effect" amplifies the damage from charged particles. *: DNA damage. (From Nelson, 2003; ref. *55*)

It is estimated that during a three-year mission to Mars, 2% to 13% of cells in the CNS would be directly hit at least once by HZE particles (*53*).

HZE radiation is a heterogeneously composed beam including elements heavier than helium ^{4}He. On ground level experiments, however, effects of individual ions, such as ^{56}Fe, are investigated extensively to simulate effects of HZE radiation. ^{56}Fe (Z = 26) is the most abundant element in the HZE flux, followed by ^{28}Si (Z = 14) (*52*). ^{56}Fe has the highest nuclear binding energy derived from the strong nuclear force (Fig. 4). Nuclear binding energy is defined as energy required for disassembling a nucleus into free unbound neutrons and protons per nucleon. High binding energy of ^{56}Fe (8.79 MeV/nucleon) explains an increase in stability toward formation of ^{56}Fe, indicated by the arrows in Figure 4 (*59*). Much lighter elements tend to fuse together to yield heavier elements such as ^{56}Fe, and much heavier elements split apart to yield lighter elements, also leading to ^{56}Fe production.

Accumulating evidence indicates that ^{56}Fe particles can induce distinctive effect on biological materials. When behavioral toxicity caused by direct action of HZE on gastrointestinal system was evaluated using conditioned taste aversion learning, effects of ^{56}Fe was significantly greater than that of ^{4}He, ^{20}Ne, ^{40}Ar, and even the heavier ^{93}Nb (Fig. 5) (*6, 60*). One characteristic of ^{56}Fe effects is its extremely steep dose-response curve (*9, 61*), as observed in Figure 5. ^{56}Fe also can induce significant effects on motor performance assessed in wire suspension test (*5*), and prevent the acquisition of an amphetamine-induced conditioned taste aversion (*8*). Since these behaviors depend on the integrity of the central dopaminergic transmission, it has been suggested that the locus of ^{56}Fe induced change is located at the level of the nigrostriatal system (*62*).

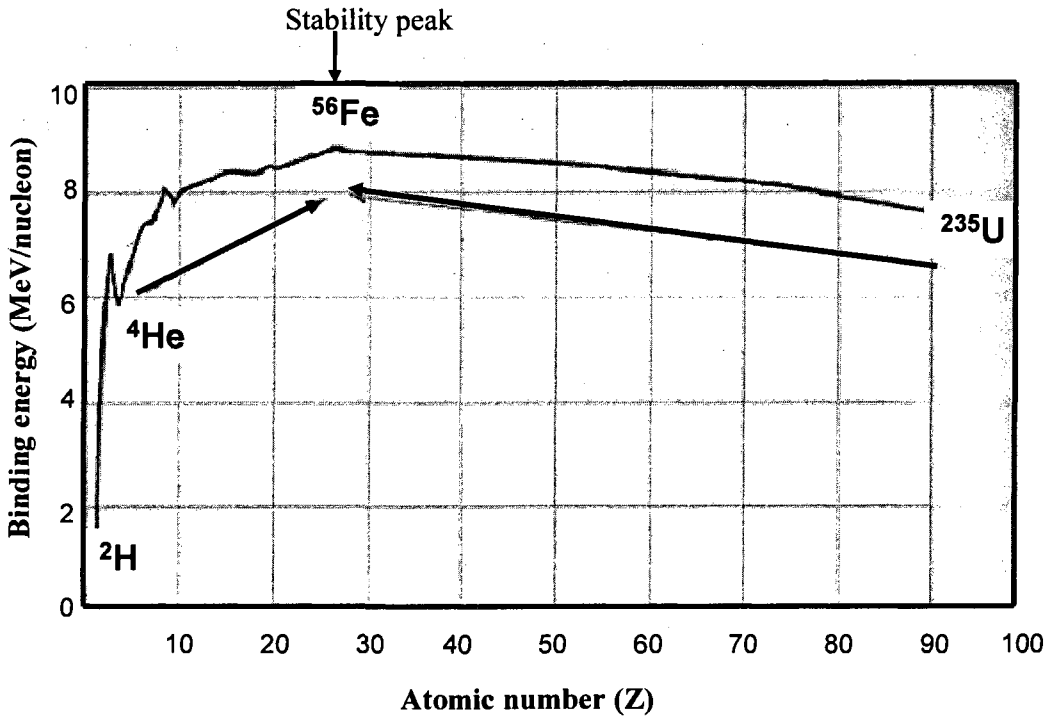

FIG. 4. Binding energy / nucleon for the most stable isotope of each naturally occurring element. ^{56}Fe possesses the highest binding energy per nucleon (8.79 MeV/n). As a result, stability is exerted in the direction toward ^{56}Fe, as indicated by the arrows. (From McMurry, 1998; ref. *59*)

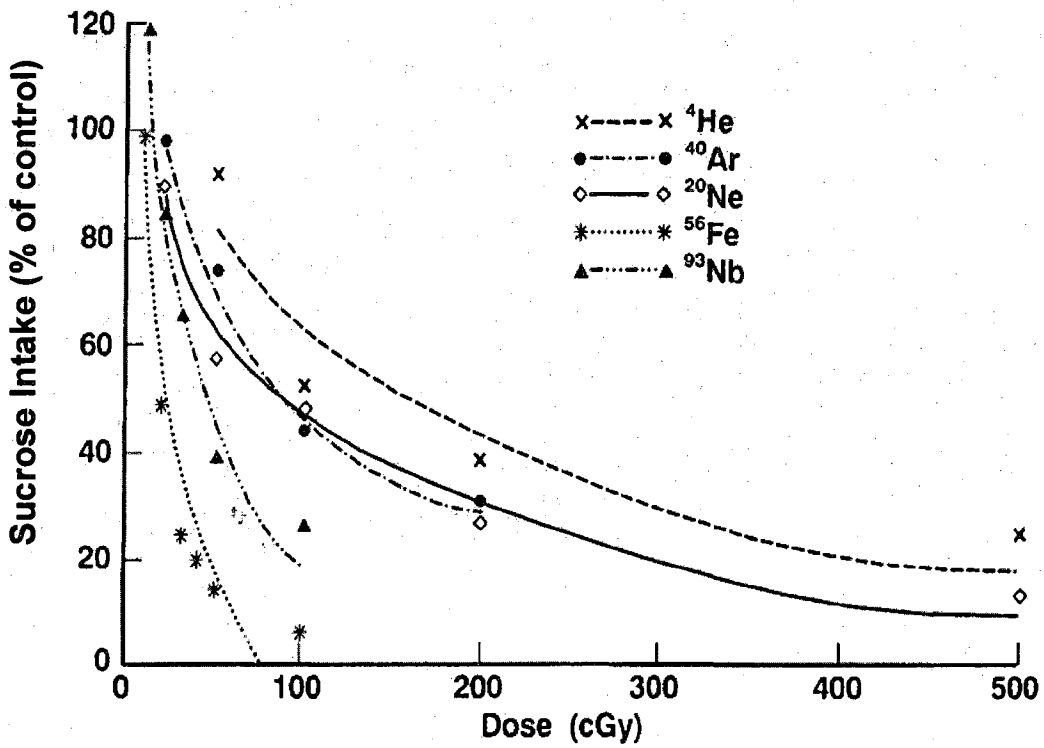

FIG. 5. Dose effects of selected HZE particles on conditioned taste aversion (CTA) production. Rats were presented a novel 10% sucrose solution and immediately exposed to one of the following HZE particles: ^{56}Fe, iron; ^{93}Nb, niobium; ^{20}Ne, neon; ^{40}Ar, argon; ^{4}He, helium. The acquisition of a CTA was assessed by subsequent intake of the normally preferred sucrose solution, and expressed as the percentage of conditioning day sucrose intake: Higher dose produced a corresponding decrease in all types of particles. Among these particles, ^{56}Fe particles showed significantly greater behavioral toxicity than other particles. (From Rabin, 1994; ref. *6*)

Joseph et al. suggested the ^{56}Fe exposure induced deficits in dopaminergic neurotransmission are due to decreased sensitivity to muscarinic receptors, which indirectly contributes to dopamine dependent behaviors. A proposed mechanism underlining the deficits is radiation induced changes in striatal membrane structure and fluidity caused by lipid peroxidation, which is known to affect a variety of neurotransmitter receptor systems (*62*). Deleterious effects of ^{56}Fe radiation on behavior were also found in hippocampal dependent learning and memory tests (*9, 10, 36*). The hippocampus plays a major role in acquisition of spatial information, temporary storage of that information, and transfer of information to long term storage to cortical areas (*63*). Failure of the hippocampus results in anterograde memory loss that interferes with proper cognitive functions. The region has been known to be highly vulnerable to insults such as trauma, ischemia, stress, aging (*64*), and also radiation. Even extremely low doses (0.005 Gy) of ^{40}Ar or ^{56}Fe induce a decrease in synaptic density and synaptic spine length in the mouse hippocampus (*65, 66*).

In animal behavioral studies, hippocampal integrity is often assayed in spatial memory tasks. 1.0 Gy to 1.5 Gy of ^{56}Fe radiation caused impairment in spatial memory performance of rodents tested in Morris water maze (*9, 27*), Barns maze (*67*), and 8-arm radial maze (*10*). These results suggest a detrimental effect of ^{56}Fe particles on hippocampus dependent cognitive functions, although the underling neurochemical mechanisms are not fully understood.

Considering these significantly pronounced effects, in this study I choose **^{56}Fe particles** to simulate effects of space radiation. ^{56}Fe particles were accelerated to energies of 1 GeV/n (giga electron volts per nucleon) in the Alternating Gradient Synchrotron in

Brookhaven National Laboratory of NASA Space Radiation Laboratory (Chapter II, Materials and Methods in detail), and utilized to irradiate rats.

PRELIMINARY RESULTS

Initially, I had tested effectiveness of ^{56}Fe particles on **catecholaminergic neurotransmission** in several brain regions three month post irradiation. I had used a **slice preparation**, which maintains integrity of local neuronal circuits and glial connection, thus, is suitable to assess neurotransmission *ex vivo*. I tested transmission of norepinephrine (NE) and dopamine (DA), which plays important roles in learning and memory (*63*), and are vulnerable to radiation (*68, 69*).

Unlike glutamatergic and GABAergic regulation which rely on dual glial-neuronal reuptake property (discussed in Chapter II), catecholamine transmitters are mostly cleared by transporters on presynaptic terminals. Thus the action of NE or DA is terminated largely by removal of these by transporters from the synaptic cleft and either recycled to synaptic vesicles or enzymatically degraded (*70*). In my experiments, pargyline, an inhibitor of monoamine oxidase, the major degradative enzyme, was added to a buffer to prevent conversion of [^{3}H]-DA or –NE to [^{3}H]-metabolites. Thus, measurement of ^{3}H indexes [^{3}H]-catecholamine release, not [^{3}H]-metabolites.

Three brain regions were tested site-by-site: **hippocampus, associative cortex and striatum.** Since NE and DA are not uniformly distributed, noradrenergic nerve terminals in hippocampal slices were labeled with [^{3}H]-NE, while dopaminergic terminals in striatum and associative cortex were labeled with [^{3}H]-DA. Basal release

was determined before a depolarization stimulus, 50 mM KCl, was applied to induce evoked release.

My results demonstrated that exposure to ≥ 2.0 Gy of ^{56}Fe HZE radiation (1 GeV/n, 150 keV/μm) perturbed neurotransmission (Fig. 6), and resulted in significant reduction in both basal and [K^+]-depolarization-evoked [^{3}H]-NE release from hippocampal slices, while [^{3}H]-DA release from cortical and striatal slices was not significantly altered under the test condition.

Using the same experimental approaches, I have measured release after X-ray exposure to assess relative biological effectiveness (RBE) of ^{56}Fe radiation. 13 Gy of X-rays produced similar neurochemical changes as observed with ≥ 2.0 Gy of ^{56}Fe radiation. It reduced both basal and [K^+]-depolarization-evoked [^{3}H]-NE release from hippocampal slices (Fig. 7), while 10 Gy of X-rays did not significantly alter neurotransmitter release (data not shown). [^{3}H]-DA release from cortical and striatal slices was not significantly altered under any test conditions (Fig. 7).

In summary, my preliminary results show 1) enhanced radio-sensitivity of the hippocampus, and 2) high effectiveness of HZE (^{56}Fe) radiation with RBE value 6.5 in inhibiting hippocampal noradrenergic transmission. The results also serve to estimate effective ^{56}Fe radiation doses for our main studies. Determination of RBE to a standard radiation, or X-rays, is a common practice in radiation research (*55, 71*). RBE is calculated as the ratio of the dose of X-rays to the dose of a test radiation that produces the same biological effect.

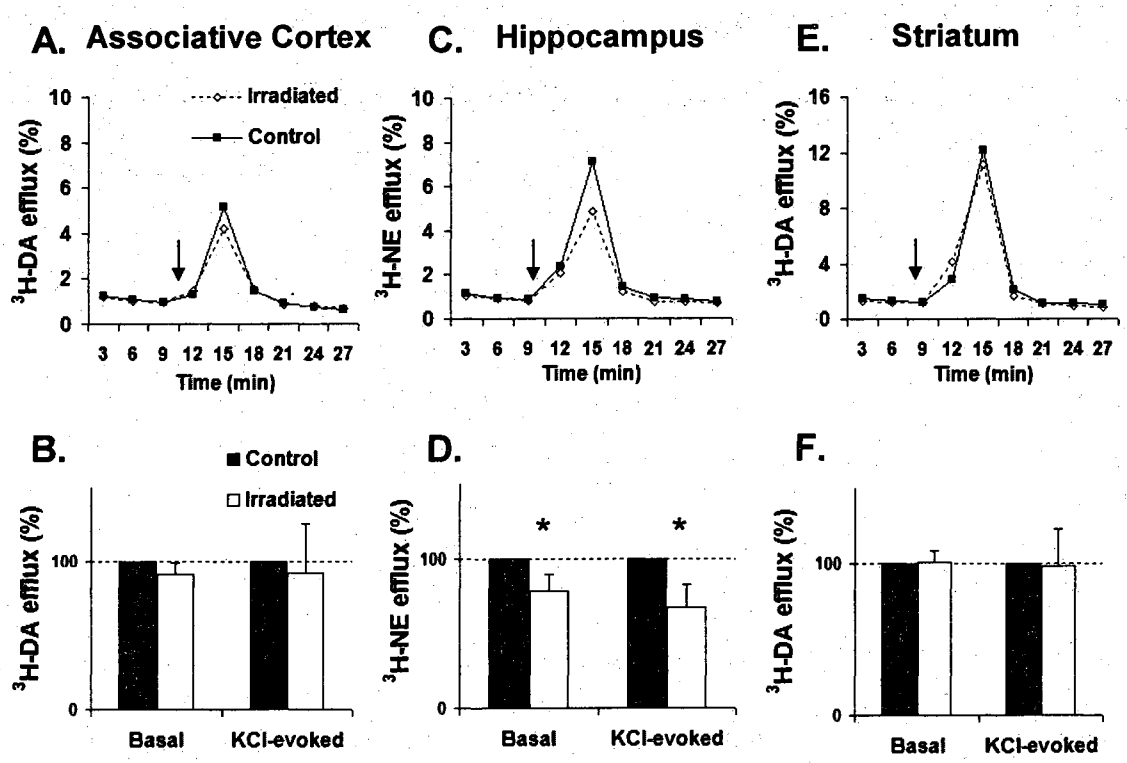

FIG. 6. Over 2 Gy of HZE (^{56}Fe, 1 GeV/n, 150 keV/μm) radiation effects on [^{3}H]-catecholaminergic release from rat brain slices: associative cortex (A, B); hippocampus (C, D); and striatum (E, F). Endogenous norepinephrine (NE) stores in hippocampal slices were labeled with [^{3}H]-NE. Endogenous dopamine (DA) stores in striatum and associative cortex slices were labeled with [^{3}H]-DA. Catecholamine release was induced by depolarization using a 1.5 min pulse of 50 mM KCl (arrow). Basal and depolarization-evoked release in response to either 2 or 2.25 Gy of ^{56}Fe radiation was determined in comparison with sham treated animals three month post irradiation. Panel A, C, E: Representative experiment. Panel B, D, F: Summary data. The fractional release values under normal conditions were set to 100% and treatment effects were normalized to control. Data are presented as mean ± SEM (n = 4 rats/treatment). *: $P < 0.05$, Student's t-test.

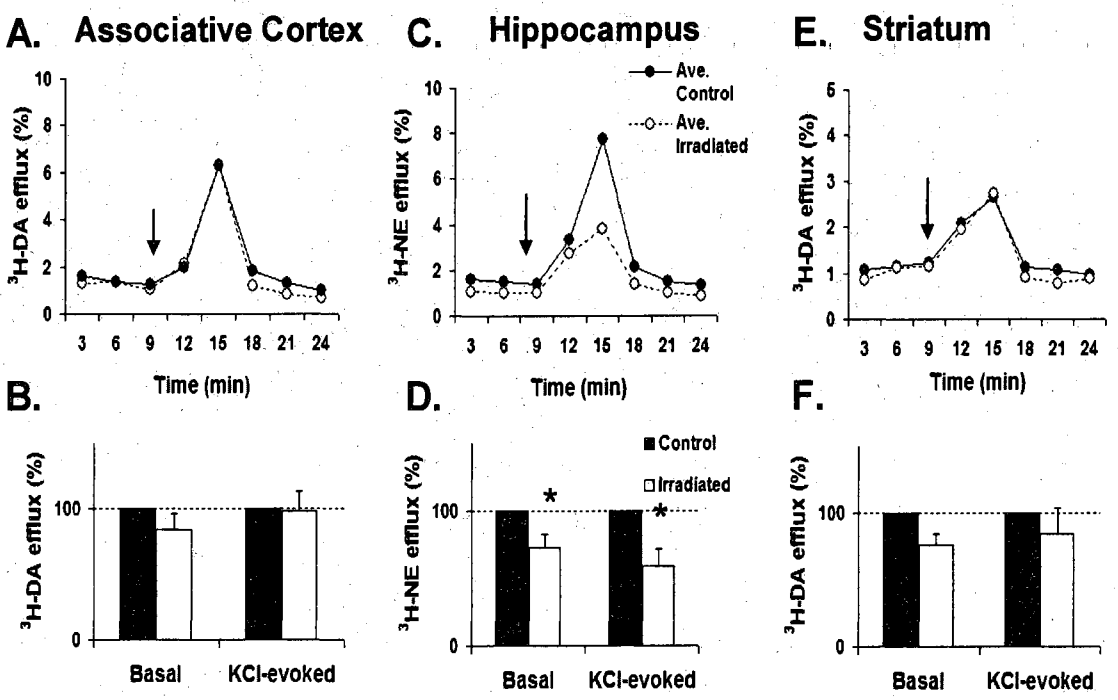

FIG. 7. Thirteen Gy of X-ray effects on [^{3}H]-catecholaminergic release from rat brain slices: associative cortex (A, B); hippocampus (C, D); and striatum (E, F). Endogenous norepinephrine (NE) stores in hippocampal slices were labeled with [^{3}H]-NE. Endogenous dopamine (DA) in striatum and associative cortex slices was labeled with [^{3}H]-DA. Catecholamine release was induced by depolarization using a 1.5 min pulse of 50 mM KCl (arrow). Basal and depolarization-evoked release in response to 13 Gy of X-rays was determined in comparison with sham treated animals at three month post irradiation. Panel A, C, E: Representative experiment. Panel B, D, F: Summary data. The fractional release values under normal conditions were set to 100%, and treatment effects were normalized to control. Data are presented as mean ± SEM (n = 3 rats/treatment). *: $P < 0.05$, Student's t-test.

CHAPTER II

EFFECTS OF HZE RADIATION ON NEUROTRANSMITTER RELEASE

BACKGROUND

In the hippocampus the majority of synaptic activity is driven by the excitatory neurotransmitter **glutamate** and I have focused my attention mostly on the glutamatergic system. Direct involvements of glutamate in learning and memory have been established, e.g. a critical role of glutamatergic **NMDA receptors** in long-term potentiation (**LTP**) (*72*), long-term depression (**LTD**) (*73*) and memory (*74*) has been shown. Disturbance of the hippocampal glutamatergic neurotransmission also has been implicated in the pathogenesis of neurological disorders, such as schizophrenia (*75*), and functional decline was found during aging (*64 for review, 76*)

The processes related to the glutamatergic neurotransmission are schematically depicted in Figure 8. The synthesis of glutamate (GLU) occurs from glutamine (GLN) through the action of glutaminase (Gln-ase) which is localized in the mitochondria of glutamatergic nerve terminals (*76*) (step 1). Glutamate is then incorporated to synaptic vesicles by **vesicular glutamate transporter (VGlut**, discussed in Chapter III) (*77*) (step 2). Glutamate is released from synaptic vesicles into the synaptic cleft upon action potential triggered by Ca^{2+} influx (step 3) and activates ionotropic receptors (AMPA, NMDA, kainate (KA) (step 4) to produce excitatory postsynaptic potential (EPSP). Glutamate also activates metabotropic receptors (mGluR), which transduce signals to enzymatic activity and/or channel activity. The main mechanism for clearing extracellular glutamate is by uptake through high-affinity neuronal glutamate transporters

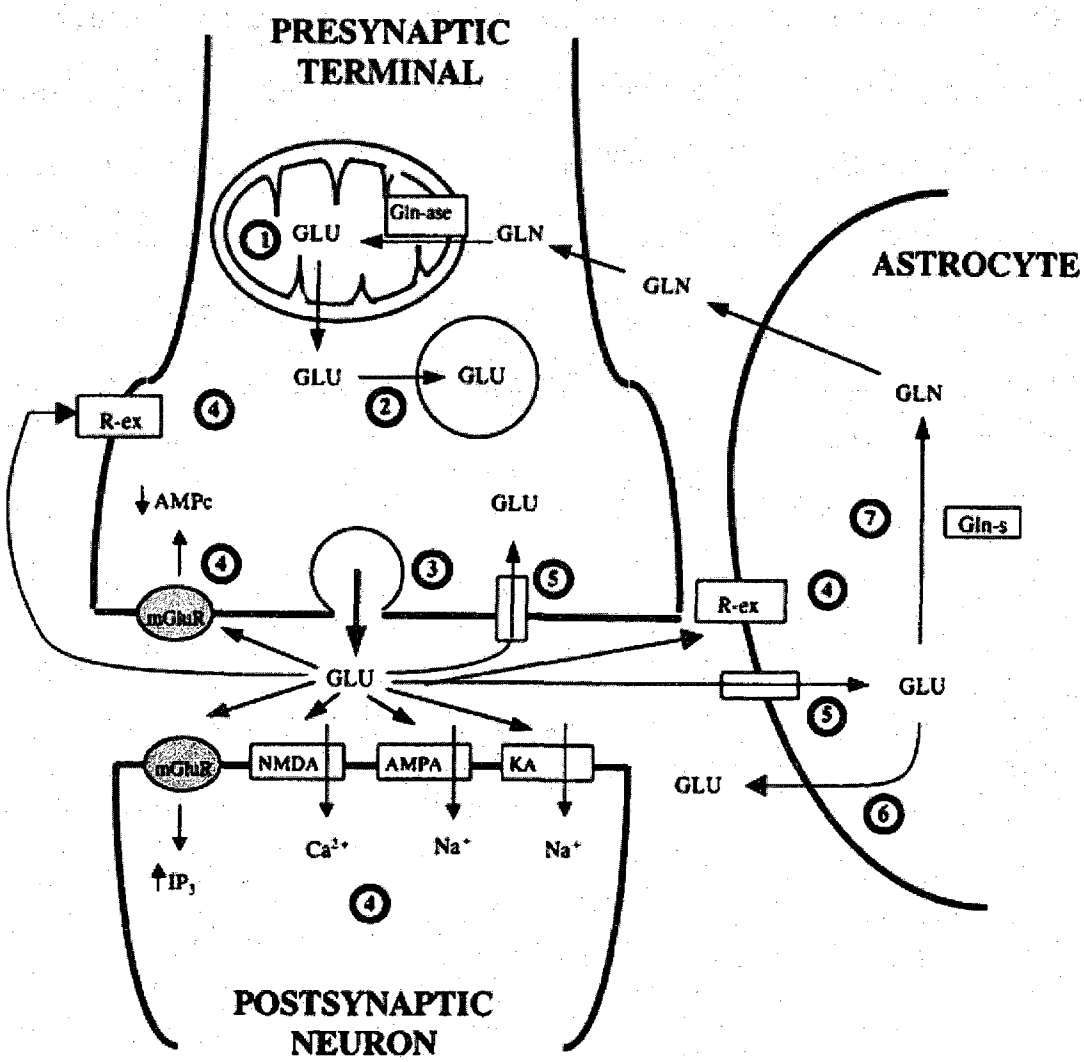

FIG. 8. Schematic representation of glutamatergic neurotransmission; 1) synthesis of glutamate (GLU) from glutamine (GLN) through the action of glutaminase (Gln-ase). 2) storing of glutamate into synaptic vesicles. 3) Ca^{2+} dependent exocitotic release of glutamate. 4) glutamate activation of its receptors (AMPA, AMPA receptors; KA, kainate receptors; NMDA, NMDA receptors; mGluR, metabotropic receptors; R-ex, extrasynaptic receptors (ionotropic or metabotropic)). 5) uptake of glutamate through high affinity transporters (empty box) located in astrocytes and presynaptic terminals. 6) synthesis of glutamine from glutamate though the action of glutamine synthetase (Gln-s). (From Segovia, 2001; ref. *64*)

(excitatory amino acid transporter (EAAT)) located in presynaptic terminal or glial glutamate transporter (GLT) located in astrocyte surrounding glutamatergic terminals (step 5). As for the catabolism of glutamate, the glial enzyme glutamine synthetase (Gln-s) converts glutamate to glutamine (*76*) (step 7), which is taken up by neurons and is converted to glutamate.

Glutamate transporters are driven by Na^+/K^+ electrochemical gradients. The transport of one molecule of glutamate is coupled to the co-transport of three Na^+ and one H^+, and the counter-transport of one K^+ (step 5). When these gradients are dissipated and ionic disequilibrium occurs, glutamate may also be "released" by reverse operation of the glutamate transporters (step 6). The physiological role of this Ca^{2+}-independent release of glutamate is questioned, but is associated with excitotoxicity in pathological circumstances, e.g. ischemia (*64*).

As Figure 8 shows, synaptic glutamate concentration is the result of a balance between these neuronal-glial release and uptake processes. This dual-component system makes it difficult to differentiate between effects on release and re-uptake when brain slices are used for release experiments. To circumvent this problem, in the present study, we have utilized isolated nerve terminals, **synaptosomes** (Fig. 9). Synaptosomes are prepared by gentle homogenization in iso-osmotic sucrose solution, followed by a series of differential centrifugations. The purity of synaptosomal preparation is estimated to be about 70% (*78*). It contains 1) mitochondria, 2) synaptic vesicles, 3) active zone, a specialized region of presynaptic plasma membrane where synaptic vesicles fuse, and 4) attached fragments of postsynaptic membranes containing signal transducing proteins (Fig. 9) (*79*). Under proper experimental conditions, synaptosomal preparation is

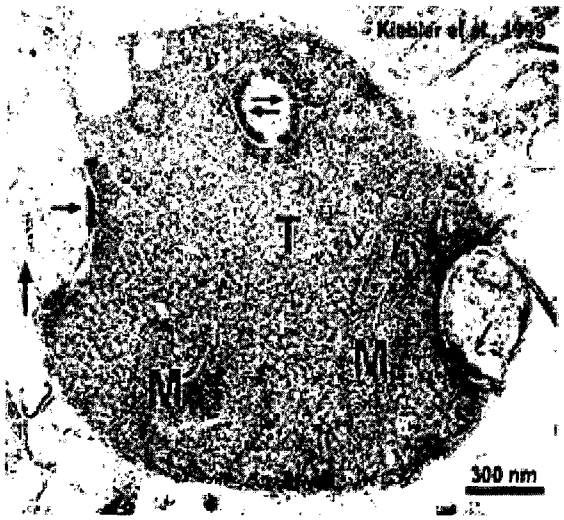

FIG. 9. Electron micrograph of rat brain synaptosome. The terminal (T) with mitochondria (M) is in contact with dendritic spine containing postsynaptic density (PSD) (small arrow) and a spine apparatus (large arrow). Bar, 300 nm. (From Kiebler, 1999; ref. *80*)

metabolically active. It respires, takes up oxygen and glucose, maintains a normal membrane potential by extruding Na^+ and accumulating K^+, and upon depolarization, releases transmitter in a Ca^{2+}-dependent manner (*78*). Since glial elements are mostly eliminated from synaptosomes, glial source of release and uptake is minimized.

In addition to glutamate, I have also investigated **GABA** and **NE** release properties. GABA is the major inhibitory neurotransmitter in the adult hippocampus, associated with synaptic inhibition by causing a hyperpolarization of postsynaptic membrane through ionotropic $GABA_A$ receptors, which is coupled to Cl^- ion conductance (*70*). $GABA_B$ receptors are metabotropic and behavioral studies have suggested that $GABA_B$ receptor blockade can improve cognition (*41*). GABA is synthesized from L-glutamate by GAD (glutamic acid decarboxylase) which localizes at neurons with the GABA containing synaptic vesicles. Similar to glutamatergic neurotransmission, GABA also has dual glial/neuronal reuptake process and after release, the action of GABA is terminated largely by removal from the synaptic cleft by these transporters.

NE plays a prominent role in hippocampal cognitive function as a neuromodulator. It enhances LTP, widely believed to be an important cellular mechanism of learning and memory. Mossy fiber LTP in the hippocampus is modulated by both β- and α1-adrenergic receptors (*43, 81, 82*). NE has also been known to display vulnerability to ionizing radiation. After X-ray exposure, NE content in rat brain and heart were reduced (*68*) and γ radiation reduced NE release in the hippocampus (*69*). The precise mechanisms underling these findings are unknown. A pharmacological study implicates reduced mobilization of intracellular Ca^{2+} stores (*83*), however, our own studies determined only a minor role for internal Ca^{2+} stores for neurotransmitter release

regulation (*84*). The involvement of hippocampal glutathione's anabolic/metabolic pathways was also suggested (*85*).

Synaptic vesicles (SV) cycle between functionally heterogeneous subpopulations is depicted in Figure 10. After the uptake of neurotransmitters (NT) (step 1), synaptic vesicles form a cluster termed **the reserve pool** (step 2). Next, vesicles are docked at the active zone (step 3), and through an ATP-dependent process, the release machinery is "primed" (step 4). During priming, fusion core complex, or SNARE complex (**s**oluble ***N***-ethylmaleimide-sensitive fusion protein **a**ttachment protein **re**ceptors), is assembled into a trans configuration, which contains synaptobrevin (vesicular SNARE motif), SNAP-25 and syntaxin (target SNARE motif on the plasma membrane). This complex spans synaptic vesicle membrane and plasma membrane, and brings these into close proximity. Also, synaptotagmin, a putative Ca^{2+} sensor, constitutively associate with SNARE complex. Though these processes, synaptic vesicles become fusion competent and form **the readily releasable pool (RRP)**. After fusion (step 5), synaptic vesicles undergo endocytosis and recycle via several routes: fast recycling without an endosomal intermediate (step 6), or clathrin-mediated endocytosis (step 7) with recycling via endosomes (step 8). The total number of vesicles that participates in exo- and endocytosis during prolonged stimulation is referred to as the **recycling pool.** This pool is composed of the RRP and the reserve pool, which serves to replenish the RRP upon its depletion (*86*). Using cultured hippocampal neurons, one study estimated 17 - 20 vesicles in the reserve pool and 4 - 8 vesicles in RRP, estimating total of 21 - 25 vesicles in the recycling pool (*86*).

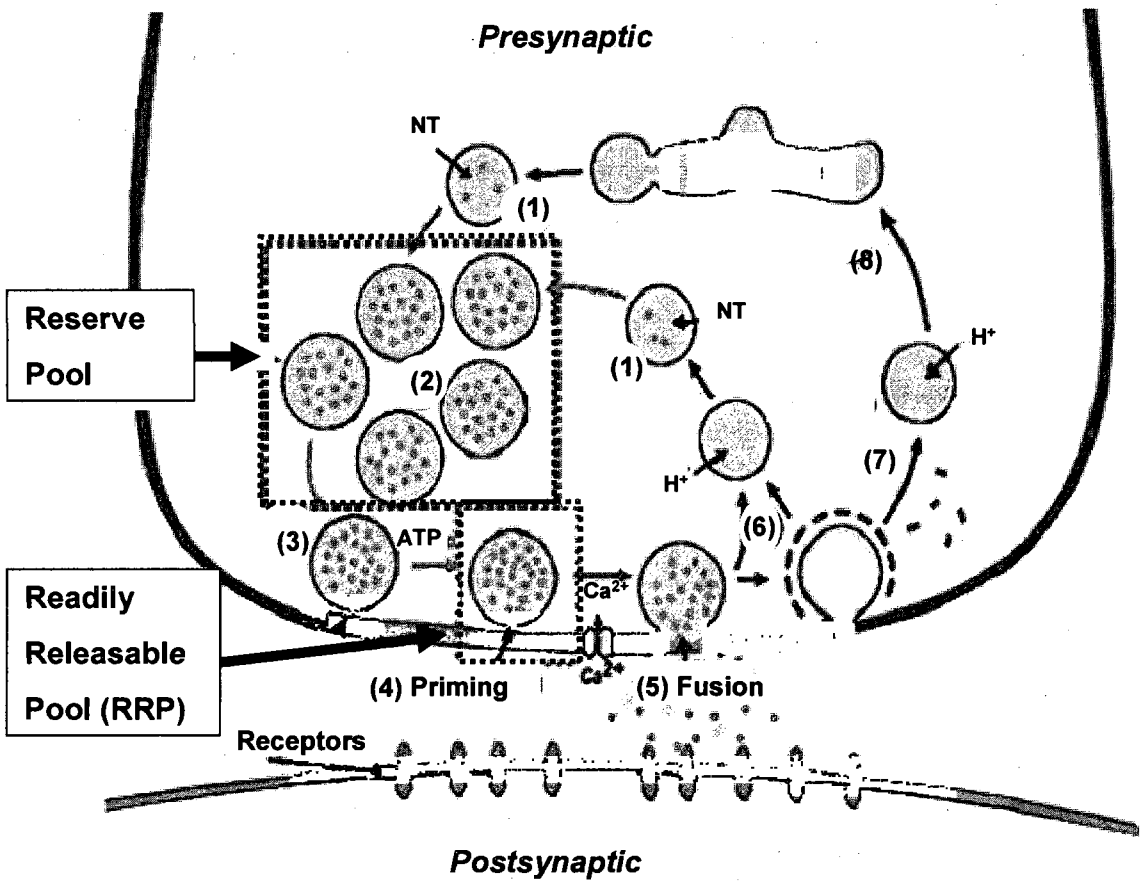

FIG. 10. Readily Releasable Pool (RRP) in synaptic vesicle cycle. After synaptic vesicles are filled with neurotransmitters (NT) (step 1), they form a vesicle cluster that serves as a reserve pool (step 2). Filled vesicles dock at the active zone (step 3), and there they undergo an ATP-dependent priming reaction (step 4) which makes them competent for Ca^{2+} triggered fusion-pore opening (step 5). Primed synaptic vesicle cluster is termed RRP. (Modified from Südhof, 2004; ref. *86*)

RRP informs on synaptic release probability (p_r) and synaptic strength (*38, 87*). These parameters are actively regulated under physiological conditions, e. g. learning and memory related processes (*88*), and under neurodegenerative conditions (*89, 90*).

I used a pulse of **hyperosmotic sucrose** to probe the size of the RRP (*38, 88*). The 30 sec pulse I applied does not induce membrane damage but mimic action potential evoked vesicular neurotransmitter release (*38, 88, 91*) with the exception that it does not require Ca^{2+} influx. This allowed me to bypass possible treatment effects on Ca^{2+} homeostasis and focus on HZE radiation induced modulation of the RRP and changes in the "proximal" release machinery proteins that are directly involved in the synaptic vesicle cycle.

Whereas action potential/depolarization evoked release is the most studied, even in the absence of action potentials, synapses exhibit low-probability "spontaneous" release. This represents mostly fusion of a single synaptic vesicle of a distinct vesicle pool (*92*). Spontaneous release had been considered as a "leak" of neurotransmitter in a random Ca^{2+} independent fashion, however, recent studies revealed that spontaneous release may also be Ca^{2+} sensitive, although to a different degree (*93*). The physiological role of spontaneous release is not clear, but several roles e.g. spine maintenance, have been suggested (*94*). **Basal release** in my assay may correlate with spontaneous release.

In my **release assay**, neurotransmitter pools in synaptosomal preparations were first labeled with ^{3}H or ^{14}C tagged neurotransmitter in a low enough concentration that would not offset the natural distribution of the endogenous neurotransmitter. In principle, release of the radiolabel accurately reflects the endogenous neurotransmitter release.

After I determined basal release, release was evoked by applying a stimulus. Basal and stimulus evoked neurotransmitter efflux was determined by counting the isotope amounts.

MATERIALS AND METHODS

Animals and Irradiation Procedures

A total of seventy-eight male[c] Wistar rats (Harlan Sprague-Dawley, Inc., Indianapolis, IN) were used in this study. 49 animals were exposed either to X-rays or ^{56}Fe radiation, while 29 rats were exposed to the same procedural steps, except that they received no radiation. These were termed as sham control animals. The animals were 3 to 4 weeks old weighing approximately 180 g when they were received at Eastern Virginia Medical School (EVMS) or Brookhaven National Laboratory (BNL, Brookhaven, NY) animal facility. They were allowed to acclimate for at least one week before radiation exposure.

At about 5 weeks of age, rats were anesthetized with I.P. ketamine (80 mg/kg)/xylazine (8 mg/kg) and placed in a custom-made irradiation jig that held their head in a fixed position by a tooth bar. The jig was placed behind a 6 mm lead shield for

---

[c] Gender differences in response to radiation have been reported in patients receiving cranial radiotherapy (*13, 95*). These reports found that girls had increased risk for neurocognitive impairments. However the underlying mechanisms of gender differences are not well understood. While gender differences to radiation have important basic science and practical implications at this exploratory stage of the project, I felt that avoiding the possible influences of menstrual cycle was more prudent. Also, previous HZE radiation studies mostly used male rodents, allowing more direct comparisons with my studies.

X-rays or a 40 mm tungsten shield for HZE that protected the anterior portion of the rats' muzzle and the posterior portion of the body from the pinnae backwards. Body doses of the cranial dose were 1-3% for X-rays and < 0.8% for HZE. Rats were given a single dose of irradiation using either X-rays or ^{56}Fe particles. For X-ray exposure, the animals were given whole brain irradiation of 10 or 13 Gy of 200 kVp X-rays at a dose rate of 3 Gy/min at EVMS. Iron-56 particle radiation (1 GeV/n, LET = 150 keV/μm) was generated using the Alternating Gradient Synchrotron (AGS) in Brookhaven National Laboratory (BNL) of NASA Space Radiation Laboratory (NSRL). The animals were given a single dose (0.6, 1.4 or 2.0 Gy) of whole brain irradiation at a dose rate of 0.5 Gy/min. After a week of recovery time, the rats were transported to EVMS.

The animals were housed either singularly or in pairs in standard cages in a group housing environment, maintained on a 12-h light/dark cycle with lights on from 7:00 AM to 7:00 PM. Ambient temperature was maintained at 24.5 ± 0.5°C. The rats were given *ad libitum* access to autoclaved rat chow and water. Their weight was monitored on a weekly basis. No specificity of weight loss was observed in any of dose groups.

Three or six months after irradiation, animals were sacrificed under anesthesia of 15% halothane in mineral oil, and brain regions of interest were dissected. These time points were selected to investigate late-developing radiation effects on the CNS (*46*). One half of the brain tissue was immediately used for making slice or synaptosomal preparations for release assay. The other half was kept as dry tissues at -80°C until use for western blotting and lipid peroxidation experiments.

The present project was conducted in accordance with the National Institutes of Health guidelines for the care and use of animals in research, and was approved by the

Institutional Animal Care and Use Committee of EVMS and by those of BNL. Animal facilities at EVMS are accredited by the Association for Assessment and Accreditation of Laboratory Animal Care, International.

Slice and Synaptosomal Preparation

After anesthesia with 15% halothane in mineral oil and decapitation, brains were rapidly removed and placed into ice-cold phosphate buffered saline (PBS), pH 7.4. The associative cortex, the hippocampus, and the striatum were dissected using visual landmarks.

For slice preparation, brain tissues were cut into minces to increase surface area for radioactive-tagged neurotransmitter uptake and oxygen/glucose supply.

Synaptosomal preparation was made as previously described (*88*). Briefly, brain tissues were homogenized at 900 rpm with a motor-driven homogenizer in ice-cold iso-osmotic solution containing 0.32 M sucrose, 100 μM EDTA, and 5 mM HEPES, pH 7.4. Debris and nuclei were pelleted by differential centrifugation at 900 x *g* at 4°C for 10 min, and supernatant containing synaptosomes was pelleted at 11,500 x *g* at 4°C for 20 min. Final pellets were resuspended in ice-cold aerated (95% O_2, 5% CO_2) Krebs-bicarbonate-HEPES buffer (KBH) composed of the following (in mM): NaCl, 118; KCl, 3.5; $CaCl_2$, 1.25; $MgSO_4$, 1.2; KH_2PO_4, 1.2; $NaCO_3$, 25; HEPES-NaOH, 5, (pH 7.4); D-glucose, 11.5, and allowed to equilibrate for at least 30 min on ice. For catecholamine release measurement, ascorbic acid, 0.6 mM; EDTA (ethylene-diamine-tetra-acetic acid), 0.1 mM; and pargyline, 0.01 mM was added to KBH buffer to reduce chemical oxidization, free radical formation, and monoamine oxidase (MAO) mediated rapid catecholamine metabolism.

Measurement of Radioactive-tagged Neurotransmitter Release from Slices

Neurotransmitter release was measured as described previously (*88*). To label endogenous neurotransmitter pool, hippocampal slices were incubated for 30 min with 173 nM [^{3}H]-norepinephrine (NE) (l-[7, 8-^{3}H] norepinephrine, 35.0 Ci/mmol specific activity, Amersham Biosciences). Frontal associative cortex and striatal slices were incubated with 110 nM [^{3}H]-dopamine (DA) (3, 4-[ring-2, 5, 6-3H]-dihydroxyphenylethylamine hydrochloride, 55 Ci/mmol specific activity, PerkinElmer) for 30 min at 35°C in freshly bubbled KBH buffer with pargyline addition. Next, slices were transferred to a superfusion chamber (0.1 ml chamber volume) containing a glass fiber filter (GF/B) and superfused continuously with bubbled KBH (warmed to 35°C, 0.2 ml/min superfusion rate) for 40 min to remove un-incorporated radioactivity. Three 3-min fractions of the superfusate were collected to determine basal level of efflux, then, evoked release was triggered by rapid switching of superfusion lines from normal KBH to a KBH containing 50 mM KCl, for 1.5 min to induce neuronal depolarization. In the depolarizing buffer the NaCl concentration was reduced from 118 mM to 72.7 mM in order to maintain iso-osmolarity. The total of nine superfusate fractions was collected continuously throughout the experiment.

Measurement of Radioactive-tagged Neurotransmitter Release from Synaptosomes

To label endogenous neurotransmitter pools, synaptosomes were incubated with 173 nM [^{3}H]-NE (l-[7, 8-^{3}H] norepinephrine, 35.0 Ci/mmol specific activity, Amersham Biosciences) for 5 min at 35°C in freshly bubbled KBH. To simultaneously measure both glutamate and GABA release, 115 nM [^{3}H]-glutamate (L-[3, 4-^{3}H]-glutamic acid, 52.0 Ci/mmol specific activity, PerkinElmer, Boston, MA) and 73 nM [^{14}C]-GABA (4-

aminobutyric acid-carboxy-^{14}C, 8.3 Ci/mmol specific activity, SIGMA) were added to synaptosomes for 5 min at 35°C in freshly bubbled KBH. Labeled synaptosomes were transferred to a superfusion chamber (0.1 ml chamber volume) containing a glass fiber filter (GF/B) covered with 50 µl of 50% Sephadex slurry, and superfused with continuously bubbled KBH (warmed to 35°C, 0.8 ml/min superfusion rate) for 12 min to remove un-incorporated radioactivity. Three 1-min fractions of the superfusate were collected to determine basal neurotransmitter efflux (basal release). Release was induced by rapid switching of superfusion lines from normal KBH to a KBH containing 0.5 M sucrose for 30 sec to produce a temporary hyperosmotic shock. The total of nine superfusate fractions was collected continuously throughout the experiment.

Determining Radioactivity and Calculating Neurotransmitter Release

Tritium and/or ^{14}C contents of individual fractions and activity remaining in the superfusion chamber was counted at the end of the experiment by liquid scintillation spectrometer (LS 3801, Beckman Instruments, Inc., Fullerton, CA), which was calibrated and validated in the range of expected radioactivity efflux values. ^{14}C and ^{3}H decay emit different energy spectra (18.3 keV, 156 keV, respectively), allowing separate detection. Release was expressed as the fractional release rate, calculated as the fraction of radioactivity released at any given time divided by the amount remaining in sample preparation at that particular time point. Total evoked release was calculated from the area under the peak.

Statistics

Effects of radiation dose and time course between 3 and 6 month points were analyzed by Kruskal-Wallis one-way ANOVA on ranks followed by Dunn's method for

pair-wise comparisons (SigmaStat 2.03). Treatment effects in comparison with controls were evaluated with Student's *t*-test or non-parametric Mann-Whitney Rank Sum test (SigmaStat 2.03) when normality tests failed. Significance was considered at $P < 0.05$.

RESULTS

Point six Gy of ^{56}Fe (1 GeV/n) radiation produced a significant inhibitory effect on [^{3}H]-glutamate efflux from the hippocampal synaptosomes

Iron-56 induced CNS effects have several characteristics in common, e.g. either an extremely steep dose-response curve or the lack of a dose-response relationship depending on the measured endpoint (*61*). To evaluate ^{56}Fe radiation dose effect on the hippocampal nerve terminal, I have tested three doses; 0.6, 1.4, and 2.0 Gy.

Dose-response analysis on 0.5 M sucrose-evoked [^{3}H]-glutamate efflux revealed that 0.6 Gy of ^{56}Fe radiation (1 GeV/n) produced the most significant inhibitory effect (14.9 ± 3.61% of control, $P \approx 0.02$, Kruskal-Wallis one-way ANOVA followed by Dunn's pairwise comparison) three months after exposure (filled circle) (Fig. 11), while 1.4 Gy radiation did not significantly alter evoked release (9.6 ± 7.06% of normal). These results suggest that the threshold for this biochemical endpoint may be equal or lower than 0.6 Gy three months post irradiation.

Furthermore, six months after exposure (open circle), the inhibitory effect induced by 0.6 Gy persisted (25.0 ± 5.23% of normal, $P = 0.002$, Kruskal-Wallis one-way ANOVA followed by Dunn's pairwise comparison), while the effects of ≥ 1.4 Gy of ^{56}Fe radiation were non-significant. Based on these findings, I choose to use a single dose of 0.6 Gy to further investigate biochemical effects of ^{56}Fe radiation on hippocampal neurotransmission.

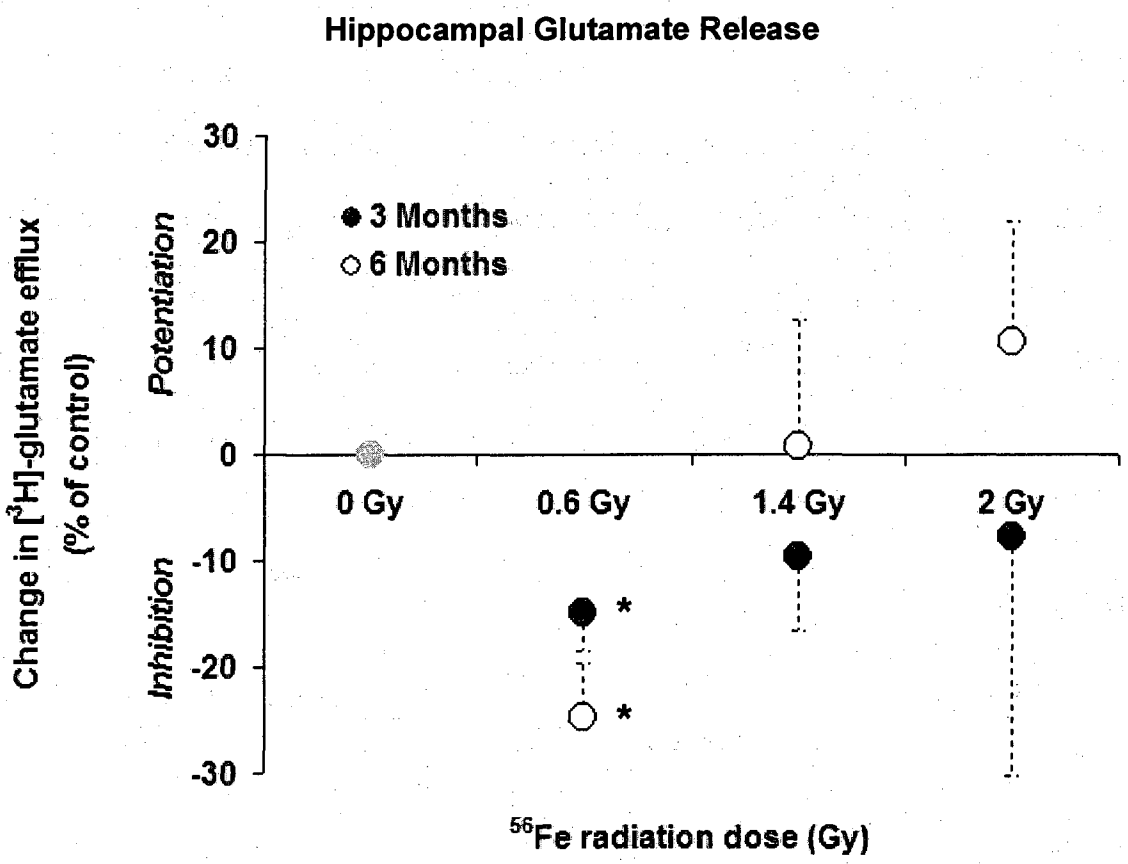

FIG. 11. Dose effects of ^{56}Fe radiation (1 GeV/n) on hyperosmotic sucrose evoked [^{3}H]-glutamate efflux from hippocampal synaptosomes at three (filled circle) and six (open circle) months post irradiation. * indicates significant differences from controls ($P < 0.05$), analyzed with Kruskal-Wallis one-way ANOVA followed by Dunn's pairwise comparison.

Figure 12A shows representative experiment on effects of 0.6 Gy of ^{56}Fe radiation on [^{3}H]–glutamate release from hippocampal synaptosomes. While basal release, observed the first 4 minute time window, was not significantly affected (95.6 ± 2.08% of control, Figs. 12B, C), hyperosmotic sucrose evoked [^{3}H]-glutamate efflux from hippocampal synaptosomes observed 5 and 6 minute time window was significantly reduced (85.2 ± 3.61% of control, $P = 0.01$, Mann-Whitney Rank Sum Test, Figs. 12B, C).

Effects of 0.6 Gy of ^{56}Fe radiation (1 GeV/n) were more pronounced on hippocampal than associative cortical synaptosomes.

Glutamate is the principal excitatory neurotransmitter in the brain, and is abundant in the hippocampus as well as in the cortex (*70, 96*). To determine if the same dose of ^{56}Fe particles exerts inhibitory effect on glutamatergic nerve terminals of different brain regions, I have evaluated [^{3}H]-glutamate release from the associative cortex. Associative cortex is functionally distinct cortical area, located in the anterior part of the cortex, which includes prefrontal cortex (PFC). The basic function of the brain area is to orchestrate goal oriented behavior. Associative cortical glutamatergic system is vulnerable to aging, and aging induced reduction of glutamate content in the area was documented (*64*).

My results showed that 0.6 Gy of ^{56}Fe radiation did not disturb [^{3}H]-glutamate release in associative cortical nerve terminals when tested three months after exposure (Fig. 13). Normalized basal and 0.5 M sucrose evoked release were 93.8 ± 4.27% and

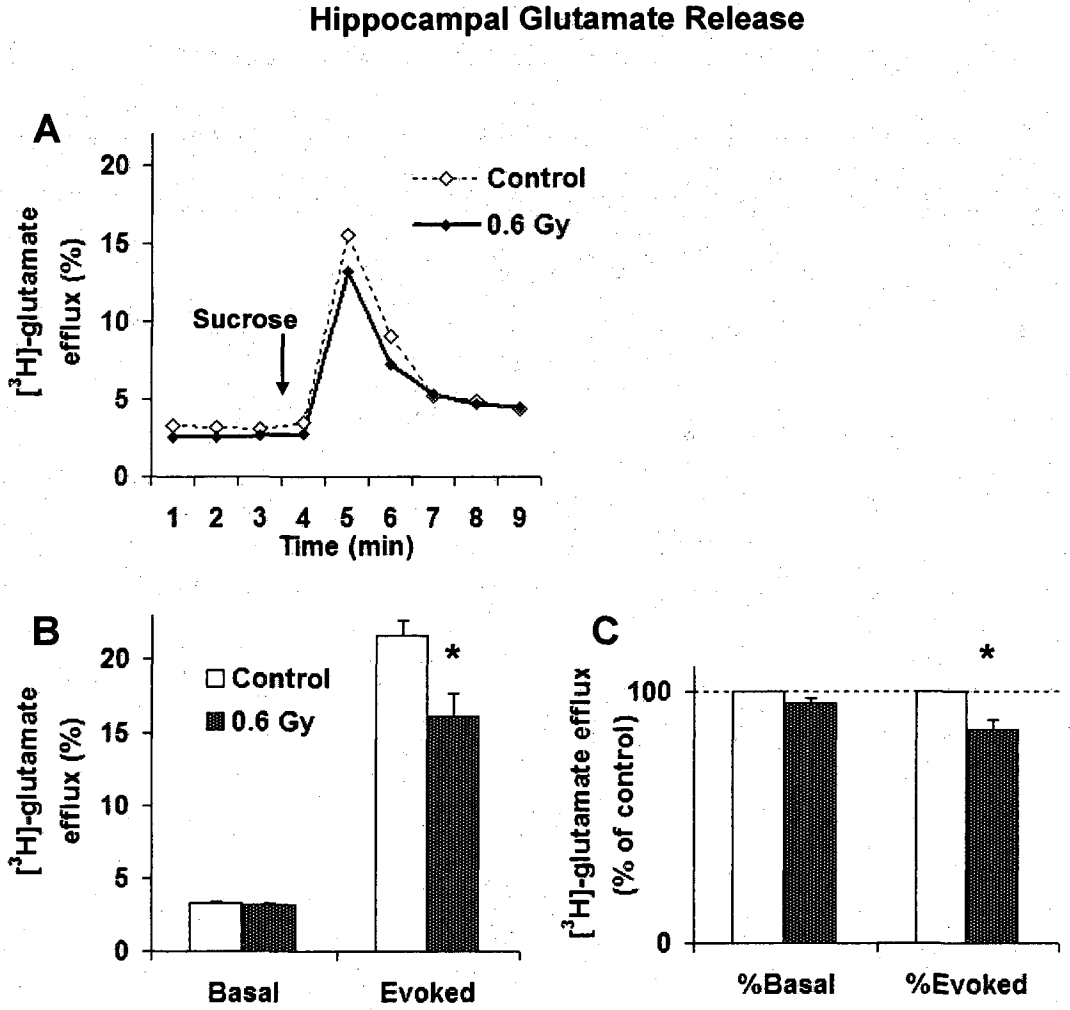

FIG. 12. Effects of 0.6 Gy of ^{56}Fe radiation (1 GeV/n) on [^{3}H]-glutamate release from rat hippocampal synaptosomes three months post irradiation. (A) Representative experiment. Glutamate release was evoked from superfused synaptosomes by 30 sec pulses of hypertonic sucrose (arrow). (B) Summary graph of experiments indicating the fractional release of [^{3}H]-glutamate basal and hypertonic sucrose evoked release calculated as the area under the peak. (C) Fractional release values under normal conditions were set to 100% and treatment effects were normalized to control. Graphs show means ± SEM (n = 8, each). *: $P < 0.05$.

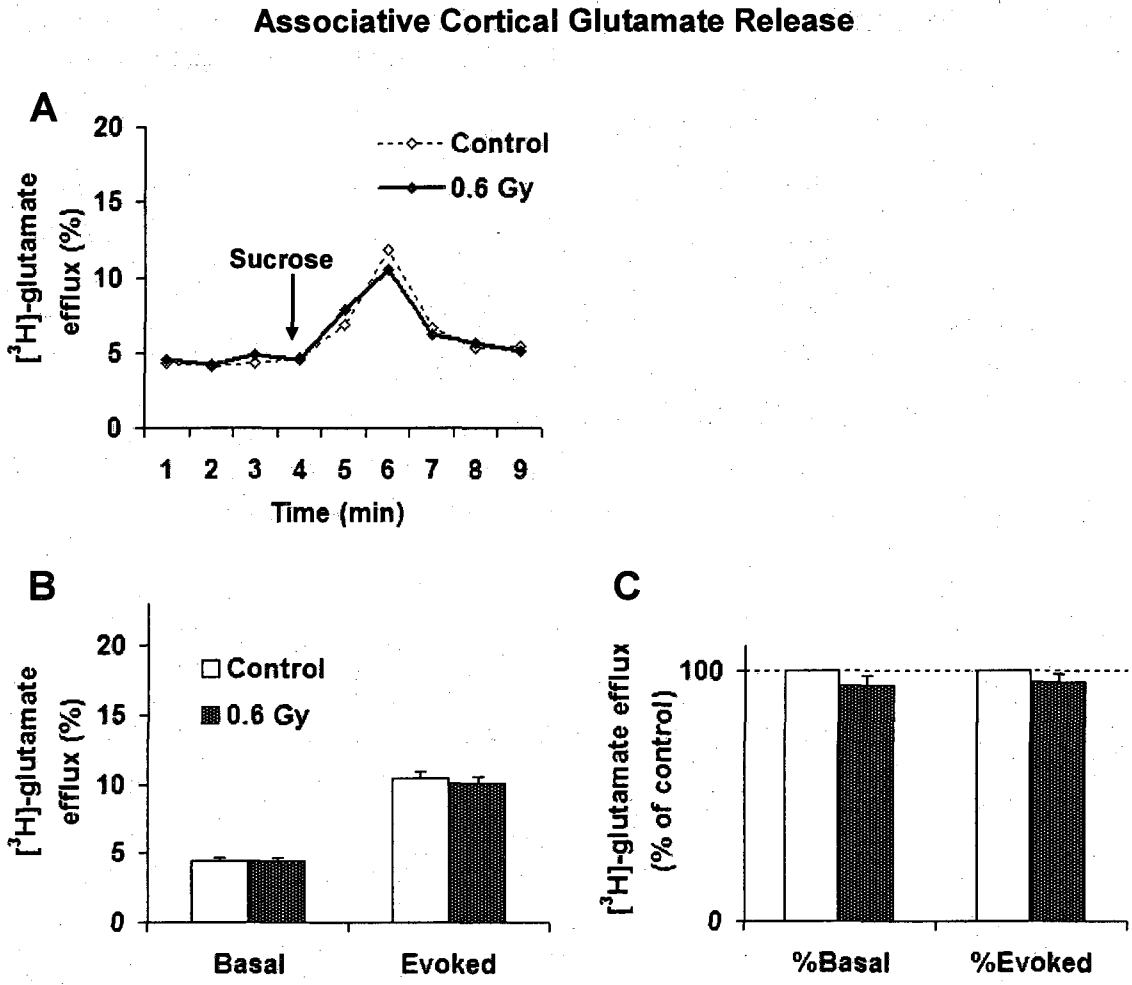

FIG. 13. Effects of 0.6 Gy of ^{56}Fe radiation (1 GeV/n) on [^{3}H]-glutamate release from associative cortical synaptosomes three months post irradiation. (A) Representative experiment. Glutamate release was evoked in superfused synaptosomes by 30 sec pulses of hypertonic sucrose (arrow). (B) Summary graph of experiments indicating the fractional release of [^{3}H]-glutamate basal and hypertonic sucrose evoked release calculated as the area under the peak. (C) Fractional release values under normal conditions were set to 100% and treatment effects were normalized to control. Graphs show means ± SEM (n = 3, each).

95.5 ± 3.05%, respectively. The results suggest that hippocampal glutamatergic nerve terminals are more sensitive to 0.6 Gy of ^{56}Fe particle radiation.

Point six Gy of ^{56}Fe radiation (1 GeV/n) produced a significant inhibitory effect on hippocampal GABA release

My next question was whether the inhibitory effect of 0.6 Gy of ^{56}Fe radiation was selective for glutamatergic nerve terminals. To address this question, I labeled hippocampal synaptosomes with [^{14}C]-GABA as well as [^{3}H]-glutamate to compare both release in the same preparation. [^{14}C]-GABA is incorporated through nerve terminal and synaptic vesicle transporters, while [^{3}H]-glutamate is incorporated by a different set of nerve terminal transporters (GLT-1 and EAAC1) and synaptic vesicle transporter (VGlut). Release was triggered by a pulse of hypertonic sucrose, and ^{14}C and ^{3}H contents were simultaneously collected, as described earlier.

Evoked [^{14}C]-GABA efflux highly correlated with that of [^{3}H]-glutamate (Fig. 14, $R^2 = 0.893$). 0.6 Gy of ^{56}Fe radiation reduced evoked [^{14}C]-GABA release significantly (82.5 ± 6.06% of control, $P \leq 0.001$, Mann-Whitney Rank Sum Test), while basal evoke was not altered (97.6 ± 2.62%, n.s., Fig. 15). These data indicate that inhibitory effect of 0.6 Gy of ^{56}Fe radiation on hippocampal nerve terminals was not selective to the glutamatergic system, and that the same cellular defects may underlie the functional impairments in both glutamatergic and GABAergic functions.

Effects of 0.6 Gy of ^{56}Fe radiation were not significant on hippocampal noradrenergic system

I have also tested the effects of 0.6 Gy of ^{56}Fe particles on noradrenergic terminals in the hippocampus. Although a trend of decrease was observed in the size of

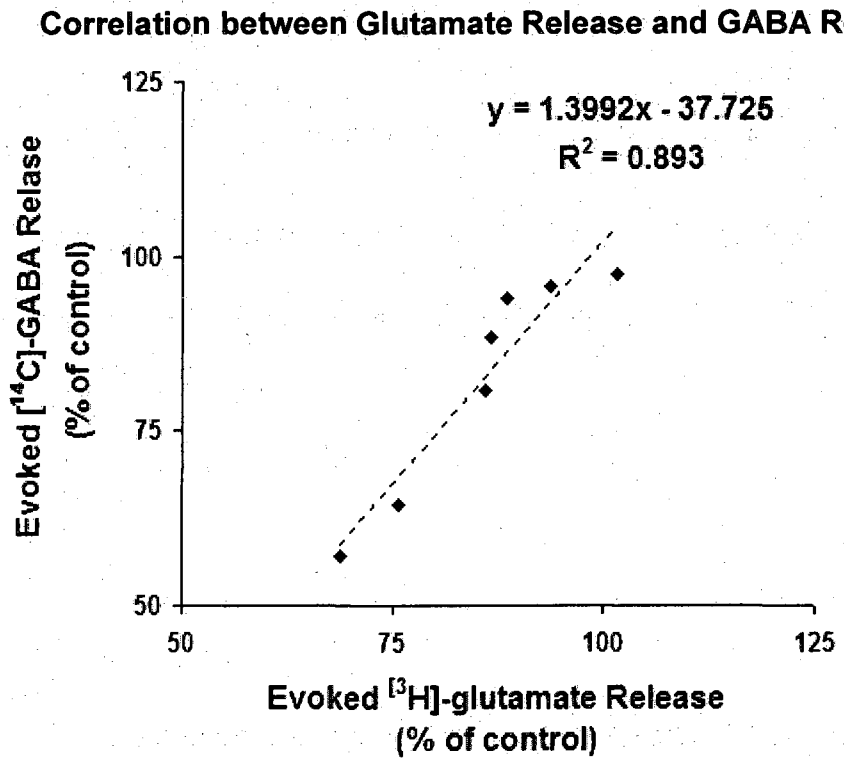

FIG. 14. Correlation between evoked [^{3}H]-glutamate release and [^{14}C]-GABA release. Hippocampal synaptosomal preparation was double labeled with [^{3}H]-glutamate and [^{14}C]-GABA. High correlation (R^2 = 0.893) indicates effects of 0.6 Gy of ^{56}Fe radiation (1 GeV/n) was not selective for neurotransmitter types.

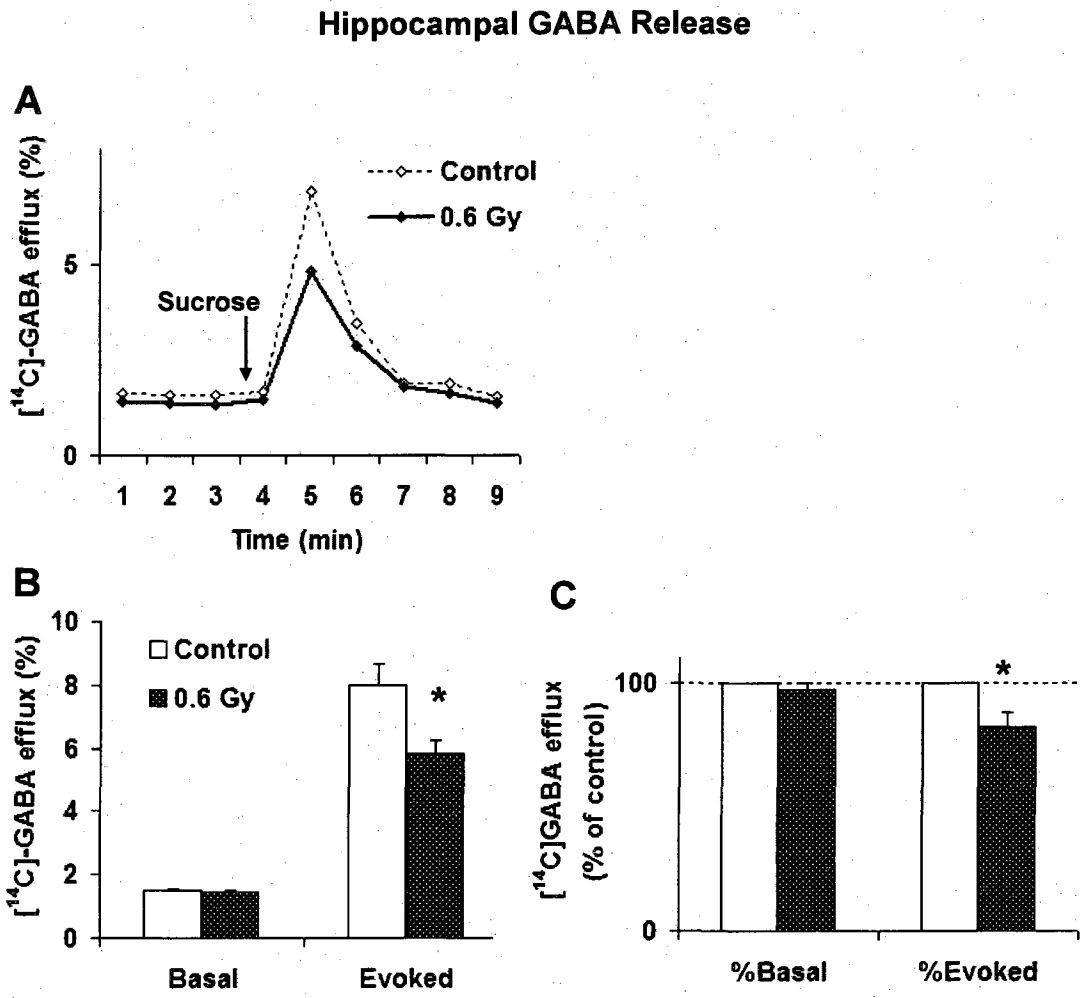

FIG. 15. Effects of 0.6 Gy of ^{56}Fe radiation (1 GeV/n) on [^{14}C]-GABA release from rat hippocampal synaptosomes three months post irradiation. (A) Representative experiment. GABA release was evoked in superfused synaptosomes by 30 sec pulses of hypertonic sucrose (arrow). (B) Summary graph of experiments indicating the fractional release of [^{14}C]-GABA basal and hypertonic sucrose evoked release calculated as the area under the peak. (C) Fractional release values under normal conditions were set to 100% and treatment effects were normalized to control. Graphs show means ± SEM (n = 8 of control, n = 7 of irradiated). *: $P < 0.05$

evoked release, it was not statistically significant (91.5 ± 5.20% of control, $P = 0.343$, Fig. 16). Basal release was spared (107.7 ± 10.65% of control).

The inhibitory effects of 0.6 Gy of ^{56}Fe radiation on [^{3}H]-glutamate and [^{14}C]-GABA release persisted at 6 month post irradiation

To test the temporal changes in HZE induced neurotransmitter release, I have evaluated the effects of 0.6 Gy of ^{56}Fe radiation six months after irradiation (Fig. 17). The results revealed that the effects were persistent on both glutamatergic (evoked release; 75.2 ± 5.23% of control, $P < 0.05$) and GABAergic release (75.8 ± 3.65 of control, $P < 0.005$) compared to control. There was a statistically significant difference in time course effect (glutamatergic, $P = 0.002$; GABAergic, $P \leq 0.001$, Kruskal-Wallis one-way ANOVA), indicating a possible progressive effect, although measures taken at 3 months and 6 months were not statistically different. Basal levels of both systems were not changed: glutamatergic, 103.8 ± 2.33%; GABAergic, 99.6 ± 6.00%. There was no effect observed in either basal or evoked release from noradrenergic nerve terminals.

DISCUSSION

I found that 0.6 Gy of ^{56}Fe radiation (1 GeV/n) led to significant reduction in hypertonic sucrose evoked release, a measure of the readily releasable pool (RRP), of two major neurotransmitters, glutamate and GABA, at three months after exposure. Moreover, these effects were persistent until six months post radiation.

While further studies with lower doses need to be carried out, 0.6 Gy may be a threshold dose for inducing impairments in hippocampal glutamatergic and GABAergic

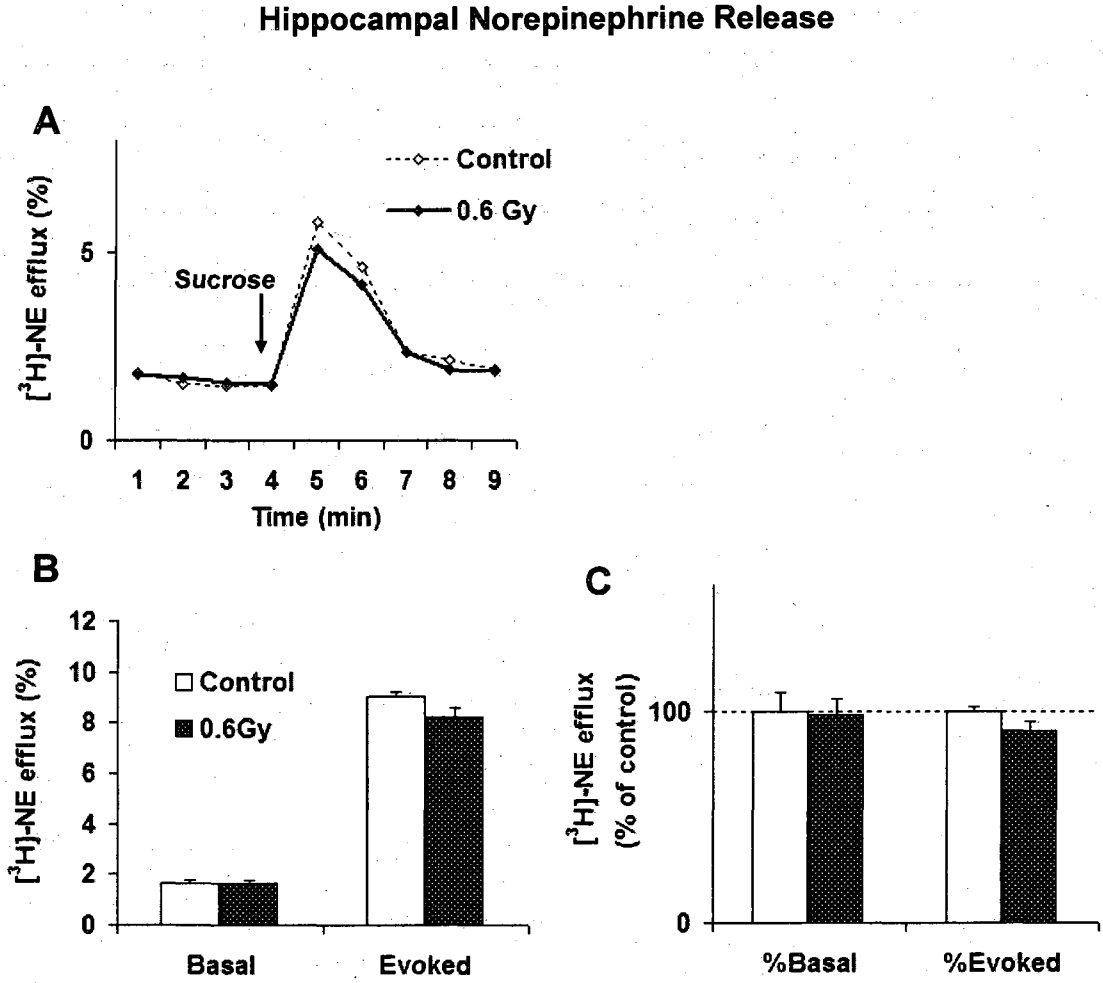

FIG. 16. Effects of 0.6 Gy of ^{56}Fe radiation (1 GeV/n) on [^{3}H]-norepinephrine (NE) release from rat hippocampal synaptosomes three months post irradiation. (A) Representative experiment. NE release was evoked in superfused synaptosomes by 30 sec pulses of hypertonic sucrose (arrow). (B) Summary graph of experiments indicating the fractional release of [^{3}H]-NE basal and hypertonic sucrose evoked release calculated as the area under the peak. (C) Fractional release values under normal conditions were set to 100% and treatment effects were normalized to control. Graphs show means ± SEM (n = 8, each).

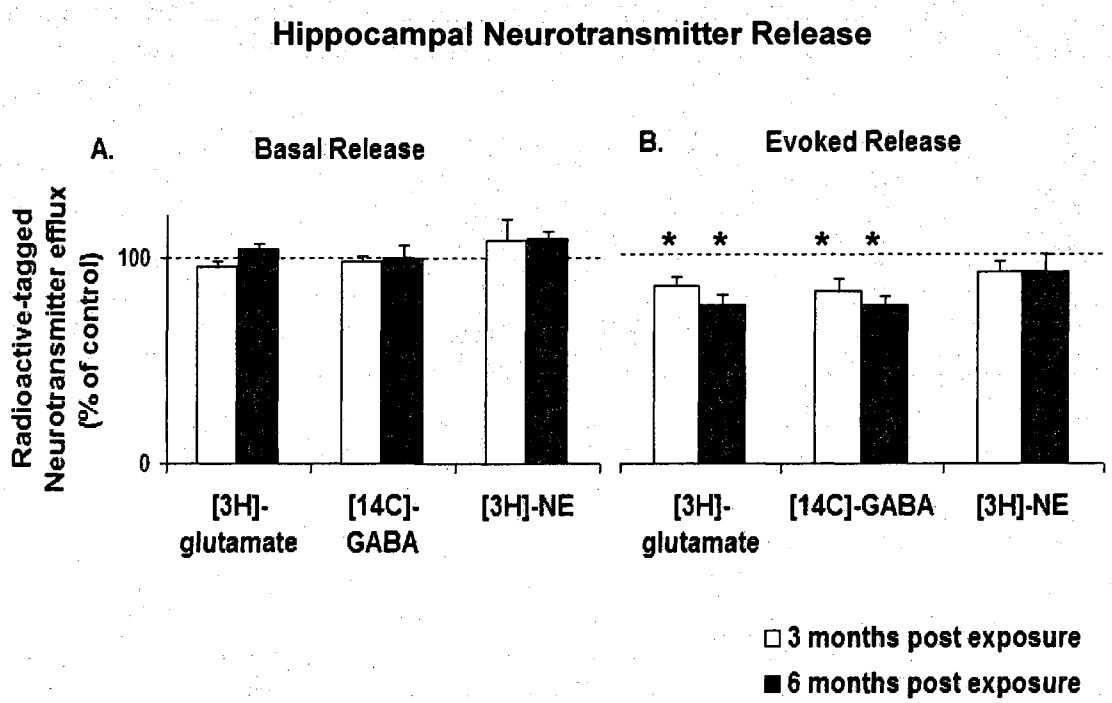

FIG. 17. Three and six months post irradiation effects of 0.6 Gy of ^{56}Fe radiation (1 GeV/n) on basal (A) and evoked release (B) from hippocampal synaptosomes. Graphs show means ± SEM (*; $P < 0.05$ compared to control, analyzed by Kruskal-Wallis one-way ANOVA followed by Dunn's pairwise comparison, $n = 5\sim8$).

neurotransmission. It is of note that the lowest dose we tested induced the largest deficits in hippocampal neurotransmission. This finding is in line with dose response studies for the induction of ROS by ^{56}Fe radiation (*26*). Limoli and co-authors found that in a range of low dose (0.25 ~ 1 Gy) of ^{56}Fe particles, ROS production was linear until a peak was reached at 1 Gy. After that point, ROS production started to decline. Rabin and co-workers also documented that the dose-response curve of ^{56}Fe particle induced changes in neurochemical function are extremely steep (*61*). They observed a significant reduction in K^+-depolarization evoked striatal DA release by doses 0.1 to 0.5 Gy, but there was no effect when dose was increased to 5 Gy. Thus, my results are consistent with the characteristics of ^{56}Fe irradiation reported by others.

In contrast to glutamatergic and GABAergic impairments, release from the noradrenergic nerve terminals was not significantly changed by the same regimen of irradiation. It is noteworthy that 2.0 Gy of ^{56}Fe particle could induce significant reduction in depolarization evoked [^{3}H]-norepinephrine release from slices of rat hippocampus (Chapter I, Preliminary Results), suggesting that threshold dose to cause perturbation in hippocampal noradrenergic neurotransmission may be higher than 0.6 Gy. Alternatively, it is possible that other elements of neurons, not terminals, which are preserved in slices, but not in synaptosomes, may be direct targets of radiation.

Glutamate and GABA are the two major neurotransmitters in the hippocampus and are involved in cognitive functions. The hippocampus is vulnerable to aging, and numerous studies suggest that disintegrating glutamatergic neurotransmission is a factor in aging (*64, 97, 98*). It is noteworthy that radiation accelerates aging, and the similarity of aged rats and ^{56}Fe irradiated rats in measures of nigrostriatal system dependent

functions (*5*) and in hippocampal dependent spatial learning and memory (*9*) have been noted.

My results also indicate that the effect of 0.6 Gy of ^{56}Fe radiation is region specific; glutamatergic chemical transmission was disturbed in nerve terminals of the hippocampus, while it was normal in the associative cortex. The nature of this region specificity is difficult to discern at the present level of investigation. One possible explanation may be regional differences in antioxidative activities. Todorović et al. found that after 2.0 Gy of γ-radiation exposure mitochondrial superoxide dismutase (SOD) activity was significantly lower in the hippocampus than in the cortex (*37*). Considering that mitochondrial SOD is induced in response to radiation, and that neurons cannot tolerate the depletion of mitochondrial SOD, their finding, at least partially, may explain the higher radio- vulnerability of the hippocampus.

Despite significant reduction in evoked release in glutamatergic and GABAergic nerve terminals, basal release remained unchanged in both nerve terminals. Basal release reflects spontaneous release, which is independent of action potential depolarization. Studies have shown that spontaneous release may originate from a different vesicle pool from the RRP with different states of releasability (*92*). The exact nature of the molecular diversity between these two vesicle pools remains to be identified, although it has been suggested that isoforms of SNARE proteins involved in basal release are different from those participated in evoked (*92, 93*). My findings of unaltered basal release and significantly altered evoked release, thus, suggest that radiation effects may have spared proteins underlining spontaneous release, and also the basic release machinery.

The question still remains, however, as to the locus of the radiation-induced deficit(s) in perturbation of glutamatergic and GABAergic release. The extent of hypertonic sucrose evoked release probes the size of the RRP, which reflects the rate of recycling of synaptic vesicles during extended stimulation (*99*). Upon depletion of vesicles in RRP, vesicles are replenished from a reserve pool. Reduction in release might reflect radiation induced change in size of the reserve pool, or total size of the recycling pool, which combines both RRP and the reserve pool. To test this, I have investigated effects of ^{56}Fe radiation on the abundance of synaptic vesicles by quantitative analysis of synaptic vesicle marker proteins (Chapter III).

Moreover, significant influence on the size of release originates Ca^{2+} dynamics, which depends on: 1) numbers and types of voltage-gated Ca^{2+}channels.; 2) Ca^{2+} buffering and transient local Ca^{2+} concentration; and 3) Ca^{2+}-binding property of Ca^{2+} sensor (*86, 99*). These factors will influence the size of hyperosmotic sucrose evoked release, even though the stimulus itself does not require influx of Ca^{2+}. Thus, any change that alters composition and tension of the participating membranes of the active zone influences neurotransmitter release, even by simply stretching the membrane (*100*). Considering oxidative effects induced by radiation and increased levels of lipid peroxidation previously documented (*27, 36*), there may be possible alterations in membrane structure and fluidity after 0.6 Gy ^{56}Fe irradiation. Consequence of lipid peroxidation is unregulated membrane potential (*101*), which may imbalance cytoplasmic Ca^{2+} concentration and ultimately affects Ca^{2+} dependent steps of the synaptic vesicle cycle. I have tested the level of lipid peroxidation in the hippocampus, and obtained supportive results (Chapter IV).

CHAPTER III

EFFECTS OF HZE RADIATION ON SELECTED SYNAPTIC PROTEIN LEVELS

BACKGROUND

In the previous chapter I reported significant reduction of hypertonic sucrose evoked release from glutamatergic and GABAergic nerve terminals in the hippocampus, three and six months after exposure to 0.6 Gy of ^{56}Fe radiation. The reduction could be a reflection of radiation induced depletion of synaptic vesicle pools. To address this, I assayed synaptic vesicle marker protein levels in hippocampal synaptosomes after ^{56}Fe irradiation. **Synaptophysin** was used as a general marker of all synaptic vesicle types and **VGlut1** (vesicular glutamatergic transporter 1) was used as a marker of glutamatergic synaptic vesicles.

Neurotransmitter receptor levels are differentially regulated during development (*102*), and in synaptic plasticity processes (*103*). Membrane structure and fluidity (*62*) and radiation (*25*) also affect neurotransmitter receptor levels. Because of the importance of those proteins in glutamatergic, GABAergic and noradrenergic transmission, I determined levels of glutamatergic **AMPA** (α-amino-3-hydroxy-5-methyl-4-isoxazole-propionic acid) and **NMDA** (*N*-methyl *D*-aspartate) receptors (**NR1, NR2A and NR2B**), GABAergic (γ-amino butyric acid) **$GABA_A$** and **$GABA_B$** receptors, and noradrenergic **α1, α2** and **β1** adrenergic receptors after 0.6 Gy of ^{56}Fe radiation exposure.

PSD-95 (postsynaptic density 95 kDa), a scaffold protein which anchors glutamatergic receptors, was also tested to evaluate whether number or size of excitatory postsynaptic contacts were affected.

To probe a possible neuronal regeneration as compensatory response after irradiation, I also have analyzed the level of **MAP2** (microtubule associated protein 2), which is involved in the stabilization and extension of dendrites (*104*).

Each protein is discussed in the following sections.

Synaptophysin

Synaptophysin is a synaptic vesicle associated protein that constitutes about 7% of the total vesicle proteins (*105*). Due to its ubiquity at all types of synaptic vesicles, it has been widely used as a general marker for nerve terminals (*106, 107*). Synaptophysin interacts with an essential SNARE protein (soluble N-ethylmaleimide-sensitive factor attachment protein receptor), synaptobrevin (also referred to as VAMP, vesicle associated membrane protein). Exact function of the synaptophysin-synaptobrevin complex is largely unknown, however it is speculated that synaptophysin may temporally restrict availability of synaptobrevin by binding to it (*106*).

Since synaptophysin levels positively correlate with the number of synaptic vesicles (*68*), I have used this protein as a general marker of total synaptic vesicle pool in nerve terminals.

VGlut1

VGlut1 is a transporter of glutamate into synaptic vesicles. VGlut1 is driven by an ATP dependent electrochemical proton gradient. Since VGlut is exclusive to vesicles containing glutamate, and undetectable in other neuron types or neuronal components

(*77*), it has been used as a marker for glutamatergic synaptic vesicles and nerve terminals. Two isoforms, VGlut1 and VGlut2, are identified in glutamatergic synapses. Both mRNA (*75*) and protein (*108*) levels of VGlut1 are predominant in hippocampus, thus, VGlut1 is more extensively used for hippocampal studies (*108*).

A recent study showed diminished VGlut1 expression in the hippocampus and prefrontal cortex of schizophrenic patients, suggesting usefulness of this marker in pathological studies (*75*). Glutamate is a ubiquitous amino acid in neural tissue and participates in a variety of intermediary metabolisms. For example, glutamate functions in the detoxification of ammonia, is a building block in the synthesis of proteins and peptides including glutathione, and is a precursor in GABA synthesis. Only 20 to 30% of neural glutamate content functions as an excitatory neurotransmitter.

To evaluate ^{56}Fe radiation effects on glutamate as a neurotransmitter, I assayed VGlut1 levels, as a measure of total glutamatergic synaptic vesicle pool.

Glutamatergic receptors

A recent study showed that rats subjected to a clinically relevant regimen of radiation induced significant reduction in performance of hippocampus dependent learning tasks, and also that the same regimen altered NMDA receptor levels in the hippocampus, indicating a role of NMDA receptors in radiation induced cognitive impairments (*25*). The importance of glutamatergic NMDA receptors in LTP (*40*) and LTD (*73*) has been well documented, providing a strong link between the glutamatergic systems and the mechanisms of learning and memory (*40, 74*). These results prompted us to evaluate NMDA receptor levels after ^{56}Fe irradiation.

The NMDA receptor functions as a glutamate gated ion channels that is highly permeable to Na^+ and Ca^{2+}. Mg^{2+} blocks this NMDA channels in a voltage-dependent manner, thus, rendering NMDA receptors voltage sensitive. NMDA receptors are heterometric complexes consisting of obligatory NR1 and various NR2 subunits. The NR1 subunit serves as a key subunit essential for ion selectivity of the NMDA channels, whereas the NR2 subunit mainly participates in channel gating by voltage and Mg^{2+}. Liu and co-authors reported that distinct NMDA subunits were critical factors to determine the direction of synaptic plasticity (*73*). They found that the activation of NR2A-containing NMDA receptors led to LTP formation, while the activation of NR2B-containing NMDA receptor produced LTD (*73*). Although this is still under debate, e.g. other group demonstrated NR2B's involvement in LTP (*109*), general consensus is that the combinations of NR1 with different NR2 subunits give rise to functional diversity.

To probe the effects of HZE radiation on these functionally different subunits, I have used antibodies against NR1, NR2A and NR2B subunits.

In addition, I have extended our investigation to AMPA receptors, another type of glutamatergic ionotropic receptors, which possess mostly Na^+-permeable channels. Excessive release of glutamate may cause overload of cellular Na^+ and Ca^{2+} through these glutamatergic ionotropic receptors, leading to excitotoxic cell death. Such scenario may play a role in cerebral ischemia and traumatic brain injury, and also, in chronic neurodegenerative disorders, such as amyotrophic lateral sclerosis (ALS) (*110*), Parkinson's disease (*111*) and Alzheimer's disease (*112*).

AMPA receptors respond faster to glutamate than NMDA receptors and mediate the bulk of rapid excitatory synaptic current induced by glutamate (*113*). Previous results

showed that LTP requires insertion of new AMPA receptors to the synapse by a mechanism that involves the association between GluR1 AMPA subunit and a PDZ domain protein, such as PSD-95 (discussed below) (*114*).

To probe the effects of HZE radiation on levels of AMPA receptors, I have used antibody against GluR1 subunit.

GABAergic receptors

GABA is the major inhibitory neurotransmitter in the adult hippocampus and can hyperpolarize postsynaptic membrane by influx of Cl^- through $GABA_A$ receptors. Metabotropic $GABA_B$ receptors are coupled to cAMP, K^+ channel or Ca^{2+} channel regulation. Behavioral studies have suggested that $GABA_B$ receptor blockade can improve cognition (*41*).

To probe the effects of HZE radiation on levels of GABA receptors, I have used antibody against $GABA_A$ and $GABA_B$ subunits.

Noradrenergic receptors

NE is a neuromodulator and plays a prominent role in learning tasks (*44*). It transmits the effects through three subtypes of receptors; i.e. Gq-coupled α1-, Gi-coupled α2-, and Gs-coupled β1-adrenergic receptors. NE activates cAMP-dependent PKA and calmodulin-dependent protein kinase (CaMKII) via β1 adrenergic receptors, and stimulation of β1 adrenergic receptors leads to profound effects on the induction of LTP in multiple hippocampal pathways (*42, 43, 115*). NE also modulates LTP through α1 adrenergic receptors (*43, 81, 82*), and reduces LTP through Gi-coupled α2 adrenergic receptors (*116*). Since NE is released during emotional arousal, its involvement in emotional influence on learning and memory has been suggested. Supporting this notion,

recent study showed that NE-driven phosphrylation of GluR1 subunit of AMPA receptors facilitates synaptic delivery of AMPA receptors in LTP expression (*117*).

To test for possible radiation effects on noradrenergic signal transmission, I have used antibodies against α1-, α2- and β1-adrenergic receptors in this study.

PSD-95

The postsynaptic compartment of excitatory synapses is characterized by an electron-dense region, referred to as the postsynaptic density (PSD) (indicated by small arrows in Figure 9) that consists of adhesion molecules, neurotransmitter receptors, and high density of scaffolding proteins. PSD-95 (PSD-95 kDa) is a major scaffold protein enriched at glutamatergic postsynaptic membranes. By homomultimerizing through N-terminus, PSD-95 molecules form a scaffold. PSD-95 contains three PDZ domains (a domain commonly discovered in PSD-95/Dlg/ZO1 proteins), which anchor various proteins such as adhesion molecules, e.g. neuroligin-1, glutamatergic NMDA receptors, and through an adapter protein, stagazin, glutamatergic AMPA receptors. PSD-95 controls subcellular localization of glutamatergic receptors by facilitating alignment of postsynaptic receptors with the presynaptic active zone.

The reduced glutamatergic release we observed (Chapter II) may produce a coordinated reduction in the levels of PSD-95. To test this possibility, I have determined PSD-95 levels by immunoblotting.

MAP2

Microtubules are major structural components of the neuronal cytoskeleton in axons and dendrites. MAPs (microtubule-associated protein) are a family of proteins involved in neuromorphogenesis, among which MAP2 is the best characterized. In

mature neurons MAP2 is compartmentalized within dendrites of neurons (*118*) and largely excluded from axons (*119*). It forms microtubule bundles with straight and rigid appearance (*120*). MAP2 also plays an important role in the extension of the dendritic cytoskeleton and in dendritic stability by forming cross-bridge between microtubules and other cytoskeletal elements (*104*). Multiple lines of evidence also indicate that MAP2 levels correlate with neuronal response to oxidative stress (*121, 122*). Treatments with H_2O_2 led to a remarkable reduction in MAP2 levels, while antioxidant treatments up-regulated MAP2 levels.

The MAP2 family consists of three isoforms, MAP2a, 2b and 2c. Each has 3 to 4 microtubule-binding repeats near the C-terminus (*123*) and an N-terminal projection domain of varying size, which has a net negative charge and exerts a long-range repulsive force (*124*) that regulates microtubule spacing (*118*). MAP2a and 2b are large proteins with longer projection domains (Mw 280 kDa), while MAP2c, which is often highly expressed during early development, is smaller (Mw 70 kDa). Different MAP2 isoforms may have distinct capacities in stabilizing the cytoskeleton. And MAP2c may have the highest capacity to interact with both microtubules and F-actin (*125*). It induces neurite initiation by reorganizing a primary actin-rich structure into a secondary microtubule-rich structure (*122*).

MAP2c may have at least two phosphorylated sites, and is a substrate for a number of protein kinases (*126*). It has been suggested that MAP2 phosphorylation state may modify microtubule stability, and thus, regulate neuronal development (*126, 127*). Previous studies found that highly phosphorylated MAP2c showed a lower affinity for

microtubule, resulting in decreases in microtubule bundling (*126*), although precise functions of individual phosphorylation sites are not known.

I measured MAP2c levels as an index of dendritic neuronal response to radiation induced oxidative stress.

MATERIALS AND METHODS

Sample Preparation for Western Blotting

Samples were prepared from hippocampal tissues as described earlier (Chapter II, Materials and Methods, *Sample Preparation*). After thawing frozen samples on ice, tissues from 4 to 6 animals were pooled. This was necessary for obtaining reliable signals in the dynamic range of detection from low density synaptic proteins. Pooled tissues were homogenized in isotonic sucrose containing 0.32 M sucrose, 100 μM EDTA, and 5 mM HEPES, pH 7.4, and synaptosomes were prepared. Total protein concentration in S1 fractions was determined using the Coomassie Plus better Bradford assay kit (Pierce) according to manufacturer's instructions.

Simultaneous Detection of Two Proteins on Western Blots using Two Near-Infrared (IR) Fluorophores

Synaptosomes were suspended in SDS-PAGE sample buffer with 8 M urea and 2% mercaptoethanol, and incubated at 60°C for 20 min to accelerate protein denaturing. Proteins were separated on 3% polyacrylamide stacking and 7.5% running gels for 20 min at 80 V followed by 40 min at 150 V, then transfer to nitrocellulose membrane (Whatman, Dassel, Germany) for 1 h at 1.5 A in a high intensity field kept at room temperature by a cooling coil (Bio-Rad, Hercules, CA). Membranes were blocked in

buffer containing 5% nonfat milk and 5% porcine serum in TBST (Tris-buffered saline Tween-20) containing Tris 20 mM, NaCl 134 mM, pH 7.6 with 0.1% v/v Tween-20 for 30 min at room temperature, and then incubated with primary antibodies overnight at 4°C.

I utilized Odyssey (Li-Cor) Multiplexed Detection which uses two IR fluorescence channels for simultaneous analysis of two targets. Two primary antibodies from different host species were incubated together to probe a blot; rabbit antibody against a protein of interest, and mouse antibody against loading controls, actin or vasolin containing protein (VCP). After washing with PBS (phosphate buffered saline) containing 0.01 M phosphate buffer, 2.7 mM KCl, and 137 mM NaCl, pH 7.4 with 1% Tween-20, incubation with two IR-conjugated secondary antibodies was carried out for 1 hour at room temperature. Five washes were carried out to remove nonspecific antibody binding in PBS with 1% Tween-20, or plain PBS.

Visualization of the Western blot signals from two IR fluorophores was done using the Odyssey IR Imaging System (LICOR, Lincoln, NE) in 700 and 800 nm channels in a single scan at 42 μm high resolution. Quantification was performed with Odyssey Application Software version 2.1 (LICOR, Lincoln, NE).

Integrated intensity signal was normalized for loading controls to gain a measure independent of sample loading errors. For each specific protein, I optimized general immunoblotting parameters (Table 2) and determined the linear range of IR fluorescence signal, by loading different protein amounts of the sample.

In some cases where the two primary antibodies were raised in the same species, diluent dilutions factor of secondary antibody were determined to obtain conditions with the least competition between the primary antibodies for the secondary antibody. Samples

TABLE 2

Optimized General Immunoblotting Parameters

	Primary Ab				Secondary Ab		Loading Control
	Protein loaded/la	Produced in	Immunogen	Dilution		Dilution	1°Ab, Dilution, 2°Ab, Dilution
NMDA NR1	25 ug	rabbit polyclonal	C-terminal of rat NR1	1:500	IRDye 800	1:15000	actin 1:5000 IRDye 680 1:15000
NMDA NR2A	25 ug	rabbit polyclonal	Mouse aa. 1265-1464	1:500	IRDye 800	1:15000	actin 1:5000 IRDye 680 1:15000
NMDA NR2B	40 ug	rabbit polyclonal		1:250	IRDye 800	1:10000	actin 1:5000 IRDye 680 1:15000
AMPA GluR1	25 ug	rabbit polyclonal	Rat aa. 276-287	1:500	IRDye 800	1:15000	actin 1:5000 IRDye 680 1:15000
$GABA_A$ α1	25 ug	rabbit polyclonal	human aa. 166-296	1:250	IRDye 800	1:15000	VCP 1:250 IRDye 680 1:15000
$GABA_B$	25 ug	mouse monoclonal	Rat R2 aa. 809-930	1:250	IRDye 680	1:15000	actin 1:5000 IRDye 680 1:15000
α1	80 ug	rabbit polyclonal	human aa. 339-349	1:250	IRDye 800	1:15000	actin 1:5000 IRDye 680 1:15000
α2A	80 ug	rabbit polyclonal	KASRWRGRGNREKR	1:250	IRDye 800	1:15000	VCP 1:250 IRDye 680 1:15000
β1	80 ug	rabbit polyclonal	Mouse aa. 394-408	1:250	IRDye 800	1:15000	actin 1:5000 IRDye 680 1:15000
Synaptophysin	20 ug	mouse monoclonal	Rat aa. 205-306	1:25000	IRDye 680	1:15000	VCP 1:250 IRDye 680 1:15000
VGlut1	<10 ug	rabbit polyclonal	Rat aa. 456-560	1:10000	IRDye 800	1:15000	actin 1:5000 IRDye 680 1:15000
PSD-95	25 ug	mouse monoclonal	Rat aa. 353-504	1:500	IRDye 680	1:15000	actin 1:5000 IRDye 680 1:15000
MAP2	25 ug	rabbit polyclonal	Mouse aa. 2-309	1:1000	IRDye 800	1:15000	actin 1:5000 IRDye 680 1:15000

IRDye 680 conjugated goat (polyclonal) anti-mouse IgG
IRDye 800 conjugated goat (polyclonal) anti-rabbit IgG
actin: mouse monoclonal
VCP: mouse monoclonal

were assayed in duplicates for each experiment, and each experiment was repeated at least three times.

Antibodies

The rabbit polyclonal antibodies against; NR2A, NR1 and GluR1 were purchased from Millipore (Temecula, CA), NR2B, α1 and β1 were from Abcam (Cambridge, MA), $GABA_A$ was from BD Biosciences (San Jose, CA), α2 was from Neuromics (Edina, MN), and VGlut1 and MAP2 were from Synaptic Systems (Goettingen, Germany). The mouse monoclonal antibodies against synaptophysin, actin, PSD-95, $GABA_B$ and VCP were purchased from BD Biosciences (San Jose, CA). Goat anti-rabbit or goat anti-mouse antibodies conjugated to IR dyes (IRDye 800CW, IRDye 680, respectively, were purchased from LI-COR, Lincoln, NE).

Statistics

The results were analyzed by Student's *t*-test to evaluate treatment effects in comparison with sham-control. Time course effects were evaluated by Kruskal-Wallis one-way ANOVA followed by Dunn's pairwise comparison to assess three and six months post radiation effects. Differences between means were considered significant at $P < 0.05$.

RESULTS

Reduction of [^{3}H]-glutamate release was not due to decrease in nerve terminal number or in glutamatergic synaptic vesicle number.

My findings on 0.6 Gy of ^{56}Fe radiation induced reduction in RRP (Chapter II

Background in detail) raised the possibility of nerve terminal loss or reduced glutamatergic synaptic vesicle numbers. I have assessed the levels of VGlut1 and synaptophysin in hippocampal synaptosomes obtained from rats subjected to ^{56}Fe irradiation to investigate synaptic vesicle densities on nerve terminal.

VGlut1 antibody detected a single band at approximately 70 kDa (Fig. 18B). The synaptophysin antibody also detected a single band migrating at approximately 40 kDa (Fig. 18B). These immunoreactive bands corresponds to the previously published molecular weights of VGlut1 (70-80 kDa) and synaptophysin (38 kDa) (*106, 108*). Normalized levels of integrated intensity showed that ^{56}Fe radiation did not have a significant effect on VGlut1 or synaptophysin immunoreactivity (Fig 18A, Table 3) three and six months post irradiation. These results suggest that radiation did not cause global changes in glutamatergic nerve terminal population, or in glutamatergic synaptic vesicle numbers.

0.6 Gy of ^{56}Fe radiation significantly reduced levels of NMDA, but not AMPA receptors 3 months post irradiation

It was previously reported that ionizing radiation affected glutamatergic NMDA receptor levels (*25*). I assessed NMDA and AMPA receptor abundance in hippocampal synaptosomes obtained from rats subjected to 0.6 Gy of ^{56}Fe irradiation. The NR1 antibody detected a strong band at 120 kDa, and the NR2A antibody detected a strong band at 170 kDa (Fig. 19B). The NR2B antibody detected two bands at approximately 180 kDa and 150 kDa. The lower band was probably a product of proteolytic degradation (*128*). Our results showed that degradation rate calculated as intensities of 150 kDa over 180 kDa was not significantly altered after irradiation.

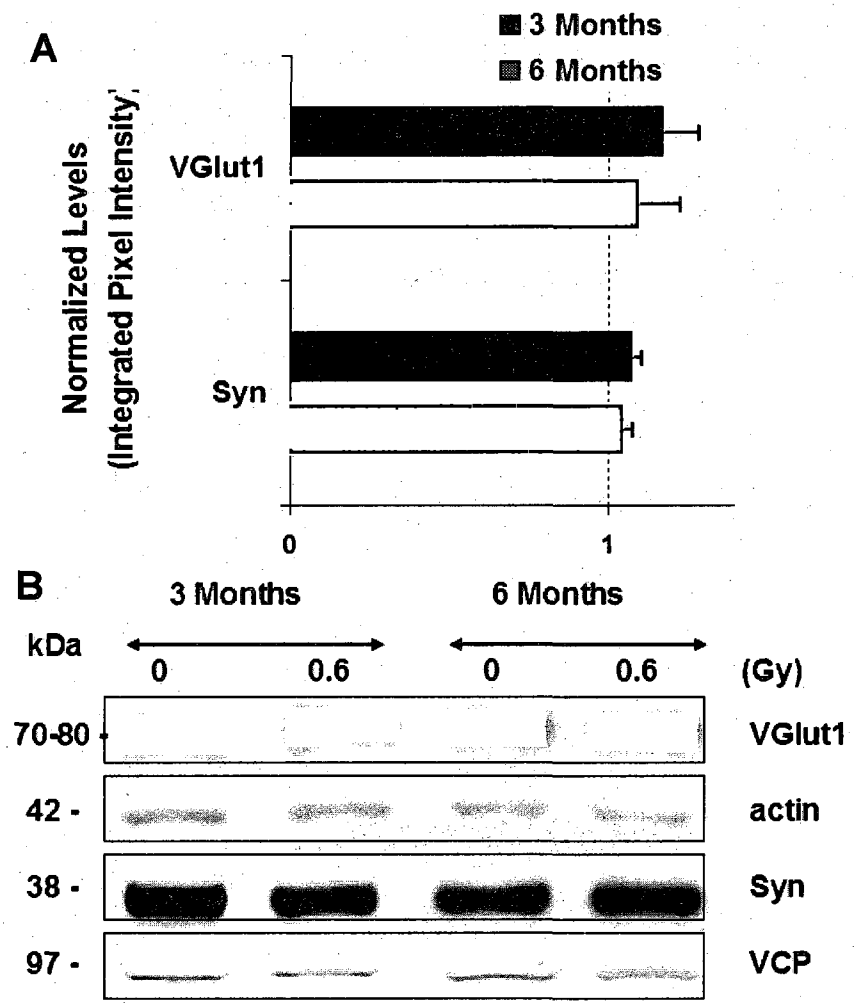

FIG. 18. Effects of 0.6 Gy of ^{56}Fe radiation (1 GeV/n) on VGlut1 and synaptophysin levels. Protein levels were analyzed by quantitative western blotting, using VGlut1 and synaptophysin antibodies. Data were normalized to sham irradiated values, which was set to 1. Data shown are means ± SEMs. (A) Summary graph of VGlut1 and synaptophysin (Syn) levels in hippocampal synaptosomes three and six months post irradiation. (B) Representative immunoblots of VGlut1 and synaptophysin (Syn) with loading controls, actin and VCP, respectively.

TABLE 3

Change of Levels in Selected Synaptic Proteins 3 and 6 Months Post 0.6 Gy ^{56}Fe Irradiation

Proteins	*3 Months* Integrated intensity	p value	*6 Months* Integrated intensity	p value
NMDA NR1	0.894 ± 0.023	*0.010	1.282 ± 0.055	*0.007
NMDA NR2A	0.792 ± 0.023	*0.001	0.905 ± 0.035	*0.033
NMDA NR2B	0.783 ± 0.073	*0.024	0.933 ± 0.073	0.396
AMPA GluR1	1.038 ± 0.063	0.583	0.913 ± 0.126	0.528
$GABA_A$ α1	0.972 ± 0.100	0.672	1.003 ± 0.154	0.984
$GABA_B$	0.904 ± 0.161	0.584	0.963 ± 0.123	0.712
α1	0.876 ± 0.117	0.260	0.954 ± 0.108	0.692
α2A	0.917 ± 0.175	0.607	1.120 ± 0.072	0.172
β1	0.612 ± 0.156	*0.038	0.998 ± 0.045	0.959
Synaptophysin	1.076 ± 0.031	0.069	1.046 ± 0.032	0.220
VGut1	1.172 ± 0.114	0.183	1.093 ± 0.136	0.531
PSD-95	0.899 ± 0.047	0.097	0.907 ± 0.136	0.519
MAP2c	0.861 ± 0.047	*0.018	1.238 ± 0.044	*0.006

*: $P < 0.05$, analyzed by Student's *t*-test (two-tailed distribution)

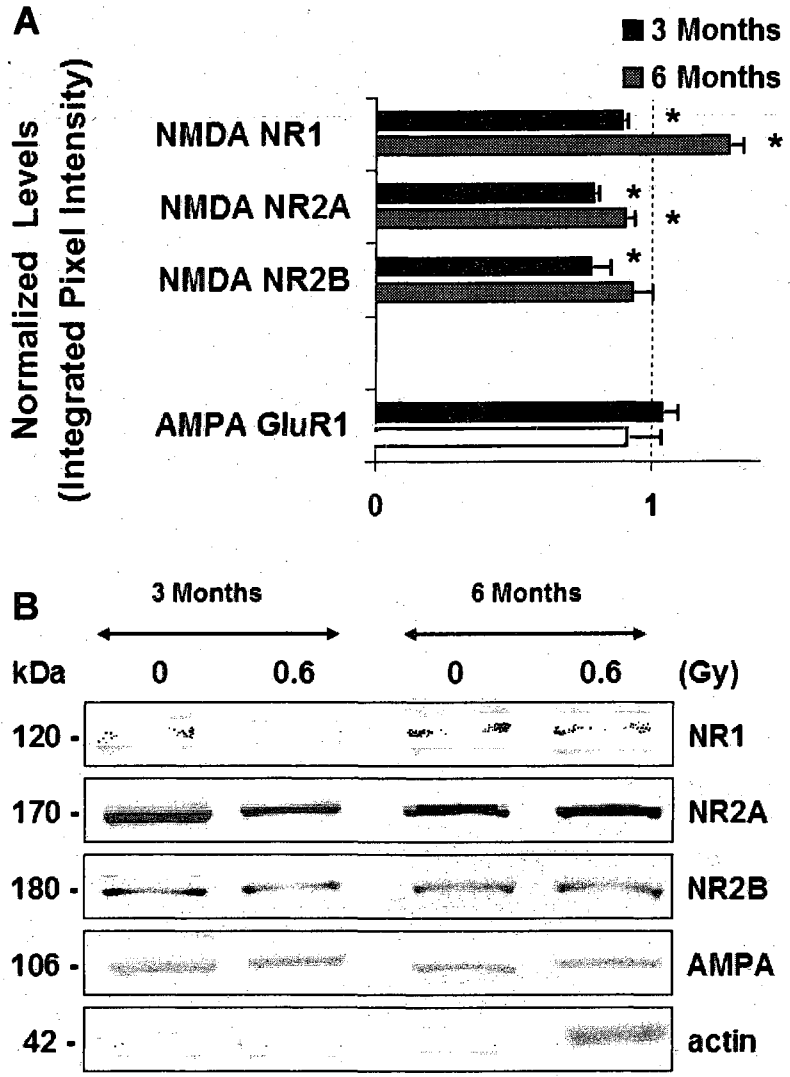

FIG. 19. Effects of 0.6 Gy of ^{56}Fe radiation (1 GeV/n) on selected glutamatergic receptor levels. Protein levels were analyzed by quantitative western blotting. Data were normalized to sham irradiated values, which was set to 1. Data shown are means ± SEMs. (A) Summary graph of NMDA NR1, 2A, 2B and AMPA GluR1 levels in hippocampal synaptosomes three and six months post irradiation. (B) Representative immunoblots. *: $P < 0.05$ analyzed by Student's *t*-test compared to control.

The 150 kDa unit is a constituent of the NMDA receptor complex. It is stable and maintains basic properties, suggesting functionality (*128*). Thus, I added up intensities from both bands to quantify NR2B levels. A representative band at 180 kDa is shown in Figure 19B. The AMPA antibody detected a strong band at 100 kDa.

For all three NMDA receptor subunits, normalized integrated intensity was significantly reduced three months post irradiation, while AMPA receptor immunoreactivity was spared (Fig 19A, Table 3). The effects were statistically significant, and were more pronounced on NR2 subunits. Both NR2A and NR2B isoform levels were reduced by ≈ 20% (NR2A: 0.79 ± 0.02 of control: NR2B, 0.78 ± 0.07 of control).

Six months post irradiation, however, the levels returned to normal. The levels of NR2 subunits were comparable to controls, whereas NR1 levels were up-regulated by 28%. Statistical analysis revealed a significant time course effect on NR1 receptors between three and six months (Kruskal-Wallis one-way ANOVA on ranks followed by Dunn's pairwise comparison, $P = 0.004$). AMPA levels were unaltered six months post irradiation.

Radiation exposure did not change PSD-95 levels

Either directly or indirectly, reduction in glutamatergic release and level of NMDA receptors might produce a coordinated change in a major glutamatergic receptor scaffolding protein, PSD-95. The PSD-95 antibody I used detected a single band at approximately 95 kDa, as expected (Fig. 20B). Three months after exposure the level of PSD-95 showed a trend of decrease (0.90 ± 0.05 of controls), but this was not statistically

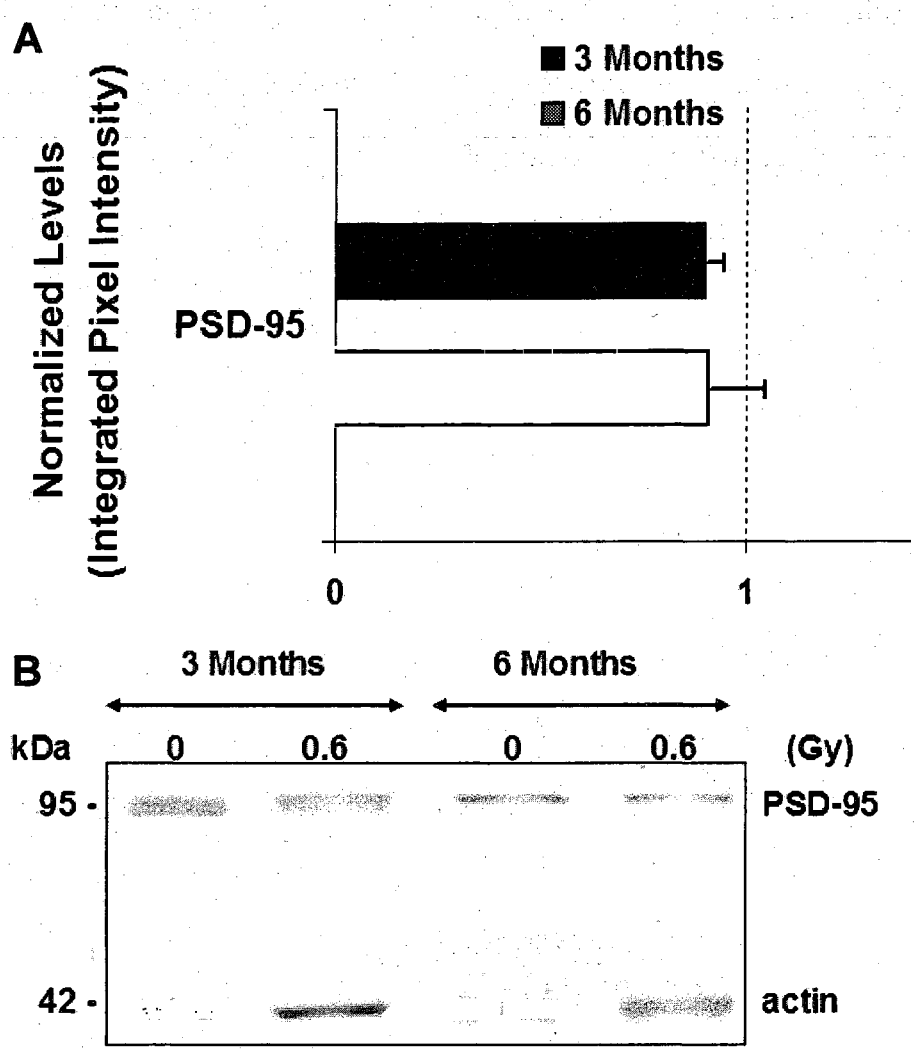

FIG. 20. Effects of 0.6 Gy of ^{56}Fe radiation (1 GeV/n) on PSD-95 levels. Protein levels were analyzed by quantitative western blotting, using PSD-95 antibodies. Data were normalized to sham irradiated values, which was set to 1. Data shown are means ± SEMs. (A) Summary graph of PSD-95 levels in hippocampal synaptosomes three and six months post irradiation. (B) Representative immunoblots.

significant (Fig. 20A, Table 3). The level was unchanged when tested six months after irradiation (0.91 ± 0.14 of controls).

β1 adrenergic receptor displayed significant radio-sensitivity 3 months post irradiation, whereas GABA and α-adrenergic receptors did not.

In addition to glutamatergic receptors, I have evaluated levels of GABAergic and noradrenergic receptors. I found both $GABA_A$ and $GABA_B$ receptors were relatively resistant to 0.6 Gy of ^{56}Fe irradiation. The levels of these receptors did not show any significant changes in comparison with control at either 3 or 6 month time point (Table 3). Among three noradrenergic receptors tested, only the level of β1 adrenergic receptor was significantly reduced three months after irradiation (Fig. 21, Table 3), while α subunits of adrenergic receptors were not altered (Table 3). β receptor levels returned to normal six months post irradiation (Table 3).

Radiation induced a reduction in MAP2c levels 3 months post irradiation that recovered 6 months post irradiation

To assess the possibility of neurite degeneration/regeneration, I tested MAP2 levels in hippocampal synaptosomes. The MAP2 antibody detected two strong bands for MAP2 isoforms at approximately 280 kDa (MAP2a and 2b), and 70 kDa (MAP2c), as previously documented (*129*). Thirty percent of total signal came from MAP2c alone (30.9 ± 3.92% in sham-control). The results verified that MAP2c, which is highly expressed during early neuronal development (*118*), was still detectable in the 4 ~ 7 months old test subjects. Although MAP2a/2b levels did not significantly change, MAP2c levels showed significant changes both at three and six months post irradiation. Western blots identified three major MAP2c species with slightly different

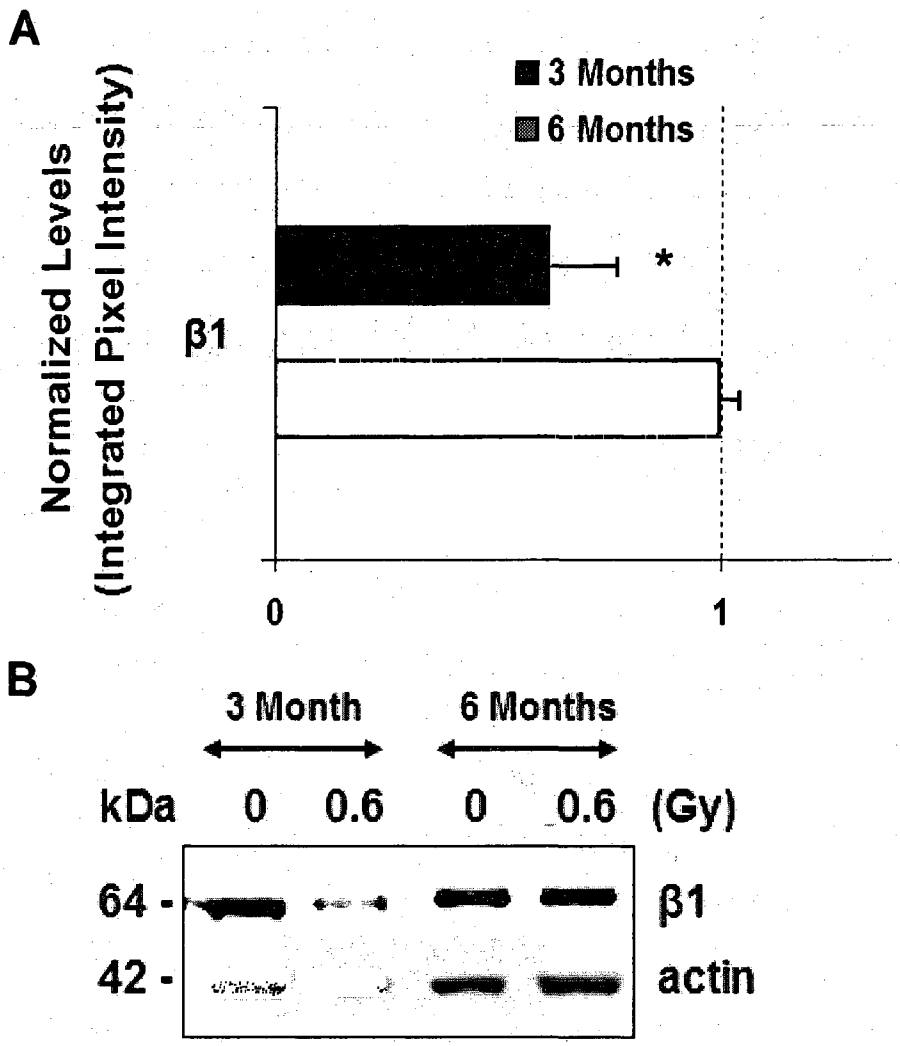

FIG. 21. Effects of 0.6 Gy of ^{56}Fe radiation (1 GeV/n) on β1 adrenergic receptor levels. Protein levels were analyzed by quantitative western blotting. Data were normalized to sham irradiated values, which was set to 1. Data shown are means ± SEMs. (A) Summary graph of β1 adrenergic receptor levels in hippocampal synaptosomes three and six months post irradiation. (B) Representative immunoblots. *: $P < 0.05$ analyzed by Student's *t*-test compared to control.

electrophoretic mobility, which may be due to different phosphorylation states (*126*) (Fig. 22B). The highest electrophoretic mobility MAP2c species (band 1), which showed the strongest immunoreactivity, is likely to be in de-phosphorylated state. Levels of band 1 showed 14% reduction three months after exposure (Fig 22A, $P = 0.02$, Student's *t*-test). More interestingly, at six months post-irradiation, intensity of this MAP2c species were up-regulated by 24% in comparison with sham-control (Fig 22A, $P = 0.01$). The difference in the mean values between these two time points was statistically significant (one-way ANOVA; $P \leq 0.001$).

As the phosphorylated states of MAP2c species, i.e. band 2 / band 1 and band 3 / band 1 ratios, were unaltered at three months post irradiation, no radiation effects on phosphorylation were suggested. However, at six months post irradiation, band 3 / band 1 ratio was significantly reduced compared to control by 20%, indicating reduced phosphorylation state of MAP2c. Since MAP2c species in de-phosphorylated state are more likely to regulate microtubule growth and stability (*126*), the band 1 level results, i.e. reduction at 3 months and up-regulation at 6 months post irradiation, suggest dendritic degeneration and dendritic growth, respectively, which may correspond with our findings on NMDA and β1 receptor levels.

DISCUSSION

The most significant finding in this study was the inhibitory effects of 0.6 Gy of ^{56}Fe radiation on the levels of glutamatergic NMDA receptors and β1 adrenergic receptors. For all three NMDA receptor subunits tested, namely NR1, NR2A and NR2B, levels were significantly reduced three months post irradiation. Inhibition or reduction of

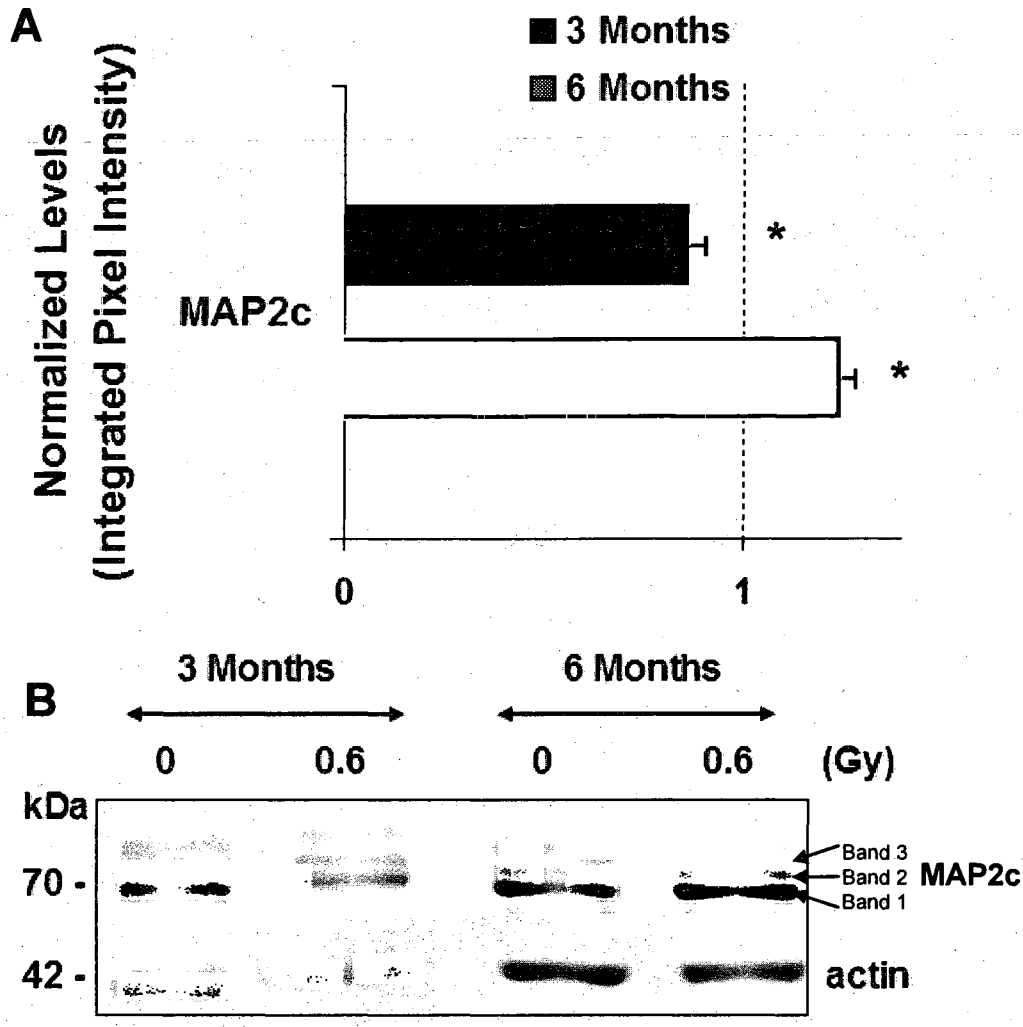

FIG. 22. Effects of 0.6 Gy of ^{56}Fe radiation (1 GeV/n) on MAP2c levels. Protein levels were analyzed by quantitative western blotting. Data were normalized to sham irradiated values, which was set to 1. Data shown are means ± SEMs. (A) Summary graph of MAP2c (Band 1) levels in hippocampal synaptosomes three and six months post irradiation. (B) Representative immunoblots. *: $P < 0.05$ analyzed by Student's *t*-test compared to control.

NMDA receptor levels in the hippocampus are considerably associated with impairments in learning and memory. Specifically, L-AP5, a NMDA receptor antagonist, blocks the induction of LTP in the hippocampus and decreases spatial memory performance (*130*). Also, knockout mice lacking the obligatory NR1 subunit exhibit impaired LTP and spatial memory performance (*131*). Moreover, preferential inhibition of NR2A subunits prevented the induction of LTP, and selective blocking of NR2B subunit abolished the induction of LTD (*73*). Furthermore, we have detected severe reduction of the level of β1 adrenergic receptors, which also play a critical role in LTP induction (*82*). Thus, my finding on HZE radiation induced reduction of these receptor levels provides a potential link between HZE radiation and radiation-induced cognitive dysfunction.

In contrast, glutamatergic AMPA receptor levels were unchanged. This result is consistent with a previous radiation research. Shi and co-workers found that 45 Gy of ^{137}Cs radiation, a dose for the treatment of brain tumors, induced significant alternation in NMDA receptor, but not in AMPA receptors. The nature of this specificity is difficult to discern from the present experiments, however, it is reported that NMDA possesses a unique reduction-oxidation site and ROS oxidizes the sulfhydryl residues associated with this site (*132*), which facilitates vulnerability of NMDA receptors to oxidative stress (*64, 132*). Twenty to fifty percent decreases in the density of NMDA receptors during aging have been reported, probably due to age related oxidative stress (*64*). In accordance with these reports, β1 adrenergic receptor is also susceptible to oxidative stress (*133*), and the level declines by pretreatment with H_2O_2 (*134*) and also with age (*135*). Consequently, we presume the specificity of effects of HZE radiation on levels of neurotransmitter receptors may associate with susceptibility of each receptor to oxidative stress.

Levels of a scaffold protein, PSD-95, was not significantly altered after radiation exposure. Thus, we speculate that the observed reduction in NMDA receptors did not influence number or size of downstream postsynaptic contacts. The result is in line with previous studies, which suggested relatively less functional association of PSD-95 with NMDA receptors. Mice lacking PSD-95 show normal NMDA receptor clustering and function, but reduced AMPA receptor function (*136*). In addition, over-expression of PSD-95 did not influence NMDA receptor clustering, but enhanced AMPA receptor recruitment in developing hippocampal neurons (*137*). It is likely that a predominant role of PSD-95 may be to regulate AMPA receptor insertion and retention at the synapse, therefore, that PSD-95 has the closer association with AMPA receptors. My finding of unaltered levels of AMPA is consistent with this notion.

Questions still remain about the unaltered receptor levels 6 months post irradiation. I speculate that a possible "repair mechanism" may take place after radiation damage. Recovery of HZE radiation induced damage on dendritic spine was previously reported, e.g. decrease in dendritic spine length of CA1 hippocampal neurons was less severe after one year (*65*). My finding in MAP2c levels also supports the possible recovery. Pronounced reduction in MAP2c level was found at 3 months post irradiation, whereas the level was up-regulated 6 months post irradiation. MAP2 provides scaffolds in dendrites and facilitates the localization of signal transduction apparatus there, particularly near dendritic spines (*127*). The correlation with levels of NMDA NR1 subunit and MAP2c suggest some degree of dendritic spine recovery at 6 months. This cellular process likely affected NMDA receptor sub-synaptic domains more specifically, since levels of AMPA receptors, which are also localized to dendritic spines but within

the distinct domains (*138*), were unaltered in our experiments.

My study on two synaptic vesicle markers assure that 0.6 Gy of ^{56}Fe irradiation did not affect synaptic vesicle stores in the hippocampus, thus, depletion of glutamate stores or apoptotic damage of nerve terminals are unlikely to be a cause of reduction in glutamatergic release observed in our experiments (Chapter II). In line with my results, a previous study using a higher dose (2.0 Gy) of ^{56}Fe radiation also reported unaltered levels of synaptophysin in hippocampus (*139*), supporting the notion that neurotransmitter stores are not the direct locus of radiation-induced deficits.

Overall, my findings on reduced levels of glutamatergic NMDA and β1 adrenergic receptors, both of which are critical in synaptic plasticity and in learning and memory, provide mechanistic evidence underlying HZE radiation induced cognitive dysfunction.

Although there were overall changes in neurotransmitter release (Chapter II) and neurotransmitter receptor levels by HZE irradiation, there were a number of differences. Regarding the time course of the HZE effects, I observed persisting suppression of evoked glutamate and GABA release, but a recovery in NMDA and β1 adrenergic receptor levels. Also, while both glutamate and GABA release were suppressed, only the NMDA type glutamate receptors changes, leaving GABA receptors unchanged. Moreover, while NE release was not affected, β1 adrenergic receptor levels were reduced at 3 months post irradiation. These findings suggest that the effects of HZE radiation in neurotransmitter release and neurotransmitter receptor levels are either completely independent or subjected to complex interactions that may involve homeostatic regulation.

CHAPTER VI

HZE RADIATION INDUCED LIPID PEROXIDATION

BACKGROUND

As we documented in Chapter II, ^{56}Fe radiation (0.6 Gy, 1 GeV/n)) induces significant reduction in hippocampal neurotransmitter release. The results raised a question on the integrity of cell membrane in the hippocampus after radiation exposure. One important factor that affects the membrane integrity is **lipid peroxidation**, a consequence of oxidative stress. Lipid peroxidation leads to disturbance of Ca^{2+} homeostasis that may affect functions of release machinery (discussed in Chapter II). To test this possibility, I have measured levels of lipid peroxidation in the hippocampus three and six months post irradiation.

Oxidative stress can be perceived as an imbalance of cellular pro-oxidant and anti-oxidant processes, resulting in the generation of ROS. The brain by nature provides favorable environments for generation of ROS (*47*). It consumes 20% of the oxygen utilized by the body, although the brain itself comprises only 2% of the body weight. Despite the high ratio of aerobic glycolysis, neurons contain relatively lower levels of antioxidant enzymes such as superoxide dismutase, catalase, glutathione peroxidase compared with other organs in the body (*140*). Moreover, the brain is exceptionally vulnerable to lipid peroxidation, for neurons contain high levels of peroxidizable fatty acids (*141*).

Ionizing radiation is capable of producing a variety of ROS (*26, 27, 30*). HZE radiation is a type of high LET (linear energy transfer) radiation, and predominant effects

involve direct ionization. Peroxide ($\mathbf{H_2O_2}$) pretreatment have been used extensively to study free radical chemistry of HZE radiation (*28, 29, 142*), whereas water radiolysis, in which indirect effect of ionizing radiation leads to the formation of hydroxyl radicals ($^{\bullet}OH$), has been used to model low-LET type radiation such as X-rays (*101*).

H_2O_2 is a ROS, but it is a non-radical and is relatively unreactive. It is converted to highly reactive $^{\bullet}OH$ in the presence of decompartmentalized Fe^{2+} ions:

$$H_2O_2 + \underset{\downarrow}{\overset{Fe^{2+}}{e^-}} \rightarrow OH^- + {}^{\bullet}OH \quad (Fe^{3+})$$

Because $^{\bullet}OH$ is high reactive, its diffusion radius is only 0.3 nm (*141*). Diffusible H_2O_2 penetrates cell membranes, whose thickness is between 6 nm to 10 nm, and contributes to a short-lived $^{\bullet}OH$ to be distributed both intra- and extracellularly. Thus, $^{\bullet}OH$ is able to contact oxidative targets of hydrophobic lipid tails in the cell membrane and becomes a major source of lipid peroxidation products.

Treatment of a hippocampal slice with H_2O_2 altered electrophysiological properties including decreased ability to generate action potentials (*29*). The treatment also increased lipid peroxidation, raising the possibility that the electrophysiological effects were mediated by a lipid peroxidation mechanism (*30*). In line with the finding, H_2O_2 suppressed K^+-stimulated [^{3}H]-glutamate release by 20% using cortical synaptosomal preparation (*31*). Pretreatment with antioxidants including iron chelator revealed that $^{\bullet}OH$, but not H_2O_2, was responsible for the observed effects (*30*). These results suggested that impairments in hippocampal neurotransmission after HZE irradiation may be mediated by lipid peroxidation.

Previous studies using dichlorofluorescein (DCFH) assay showed that 1.5 Gy of ^{56}Fe radiation led to increased ROS production in the frontal cortex of rats one month after exposure (*139*). Limoli and co-authors also demonstrated that a lower dose of ^{56}Fe radiation ($\leq$ 1.0 Gy) could elicit significant increase in ROS production in hippocampal precursor cells one month post irradiation (*26*). Another line of evidence showed that whole body irradiation with 1.5 Gy of ^{56}Fe particles substantially augmented lipid peroxidation in mice cerebellum one months post irradiation, and exposure also impaired the reference memory (*27*). Although the above studies support a role for ROS production and lipid peroxidation in HZE radiation induced brain damage, there are no reports that directly correspond to our experimental conditions. Therefore, we have estimated the levels of lipid peroxidation in the hippocampus three and six months post 0.6 Gy of ^{56}Fe irradiation.

Lipid peroxidation is oxidative degradation of lipids (LH) by ROS ($X^{\bullet}$), such as $OH^{\bullet}$. Most often affected is the methylene group (-CH2-) in polyunsaturated fatty acids, which possess reactive hydrogen to produce unstable lipid radical ($L^{\bullet}$);

1) $LH + X^{\bullet} \rightarrow L^{\bullet} + XH$ (Initiation)

Lipid radical readily reacts with O_2 to produce lipid peroxyl radical ($LOO^{\bullet}$);

2) $L^{\bullet} + O_2 \rightarrow LOO^{\bullet}$

Reaction can propagate, and eventually changes the membrane structure;

3) $LOO^{\bullet} + LH \rightarrow LOOH + L^{\bullet}$ (Propagation)

Hydroperoxides (LOOH) result in production of a series of new reactive species, e.g. 4-hydroxyalkenals (HAE) and malondialdehyde (MDA);

4) LOOH → short chain radicals, reactive aldehydes

The radical chain continues to proceed, until it is terminated;

5) $LOO^{\bullet} + LOO^{\bullet} \rightarrow$ non-radical product (Termination)

As this bimolecular scheme illustrates, $LOO^{\bullet}$ possesses paradoxical abilities to serve in both propagation and termination, which explains the inverse dose-response effect at radiation induced lipid peroxidation (*101, 143*). The inverse dose-response means that high production rates of free radials, which initiate lipid peroxidation, yield a smaller amount of reactive end products than low production rates. This is distinct from the dose-response of radiation effects, where high dose is more effective than low dose. It is noteworthy that these secondary reactive species such as $L^{\bullet}$, $LOO^{\bullet}$, as well as degradation products of LOOH, are also capable to interact with lipids and membrane proteins.

The alteration of membrane structures leads to increased membrane permeability. Inactivation of ion channels and increase of unspecific membrane leak was found after oxidative insult (*101*). These allow membrane depolarization (*144*) and non-specific Ca^{2+} influx (*145*). An important pathophysiological consequence is disruption of Ca^{2+} homeostasis and alteration of neural transmission.

I assayed levels of MDA and HAE, end products of LOOH (Eq. 4). Measurements of them have been used as an indicator of lipid peroxidation. As a result, I have found that 0.6 Gy of ^{56}Fe radiation (1 GeV/n) induced high levels of lipid peroxidation in the hippocampus three months post irradiation. The high levels persisted six months post irradiation.

MATERIALS AND METHODS

Sample Preparation

Hippocampus was dissected and stored at -80°C to prevent loss of MDA and HAE, and to prevent further oxidation. Frozen samples were thawed on ice. Tissues from 4 animals were pooled, and then homogenized in ice-cold PBS containing 5 mM butylated hydroxytoluene (BHT), an antioxidant, to prevent new lipid peroxidation during homogenization. Homogenates were centrifuged at 3000 x *g* at 4°C for 10 min to pellet cell debris. Aliquots of supernatant were taken to determine protein concentration using the Coomassie Plus better Bradford assay kit (Pierce) according to manufacturer's instructions. Protein concentration of samples was adjusted to 15 - 60 mg/ml. Samples were kept on ice until use.

Lipid Peroxidation Assay

Measurement of MDA in combination with HAE was performed using a micro-plate assay kit (Oxford Biomedical Research, Oxford, MI) according to the manufacturer's directions. The assay is based on a color reaction of a chromogenic reagent, N-methyl-2-phenylindole, with MDA and HAE. One molecule of either MDA or HAE reacts with 2-molecules of the reagent to yield a stable chromophore with absorbance at 570 nm. Samples were added to the reagent, and incubated at 45°C for 60 min, followed by centrifugation at 15,000 x *g* for 10 min to obtain a supernatant clear from precipitates. Values were expressed as MDA + HAE nmol/mg protein. Samples were assayed in triplicate in each experiment. Each measurement was repeated at least three times.

Statistics

The results were analyzed by Student's *t*-test. Differences between means were considered significant at $P < 0.05$.

RESULTS

Point six Gy of ^{56}Fe radiation (1 GeV/n) leads to a significant increase in lipid peroxidation in the hippocampus three and six months post irradiation

My results showed that the level of MDA + HAE was about two times higher in 0.6 Gy irradiated samples than in the sham control animals (control: 1.8 ± 0.30 nmol/mg protein; irradiated: 3.8 ± 0.82 nmol/mg protein, $P < 0.05$, Student's *t*-test, $n = 4$, Fig. 23.) The effects persisted six months post irradiation (irradiated: 4.0 ± 0.48 nmol/mg protein, $P < 0.05$, Student's *t*-test, $n = 4$, Fig. 23.)

The temporal correlation between lipid peroxidation and reduction in hippocampal glutamate and GABA transmitter release caused by 0.6 Gy of ^{56}Fe radiation raises the possibility of a causal relationship.

DISCUSSION

My results demonstrate an inverse relationship between hippocampal neurotransmitter release and level of lipid peroxidation in the hippocampus of animals exposed to 0.6 Gy of ^{56}Fe radiation. These two phenomena correlated well and the inverse relationship persisted even through 6 months. This delayed effect of oxidative insults on membrane might be a contributing factor to the observed reduction of hippocampal neurotransmission.

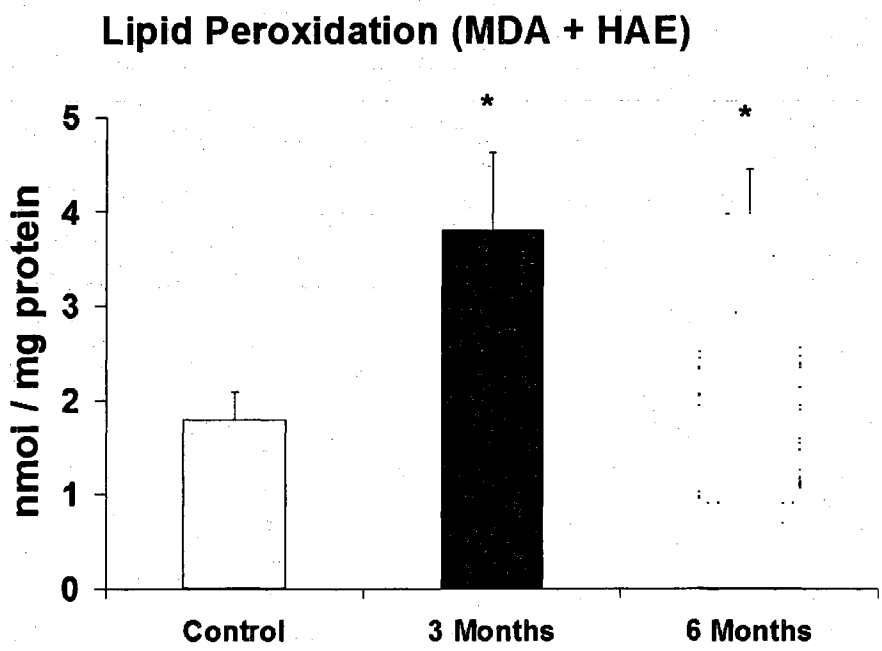

FIG. 23. Point six Gy of ^{56}Fe radiation (1 GeV/n) induced changes in products of lipid peroxidation in the hippocampus. Levels of lipid peroxidation were evaluated as described in the Materials and Methods. Briefly, hippocampal homogenate was loaded with a chromogenic reagent, *N*-methyl-2-phenylindole at 45°C for 60 min, and lipid peroxidation was assessed by measuring the levels of MDA (malondialdehyde) in combination with a derivative, HAE (4-hydroxyalkenals) at three months and six months post irradiation. Values are expressed as means of MDA + HAE (nmol/mg protein) ± SEM. Asterisks indicate statistical significance analyzed by two- tail Student's *t*-test. ($n = 4$).

Radiation induced lipid peroxidation is a non-enzymatic random reaction (*146*), but extremely common phenomena in the brain. It is noteworthy that this radiation induced insult was one of a few uniform responses among irradiated subjects, based on a long-term investigations after the Chernobyl nuclear accident (*45*). Generally, radiation effects display high variability among subjects due to different radio-sensitivity of each individual.

While previous studies focused on the early delayed effects of HZE radiation on ROS production (*147*) and lipid peroxidation (*27*) detected one month post irradiation, my results indicate that the effects can persist well beyond one month, for as long as 6 months, suggesting that production of ROS can be continuous and may play a critical role in late delayed effects of HZE radiation on neurotransmission. Mechanistic explanation of this prolonged membrane oxidization is beyond the scope of this study, however, it has been suggested that paradoxical ability of reactive species, which both initiate and terminate chain reaction that results in lipid peroxidation, might be relevant to prolonged production (*143*). In order to terminate the chain of events, it is necessary to reduce lipid hydroperoxides as well as to decompose concomitant formation of $LOO^{\bullet}$. Consequently, the role of endogenous antioxidants has received extensive attention. It is likely that an optimal concentration of antioxidants may exist that will restore the free radical level to yield the best combination of inhibition and termination to minimize net lipid peroxidation, and any concentration other than this optimal leads to increased, thus, prolonged lipid peroxidation (*143*).

CHAPTER V

SUMMARY

The main findings of the present study were: 1) 0.6 Gy of ^{56}Fe radiation (1 GeV/n) significantly perturbed chemical neurotransmission of rat hippocampal nerve terminals, resulting in a persisted reduction of hypertonic sucrose evoked [^{3}H]-glutamate and [^{14}C]-GABA release; 2) exposure to 0.6 Gy of ^{56}Fe radiation also significantly reduced levels of glutamatergic NMDA receptors as well as β1 adrenergic receptors three months post irradiation, however, partial repair may take place by six months post irradiation; 3) the same radiation regimen significantly enhanced oxidative stress as indicated by increased levels of lipid peroxidation products in the hippocampus both three and six months post irradiation, suggesting that increased levels of lipid peroxidation played an important role in reduction of neurotransmitter release.

Although it is presently untested whether these alterations within the hippocampus directly contribute to aspects of radiation induced cognitive impairments, our findings demonstrate that, after a single dose of ^{56}Fe radiation as low as 0.6 Gy, the neurochemical environment in the hippocampus becomes significantly altered, which may underlie impairments in cognitive functions. It is of importance that synaptic plasticity may be significantly altered via reduction of NMDA and β1 adrenergic receptor levels in the hippocampus.

Although precise mechanisms are still under debate, a generally accepted model of radiation-induced cognitive dysfunction is depicted in Figure 24. In this classic paradigm, neuronal cell death due to radiation induced generation of ROS leads to cell

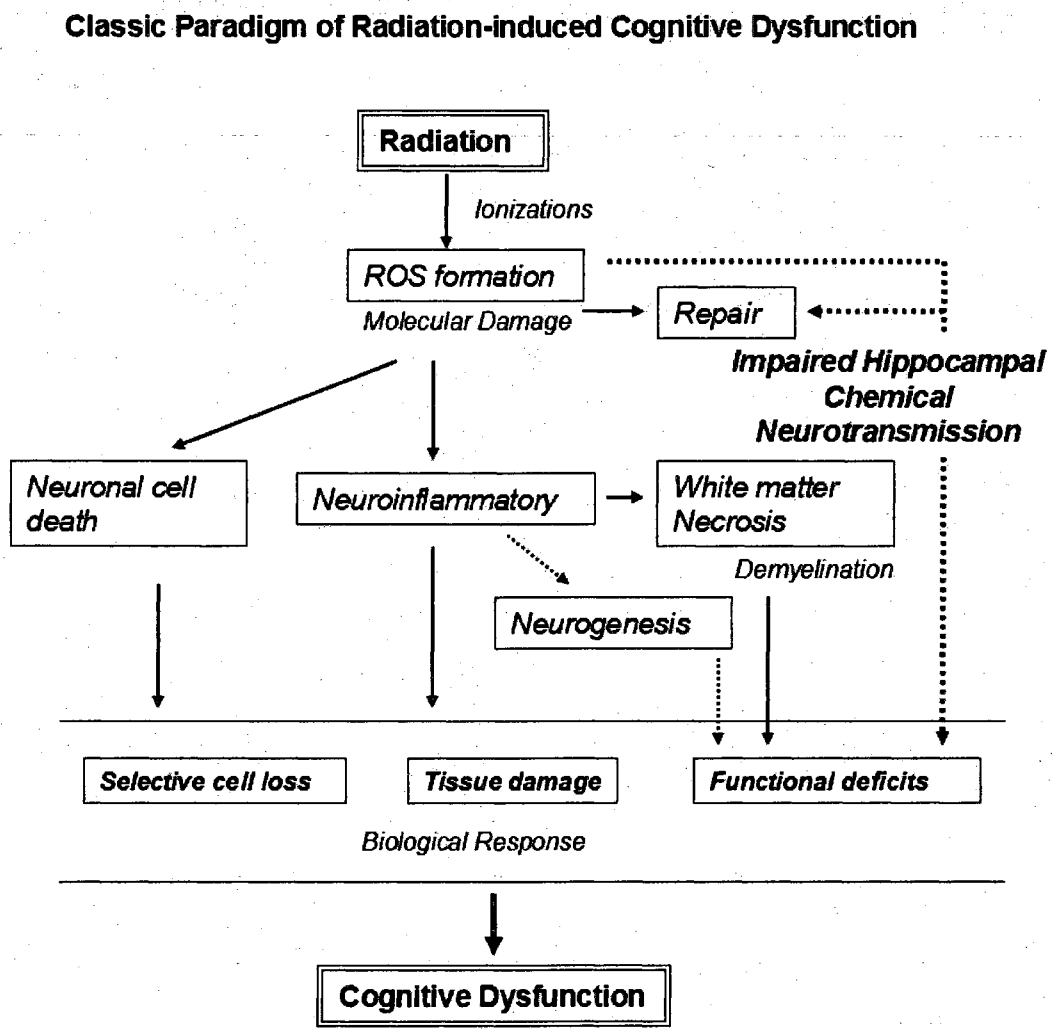

FIG. 24. Classic paradigm of radiation-induced cognitive dysfunction. The solid arrows indicate the generally accepted sequence of events from the absorption of radiation to the expression of the various forms of biological damage, which consequently leads to cognitive dysfunction. Dotted line indicates postulated neurogenesis hypothesis (*19, 36*). Dashed line indicates a pathway proposed by the present work.

loss and/or tissue damage, which can deteriorate functions of the CNS (*46*). With high dose radiation exposure, white matter necrosis is the dominant histopathological presentation and consistently associated with demyelination (*47*). Demyelination impairs the conduction of action potentials, and consequently impairs cognitive performance. Whereas high doses of radiation produce overt histopathological changes, lower dose exposures produce cognitive dysfunction without inducing obvious morphological changes. Recently it was reported that radiation impaired neurogenesis via neuroinflammatory process. Two Gy of ^{56}Fe radiation reduced the rate of proliferation among neuronal progenitors within the dentate gyrus, and also impaired hippocampus dependent performance (*19, 36*). My findings with 0.6 Gy, which is regarded sub-threshold for impairing neurogenesis, raise the possibility that HZE radiation could cause functional deficits in cognitive behavior without involving neurogenesis or histopathological changes as previously proposed (dashed line in Fig. 24).

Overall, this work contributes to Phase 1 of NASA Strategic Program Plan by 1) uncovering a risk to the integrity of hippocampal chemical neurotransmission in the CNS, and 2) collecting specific evidence for radiation induced alterations in synaptic functions / elements that are critical for normal cognitive functions.

In future studies, I would like to further extend my investigation to 1) validate permissible exposure limits using a series of our assays. Also, assuming that lipid peroxidation may at least partially underlie the observed reduction in neurotransmitter release, optimized concentration of cellular antioxidants may rescue the radiation induced deficits. Thus, the current assays would facilitate to: 4) develop effective mitigation strategies. Pretreatment with ROS scavengers, such as polyethylene glycol-conjugated

catalase (PEG-CAT), a cell permeable H_2O_2 scavenging enzyme, may reduce radiation-induced deficiencies. Also, diet antioxidants, such as vitamin E, are known to inhibit lipid peroxidation and might ameliorate HZE radiation effects on neurotransmission.

REFERENCES

1. The NASA Space Radiation Project Element, Human Research Program, Johnson Space Center. http://hacd.jsc.nasa.gov/projects/space_radiation_overview.cfm.

2. T. Straume, S. A. Amundson, W. F. Blakely, F. J. Burns, A. Chen, N. Dainiak, S. Franklin, J. A. Leary, D. J. Loftus, et al., NASA Radiation Biomarker Workshop, September 27-28, 2007. *Radiat. Res.* **170**, 393-405 (2008).

3. S. J. Graham, Radiation Hazards to Crews of Interplanetary Missions: Biological Issues and Research Strategies. The Committee on Space Biology and Medicine (1996).

4. R. B. Setlow, The U.S. National Research Council's views of the radiation hazards in space. *Mutat. Res.* **430**, 169-175 (1999).

5. J. A. Joseph, W. A. Hunt, B. M. Rabin and T. K. Dalton, Possible "accelerated striatal aging" induced by ^{56}Fe heavy-particle irradiation: implications for manned space flights. *Radiat. Res.* **130**, 88-93 (1992).

6. B. M. Rabin, J. A. Joseph, W. A. Hunt, T. B. Dalton, S. B. Kandasamy, A. H. Harris and B. Ludewigt, Behavioral endpoints for radiation injury. *Adv. Space Res.* **14**, 457-466 (1994).

7. B. M. Rabin, J. A. Joseph and S. Erat, Effects of exposure to different types of radiation on behaviors mediated by peripheral or central systems. *Adv. Space Res.* **22**, 217-225 (1998).

8. B. M. Rabin, J. A. Joseph, B. Shukitt-Hale and J. McEwen, Effects of exposure to heavy particles on a behavior mediated by the dopaminergic system. *Adv. Space Res.* **25**, 2065-2074 (2000).

9. B. Shukitt-Hale, G. Casadesus, J. J. McEwen, B. M. Rabin and J. A. Joseph, Spatial learning and memory deficits induced by exposure to iron-56-particle radiation. *Radiat. Res.* **154**, 28-33 (2000).

10. B. Shukitt-Hale, G. Casadesus, I. Cantuti-Castelvetri, B. M. Rabin and J. A. Joseph, Cognitive deficits induced by ^{56}Fe radiation exposure. *Adv. Space Res.* **31**, 119-126 (2003).

11. NASA, Human Research Program IWS: Overview (S. R. P. Element, Ed.). NASA (2005). http://hacd.jsc.nasa.gov/documents/Radiation_IWS_Banner1_Final.pdf.

12. NASA, Bioastronautics Roadmap (2005). http://hacd.jsc.nasa.gov/documents/Radiation_IWS_Banner1_Final.pdf.

13. P. C. Nathan, S. K. Patel, K. Dilley, R. Goldsby, J. Harvey, C. Jacobsen, N. Kadan-Lottick, K. McKinley, A. K. Millham, et al., Guidelines for identification of, advocacy for, and intervention in neurocognitive problems in survivors of childhood cancer: a report from the Children's Oncology Group. *Arch. Pediat. Adolescent Med.* **161**, 798-806 (2007).

14. M. D. Ris, R. Packer, J. Goldwein, D. Jones-Wallace and J. M. Boyett, Intellectual outcome after reduced-dose radiation therapy plus adjuvant chemotherapy for medulloblastoma: a Children's Cancer Group study. *J. Clin. Oncol.* **19**, 3470-3476 (2001).

15. W. E. Reddick, J. O. Glass, S. L. Palmer, S. Wu, A. Gajjar, J. W. Langston, L. E. Kun, X. Xiong and R. K. Mulhern, Atypical white matter volume development in children following craniospinal irradiation. *Neurooncology* **7**, 12-19 (2005).

16. W. E. Reddick, H. A. White, J. O. Glass, G. C. Wheeler, S. J. Thompson, A. Gajjar, L. Leigh and R. K. Mulhern, Developmental model relating white matter volume to neurocognitive deficits in pediatric brain tumor survivors. *Cancer* **97**, 2512-2519 (2003).

17. K. Akiyama, R. Tanaka, M. Sato and N. Takeda, Cognitive dysfunction and histological findings in adult rats one year after whole brain irradiation. *Neurol. Med. Chir. (Tokyo)* **41**, 590-598 (2001).

18. J. Raber, R. Rola, A. LeFevour, D. Morhardt, J. Curley, S. Mizumatsu, S. R. VandenBerg and J. R. Fike, Radiation-induced cognitive impairments are associated with changes in indicators of hippocampal neurogenesis. *Radiat. Res.* **162**, 39-47 (2004).

19. M. L. Monje, S. Mizumatsu, J. R. Fike and T. D. Palmer, Irradiation induces neural precursor-cell dysfunction. *Nat. Med.* **8**, 955-962 (2002).

20. S. Mizumatsu, M. L. Monje, D. R. Morhardt, R. Rola, T. D. Palmer and J. R. Fike, Extreme sensitivity of adult neurogenesis to low doses of X-irradiation. *Cancer Res.* **63**, 4021-4027 (2003).

21. T. J. Shors, D. A. Townsend, M. Zhao, Y. Kozorovitskiy and E. Gould, Neurogenesis may relate to some but not all types of hippocampal-dependent learning. *Hippocampus* **12**, 578-584 (2002).

22. J. S. Snyder, N. S. Hong, R. J. McDonald and J. M. Wojtowicz, A role for adult neurogenesis in spatial long-term memory. *Neuroscience* **130**, 843-852 (2005).

23. C. L. Zhang, Y. Zou, W. He, F. H. Gage and R. M. Evans, A role for adult TLX-positive neural stem cells in learning and behaviour. *Nature* **451**, 1004-1007 (2008).

24. B. Leuner, E. Gould and T. J. Shors, Is there a link between adult neurogenesis and learning? *Hippocampus* **16**, 216-224 (2006).

25. L. Shi, M. M. Adams, A. Long, C. C. Carter, C. Bennett, W. E. Sonntag, M. M. Nicolle, M. Robbins, R. D'Agostino and J. K. Brunso-Bechtold, Spatial learning and memory deficits after whole-brain irradiation are associated with changes in NMDA receptor subunits in the hippocampus. *Radiat. Res.* **166**, 892-899 (2006).

26. C. L. Limoli, E. Giedzinski, J. Baure, R. Rola and J. R. Fike, Redox changes induced in hippocampal precursor cells by heavy ion irradiation. *Radiat. Env. Biophysics* **46**, 167-172 (2007).

27. K. Manda, M. Ueno and K. Anzai, Memory impairment, oxidative damage and apoptosis induced by space radiation: ameliorative potential of alpha-lipoic acid. *Behavioural Brain Res.* **187**, 387-395 (2008).

28. L. S. Myers, Jr., A. J. Carmichael and T. C. Pellmar, Radiation chemistry of the hippocampal brain slice. *Adv. Space Res.* **14**, 453-456 (1994).

29. T. C. Pellmar, Peroxide alters neuronal excitability in the CA1 region of guinea-pig hippocampus in vitro. *Neuroscience* **23**, 447-456 (1987).

30. T. C. Pellmar, Use of brain slices in the study of free-radical actions. *J. Neurosci. Methods* **59**, 93-98 (1995).

31. S. C. Gilman, M. J. Bonner and T. C. Pellmar, Peroxide effects on [^{3}H]-glutamate release by synaptosomes isolated from the cerebral cortex. *Neurosci. Lett.* **140**, 157-160 (1992).

32. P. Haerich, G. A. Nelson and M. J. Pecaut, HZE radiation and dopaminergic modification of startle and prepulse inhibition in mice. *Physiol. Behavior* **86**, 103-110 (2005).

33. Y. Koike, M. A. Frey, F. Sahiar, R. Dodge and S. Mohler, Effects of HZE particle on the nigrostriatal dopaminergic system in a future Mars mission. *Acta Astronautica* **56**, 367-378 (2005).

34. T. W. Robbins and B. J. Everitt, Neurobehavioural mechanisms of reward and motivation. *Curr. Opi. Neurobiol.* **6**, 228-236 (1996).

35. R. Villalobos-Molina, J. A. Joseph, B. M. Rabin, S. B. Kandasamy, T. K. Dalton and G. S. Roth, Iron-56 irradiation diminishes muscarinic but not alpha 1-adrenergic-stimulated low-Km GTPase in rat brain. *Radiat. Res.* **140**, 382-386 (1994).

36. K. Manda, M. Ueno and K. Anzai, Space radiation-induced inhibition of neurogenesis in the hippocampal dentate gyrus and memory impairment in mice: ameliorative potential of the melatonin metabolite, AFMK. *J. Pineal Res.* **45**, 430-438 (2008).

37. A. Todorovic, J. Kasapovic, S. Pejic, V. Stojiljkovic and S. B. Pajovic, Differences in antioxidative response of rat hippocampus and cortex after exposure to clinical dose of gamma-rays. *Annals of the New York Academy of Sciences* **1048**, 369-372 (2005).

38. C. Rosenmund and C. F. Stevens, Definition of the readily releasable pool of vesicles at hippocampal synapses. *Neuron* **16**, 1197-1207 (1996).

39. C. F. Stevens, Presynaptic function. *Curr. Opi. Neurobiol.* **14**, 341-345 (2004).

40. D. R. Grosshans and M. D. Browning, Protein kinase C activation induces tyrosine phosphorylation of the NR2A and NR2B subunits of the NMDA receptor. *J. Neurochem.* **76**, 737-744 (2001).

41. K. A. Helm, R. P. Haberman, S. L. Dean, E. C. Hoyt, T. Melcher, P. K. Lund and M. Gallagher, $GABA_B$ receptor antagonist SGS742 improves spatial memory and reduces protein binding to the cAMP response element (CRE) in the hippocampus. *Neuropharmacology* **48**, 956-964 (2005).

42. Y. Y. Huang and E. R. Kandel, Modulation of both the early and the late phase of mossy fiber LTP by the activation of beta-adrenergic receptors. *Neuron* **16**, 611-617 (1996).

43. Y. Izumi and C. F. Zorumski, Norepinephrine promotes long-term potentiation in the adult rat hippocampus in vitro. *Synapse* **31**, 196-202 (1999).

44. C. F. Murchison, X. Y. Zhang, W. P. Zhang, M. Ouyang, A. Lee and S. A. Thomas, A distinct role for norepinephrine in memory retrieval. *Cell* **117**, 131-143 (2004).

45. A. G. Kudyasheva, L. N. Shishkina, O. G. Shevchenko, L. A. Bashlykova and N. G. Zagorskaya, Biological consequences of increased natural radiation background for Microtus oeconomus Pall. populations. *J. Env. Radioactivity* **97**, 30-41 (2007).

46. E. J. Hall, *Radiobiology for the Radiologist*, 6th ed. Lippincott, Williams & Wilkins, Philadelphia (2006).

47. J. H. Kim, S. L. Brown, K. A. Jenrow and S. Ryu, Mechanisms of radiation-induced brain toxicity and implications for future clinical trials. *J. Neuro-oncology* **87**, 279-286 (2008).

48. A. Nagy and A. V. Delgado-Escueta, Rapid preparation of synaptosomes from mammalian brain using nontoxic isoosmotic gradient material (Percoll). *J. Neurochem.* **43**, 1114-1123 (1984).

49. T. Lomo, The discovery of long-term potentiation. *Philosophical Transactions of the Royal Society of London* **358**, 617-620 (2003).

50. B. Shukitt-Hale, A. Szprengiel, J. Pluhar, B. M. Rabin and J. A. Joseph, The effects of proton exposure on neurochemistry and behavior. *Adv. Space Res.* **33**, 1334-1339 (2004).

51. B. Shukitt-Hale, J. J. McEwen, A. Szprengiel and J. A. Joseph, Effect of age on the radial arm water maze-a test of spatial learning and memory. *Neurobiol. Aging* **25**, 223-229 (2004).

52. P. A. Craven and M. J. Rycroft, Fluxes of galactic iron nuclei and associated HZE secondaries, and resulting radiation doses, in the brain of an astronaut. *Adv. Space Res.* **14**, 873-878 (1994).

53. S. B. Curtis, M. E. Vazquez, J. W. Wilson, W. Atwell, M. Kim and J. Capala, Cosmic ray hit frequencies in critical sites in the central nervous system. *Adv. Space Res.* **22**, 197-207 (1998).

54. M. Dingfelder, I. G. Jorjishvili, J. A. Gersh and L. H. Toburen, Heavy ion track structure simulations in liquid water at relativistic energies. *Radiat. Protection Dosimetry* **122**, 26-27 (2006).

55. G. A. Nelson, Fundamental space radiobiology. *Gravit. Space Biol. Bull.* **16**, 29-36 (2003).

56. H. Nagasawa and J. B. Little, Induction of sister chromatid exchanges by extremely low doses of alpha-particles. *Cancer Res.* **52**, 6394-6396 (1992).

57. S. A. Lorimore, M. A. Kadhim, D. A. Pocock, D. Papworth, D. L. Stevens, D. T. Goodhead and E. G. Wright, Chromosomal instability in the descendants of unirradiated surviving cells after alpha-particle irradiation. *Proc. Natl. Acad. Sci. USA* **95**, 5730-5733 (1998).

58. C. Mothersill and C. Seymour, Radiation-induced bystander effects: past history and future directions. *Radiat. Res.* **155**, 759-767 (2001).

59. J. McMurry and R. C. Fay, *Chemistry*. Prentice Hall, Upper Saddle River, NJ (1998).

60. B. M. Rabin, W. A. Hunt and J. A. Joseph, An assessment of the behavioral toxicity of high-energy iron particles compared to other qualities of radiation. *Radiat. Res.* **119**, 113-122 (1989).

61. B. M. Rabin, J. A. Joseph and B. Shukitt-Hale, Heavy particle irradiation, neurochemistry and behavior: thresholds, dose-response curves and recovery of function. *Adv. Space Res.* **33**, 1330-1333 (2004).

62. J. A. Joseph, R. Villalobos-Molina, B. M. Rabin, T. K. Dalton, A. Harris and S. Kandasamy, Reductions of ^{56}Fe heavy-particle irradiation-induced deficits in striatal muscarinic receptor sensitivity by selective cross-activation/inhibition of second-messenger systems. *Radiat. Res.* **139**, 60-66 (1994).

63. E. R. Kandel, J. H. Schwartz, T. M. Jessell, *Principles of Neural Science,* 4th ed. McGraw-Hill, New York (2000).

64. G. Segovia, A. Porras, A. Del Arco and F. Mora, Glutamatergic neurotransmission in aging: a critical perspective. *Mechanisms of Ageing and Development* **122**, 1-29 (2001).

65. D. E. Philpott, W. Sapp, J. Miquel, K. Kato, R. Corbett, J. Stevenson, S. Black, K. A. Lindseth and E. V. Benton, The effect of high energy (HZE) particle radiation (40Ar) on aging parameters of mouse hippocampus and retina. *Scanning Electron Microscopy*, 1177-1182 (1985).

66. D. E. Philpott and J. Miquel, Long term effects of low doses of ^{56}Fe ions on the brain and retina of the mouse: ultrastructural and behavioral studies. *Adv. Space Res.* **6**, 233-242 (1986).

67. R. Rola, J. Raber, A. Rizk, S. Otsuka, S. R. VandenBerg, D. R. Morhardt and J. R. Fike, Radiation-induced impairment of hippocampal neurogenesis is associated with cognitive deficits in young mice. *Exp. Neurol.* **188**, 316-330 (2004).

68. S. S. V. Varagic, N. Svecenski and S. Hajdukovic, The effect of X-irradiation on the amount of catecholamines in heart atria and hypothalamus of the rabbit, and in brain and heart of the rat. *Int. J. Rad. Biol.* **12**, 113-119 (1967).

69. S. B. Kandasamy, Gamma radiation and release of norepinephrine in the hippocampus. *Adv. Exp. Med. Biol.* **469**, 655-659 (1999).

70. F. E. B. Jack R. Cooper, Robert H. Roth, *The Biochemical Basis of Neuropharmacology*. Oxford, Oxford (2003).

71. F. A. Cucinotta, H. Wu, M. R. Shavers and K. George, Radiation dosimetry and biophysical models of space radiation effects. *Gravit. Space Biol. Bull.* **16**, 11-18 (2003).

72. D. R. Grosshans, D. A. Clayton, S. J. Coultrap and M. D. Browning, LTP leads to rapid surface expression of NMDA but not AMPA receptors in adult rat CA1. *Nature Neurosci.* **5**, 27-33 (2002).

73. L. Liu, T. P. Wong, M. F. Pozza, K. Lingenhoehl, Y. Wang, M. Sheng, Y. P. Auberson and Y. T. Wang, Role of NMDA receptor subtypes in governing the direction of hippocampal synaptic plasticity. *Science* **304**, 1021-1024 (2004).

74. B. J. McCabe and G. Horn, Learning and memory: regional changes in *N*-methyl-*D*-aspartate receptors in the chick brain after imprinting. *Proc. Natl. Acad. Sci. USA* **85**, 2849-2853 (1988).

75. S. L. Eastwood and P. J. Harrison, Decreased expression of vesicular glutamate transporter 1 and complexin II mRNAs in schizophrenia: further evidence for a synaptic pathology affecting glutamate neurons. *Schizophrenia Res.* **73**, 159-172 (2005).

76. F. Fonnum, Regulation of the synthesis of the transmitter glutamate pool. *Prog. Biophys. Mol. Biol.* **60**, 47-57 (1993).

77. S. Takamori, J. S. Rhee, C. Rosenmund and R. Jahn, Identification of a vesicular glutamate transporter that defines a glutamatergic phenotype in neurons. *Nature* **407**, 189-194 (2000).

78. V. P. Whittaker, Thirty years of synaptosome research. *J. Neurocytol.* **22**, 735-742 (1993).

79. D. G. Nicholls, Presynaptic modulation of glutamate release. In *Progress in Brain Res.* 15-22. Elsevier Science, Miamisburg (1998).

80. M. A. Kiebler, J. C. Lopez-Garcia and P. L. Leopold, Purification and characterization of rat hippocampal CA3-dendritic spines associated with mossy fiber terminals. *FEBS Lett.* **445**, 80-86 (1999).

81. W. F. Hopkins and D. Johnston, Noradrenergic enhancement of long-term potentiation at mossy fiber synapses in the hippocampus. *J. Neurophysiol.* **59**, 667-687 (1988).

82. M. J. Thomas, T. D. Moody, M. Makhinson and T. J. O'Dell, Activity-dependent beta-adrenergic modulation of low frequency stimulation induced LTP in the hippocampal CA1 region. *Neuron* **17**, 475-482 (1996).

83. S. B. Kandasamy, Effect of Bay K 8644, calcimycin and phorbol ester on radiation-induced decreases in the release of norepinephrine in the hippocampus in rats. *Radiat. Res.* **149**, 277-283 (1998).

84. G. Lonart and T. C. Sudhof, Assembly of SNARE core complexes prior to neurotransmitter release sets the readily releasable pool of synaptic vesicles. *J. Biol. Chem.* **275**, 27703-27707 (2000).

85. X. M. Shen and G. Dryhurst, Oxidation chemistry of (-)-norepinephrine in the presence of L-cysteine. *J. Med. Chem.* **39**, 2018-2029 (1996).

86. T. C. Sudhof, The synaptic vesicle cycle. *Ann. Rev.Neurosci.* **27**, 509-547 (2004).

87. L. E. Dobrunz and C. F. Stevens, Heterogeneity of release probability, facilitation, and depletion at central synapses. *Neuron* **18**, 995-1008 (1997).

88. G. Lonart, R. Janz, K. M. Johnson and T. C. Sudhof, Mechanism of action of rab3A in mossy fiber LTP. *Neuron* **21**, 1141-1150 (1998).

89. M. Verhage, Presynaptic plasticity: modulation of secretion, co-transmission and neurodegeneration. *Parkinsonism and Related Disorders* **13**, S250 (2007).

90. R. F. Toonen, K. Wierda, M. S. Sons, H. de Wit, L. N. Cornelisse, A. Brussaard, J. J. Plomp and M. Verhage, Munc18-1 expression levels control synapse recovery by regulating readily releasable pool size. *Proc. Natl. Acad. Sci. USA* **103**, 18332-18337 (2006).

91. W. J. Tyler, X. L. Zhang, K. Hartman, J. Winterer, W. Muller, P. K. Stanton and L. Pozzo-Miller, BDNF increases release probability and the size of a rapidly recycling vesicle pool within rat hippocampal excitatory synapses. *J. Physiol.* **574**, 787-803 (2006).

92. Y. Sara, T. Virmani, F. Deak, X. Liu and E. T. Kavalali, An isolated pool of vesicles recycles at rest and drives spontaneous neurotransmission. *Neuron* **45**, 563-573 (2005).

93. M. D. Glitsch, Spontaneous neurotransmitter release and Ca^{2+}--how spontaneous is spontaneous neurotransmitter release? *Cell Calcium* **43**, 9-15 (2008).

94. R. A. McKinney, M. Capogna, R. Durr, B. H. Gahwiler and S. M. Thompson, Miniature synaptic events maintain dendritic spines via AMPA receptor activation. *Nature Neurosci.* **2**, 44-49 (1999).

95. D. Christie, A. D. Leiper, J. M. Chessells and F. Vargha-Khadem, Intellectual performance after presymptomatic cranial radiotherapy for leukaemia: effects of age and sex. *Archiv. Disease in Childhood* **73**, 136-140 (1995).

96. F. Fonnum, Glutamate: a neurotransmitter in mammalian brain. *J. Neurochem.* **42**, 1-11 (1984).

97. L. Massieu and R. Tapia, Glutamate uptake impairment and neuronal damage in young and aged rats in vivo. *J. Neurochem.* **69**, 1151-1160 (1997).

98. P. Saransaari and S. S. Oja, Age-related changes in the uptake and release of glutamate and aspartate in the mouse brain. *Mechanisms of Ageing and Development* **81**, 61-71 (1995).

99. A. M. Thomson, Facilitation, augmentation and potentiation at central synapses. *Trends Neurosci.* **23**, 305-312 (2000).

100. B. Katz, *The Release of Neural Transmitter Substanes* Liverpool Univ. Press, Liverpool (1969).

101. G. Stark, Functional consequences of oxidative membrane damage. *J. Mem. Biol.* **205**, 1-16 (2005).

102. S. Cohen-Cory, The developing synapse: construction and modulation of synaptic structures and circuits. *Science* **298**, 770-776 (2002).

103. C. Luscher, R. A. Nicoll, R. C. Malenka and D. Muller, Synaptic plasticity and dynamic modulation of the postsynaptic membrane. *Nature Neurosci.* **3**, 545-550 (2000).

104. V. Fontaine-Lenoir, B. Chambraud, A. Fellous, S. David, Y. Duchossoy, E. E. Baulieu and P. Robel, Microtubule-associated protein 2 (MAP2) is a neurosteroid receptor. *Proc. Natl. Acad. Sci. USA* **103**, 4711-4716 (2006).

105. H. T. McMahon, V. Y. Bolshakov, R. Janz, R. E. Hammer, S. A. Siegelbaum and T. C. Sudhof, Synaptophysin, a major synaptic vesicle protein, is not essential for neurotransmitter release. *Proc. Natl. Acad. Sci. USA* **93**, 4760-4764 (1996).

106. F. Valtorta, M. Pennuto, D. Bonanomi and F. Benfenati, Synaptophysin: leading actor or walk-on role in synaptic vesicle exocytosis? *Bioessays* **26**, 445-453 (2004).

107. Y. Gao, Y. B. Bezchlibnyk, X. Sun, J. F. Wang, B. S. McEwen and L. T. Young, Effects of restraint stress on the expression of proteins involved in synaptic vesicle exocytosis in the hippocampus. *Neuroscience* **141**, 1139-1148 (2006).

108. K. Tabuchi, J. Blundell, M. R. Etherton, R. E. Hammer, X. Liu, C. M. Powell and T. C. Sudhof, A neuroligin-3 mutation implicated in autism increases inhibitory synaptic transmission in mice. *Science* **318**, 71-76 (2007).

109. Y. P. Tang, E. Shimizu, G. R. Dube, C. Rampon, G. A. Kerchner, M. Zhuo, G. Liu and J. Z. Tsien, Genetic enhancement of learning and memory in mice. *Nature* **401**, 63-69 (1999).

110. P. N. Leigh and B. S. Meldrum, Excitotoxicity in ALS. *Neurology* **47**, S221-227 (1996).

111. F. Bibbiani, J. D. Oh, A. Kielaite, M. A. Collins, C. Smith and T. N. Chase, Combined blockade of AMPA and NMDA glutamate receptors reduces levodopa-induced motor complications in animal models of PD. *Exp. Neurol.* **196**, 422-429 (2005).

112. C. P. Jacob, E. Koutsilieri, J. Bartl, E. Neuen-Jacob, T. Arzberger, N. Zander, R. Ravid, W. Roggendorf, P. Riederer and E. Grunblatt, Alterations in expression of glutamatergic transporters and receptors in sporadic Alzheimer's disease. *J Alzheimers Dis.* **11**, 97-116 (2007).

113. B. S. Meldrum, Glutamate as a neurotransmitter in the brain: review of physiology and pathology. *J. Nutrition* **130**, 1007S-1015S (2000).

114. Y. Hayashi, S. H. Shi, J. A. Esteban, A. Piccini, J. C. Poncer and R. Malinow, Driving AMPA receptors into synapses by LTP and CaMKII: requirement for GluR1 and PDZ domain interaction. *Science* **287**, 2262-2267 (2000).

115. J. N. Gelinas and P. V. Nguyen, Beta-adrenergic receptor activation facilitates induction of a protein synthesis-dependent late phase of long-term potentiation. *J. Neurosci.* **25**, 3294-3303 (2005).

116. M. Mondaca, A. Hernandez, H. Perez, L. Valladares, W. Sierralta, V. Fernandez and R. Soto-Moyano, Alpha2-adrenoceptor modulation of long-term potentiation elicited in vivo in rat occipital cortex. *Brain Res.* **1021**, 292-296 (2004).

117. H. Hu, E. Real, K. Takamiya, M. G. Kang, J. Ledoux, R. L. Huganir and R. Malinow, Emotion enhances learning via norepinephrine regulation of AMPA-receptor trafficking. *Cell* **131**, 160-173 (2007).

118. L. Dehmelt and S. Halpain, The MAP2/Tau family of microtubule-associated proteins. *Genome Biol.* **6**, 204 (2005).

119. A. Caceres, G. A. Banker and L. Binder, Immunocytochemical localization of tubulin and microtubule-associated protein 2 during the development of hippocampal neurons in culture. *J. Neurosci.* **6**, 714-722 (1986).

120. A. Vandecandelaere, B. Pedrotti, M. A. Utton, R. A. Calvert and P. M. Bayley, Differences in the regulation of microtubule dynamics by microtubule-associated proteins MAP1B and MAP2. *Cell Motility and the Cytoskeleton* **35**, 134-146 (1996).

121. B. Prieto-Gomez, M. Velazquez-Paniagua, L. O. Cisneros, C. Reyes-Vazquez, F. Jimenez-Trejo, M. E. Reyes, J. Mendoza-Torreblanca and G. Gutierrez-Ospina, Melatonin attenuates the decrement of dendritic protein MAP-2 immuno-staining in the hippocampal CA1 and CA3 fields of the aging male rat. *Neurosci. Lett.* **448**, 56-61 (2008).

122. L. Dehmelt, F. M. Smart, R. S. Ozer and S. Halpain, The role of microtubule-associated protein 2c in the reorganization of microtubules and lamellipodia during neurite initiation. *J. Neurosci.* **23**, 9479-9490 (2003).

123. S. A. Lewis, D. H. Wang and N. J. Cowan, Microtubule-associated protein MAP2 shares a microtubule binding motif with tau protein. *Science* **242**, 936-939 (1988).

124. R. Mukhopadhyay and J. H. Hoh, AFM force measurements on microtubule-associated proteins: the projection domain exerts a long-range repulsive force. *FEBS Lett.* **505**, 374-378 (2001).

125. R. S. Ozer and S. Halpain, Phosphorylation-dependent localization of microtubule-associated protein MAP2c to the actin cytoskeleton. *Mol. Biol. Cell* **11**, 3573-3587 (2000).

126. C. Sanchez, M. Perez and J. Avila, GSK3beta-mediated phosphorylation of the microtubule-associated protein 2C (MAP2C) prevents microtubule bundling. *Eur. J. Cell Biol.* **79**, 252-260 (2000).

127. C. Sanchez, J. Diaz-Nido and J. Avila, Phosphorylation of microtubule-associated protein 2 (MAP2) and its relevance for the regulation of the neuronal cytoskeleton function. *Prog. Neurobiol.* **61**, 133-168 (2000).

128. R. P. Guttmann, D. L. Baker, K. M. Seifert, A. S. Cohen, D. A. Coulter and D. R. Lynch, Specific proteolysis of the NR2 subunit at multiple sites by calpain. *J. Neurochem.* **78**, 1083-1093 (2001).

129. C. C. Garner, B. Brugg and A. Matus, A 70-kilodalton microtubule-associated protein (MAP2c), related to MAP2. *J. Neurochem.* **50**, 609-615 (1988).

130. R. G. Morris, E. Anderson, G. S. Lynch and M. Baudry, Selective impairment of learning and blockade of long-term potentiation by an *N*-methyl-*D*-aspartate receptor antagonist, AP5. *Nature* **319**, 774-776 (1986).

131. J. Z. Tsien, P. T. Huerta and S. Tonegawa, The essential role of hippocampal CA1 NMDA receptor-dependent synaptic plasticity in spatial memory. *Cell* **87**, 1327-1338 (1996).

132. E. Aizenman, K. A. Hartnett and I. J. Reynolds, Oxygen free radicals regulate NMDA receptor function via a redox modulatory site. *Neuron* **5**, 841-846 (1990).

133. C. Nicolas, D. Lacasa, Y. Giudicelli, Y. Demarne, B. Agli, M. J. Lecourtier and C. Lhuillery, Dietary (n-6) polyunsaturated fatty acids affect beta-adrenergic

receptor binding and adenylate cyclase activity in pig adipocyte plasma membrane. *J. Nutrition* **121**, 1179-1186 (1991).

134. S. Persad and N. S. Dhalla, Modification of beta-adrenoceptors and adenylyl cyclase in hearts perfused with hypochlorous acid. *Canadian J. Physiol. Pharmacol.* **76**, 961-966 (1998).

135. L. H. Greenberg and B. Weiss, beta-Adrenergic receptors in aged rat brain: reduced number and capacity of pineal gland to develop supersensitivity. *Science* **201**, 61-63 (1978).

136. J. C. Beique, D. T. Lin, M. G. Kang, H. Aizawa, K. Takamiya and R. L. Huganir, Synapse-specific regulation of AMPA receptor function by PSD-95. *Proc. Natl. Acad. Sci. USA* **103**, 19535-19540 (2006).

137. A. E. El-Husseini, E. Schnell, D. M. Chetkovich, R. A. Nicoll and D. S. Bredt, PSD-95 involvement in maturation of excitatory synapses. *Science* **290**, 1364-1368 (2000).

138. G. Nyiri, F. A. Stephenson, T. F. Freund and P. Somogyi, Large variability in synaptic *N*-methyl-*D*-aspartate receptor density on interneurons and a comparison with pyramidal-cell spines in the rat hippocampus. *Neuroscience* **119**, 347-363 (2003).

139. N. A. Denisova, B. Shukitt-Hale, B. M. Rabin and J. A. Joseph, Brain signaling and behavioral responses induced by exposure to ^{56}Fe-particle radiation. *Radiat. Res.* **158**, 725-734 (2002).

140. R. Dringen, J. M. Gutterer and J. Hirrlinger, Glutathione metabolism in brain metabolic interaction between astrocytes and neurons in the defense against reactive oxygen species. *Eur. J. Biochem.* **267**, 4912-4916 (2000).

141. K. J. Smith, R. Kapoor and P. A. Felts, Demyelination: the role of reactive oxygen and nitrogen species. *Brain Pathol.* **9**, 69-92 (1999).

142. T. C. Pellmar, G. E. Hollinden and J. M. Sarvey, Free radicals accelerate the decay of long-term potentiation in field CA1 of guinea-pig hippocampus. *Neuroscience* **44**, 353-359 (1991).

143. J. M. McCord, Superoxide dismutase, lipid peroxidation, and bell-shaped dose response curves. *Dose Response* **6**, 223-238 (2008).

144. L. Kunz and G. Stark, Photofrin II sensitized modifications of ion transport across the plasma membrane of an epithelial cell line: I. Electrical measurements at the whole-cell level. *J. Mem. Biol.* **166**, 179-185 (1998).

145. L. Kunz and G. Stark, Photofrin II sensitized modifications of ion transport across the plasma membrane of an epithelial cell line: II. Analysis at the level of membrane patches. *J. Mem. Biol.* **166**, 187-196 (1998).

146. E. Niki, Y. Yoshida, Y. Saito and N. Noguchi, Lipid peroxidation: mechanisms, inhibition, and biological effects. *Biochem. Biophysical Res. Comm.* **338**, 668-676 (2005).

147. C. L. Limoli, E. Giedzinski, R. Rola, S. Otsuka, T. D. Palmer and J. R. Fike, Radiation response of neural precursor cells: linking cellular sensitivity to cell cycle checkpoints, apoptosis and oxidative stress. *Radiat. Res.* **161**, 17-27 (2004).

VITA
Mayumi Machida

Education:

2009	Ph.D. in Biomedical Sciences Department of Pathology and Anatomy Eastern Virginia Medical School, Norfolk, VA
2004	B.S. in Biochemistry Graduated with Distinction Old Dominion University Norfolk, VA
1979	B.A. in English Aoyama Gakuin University Tokyo, Japan

Publications:

G. Lonart, X. Tang, F. Simsek-Duran, **M. Machida**, L. D. Sanford. The role of active zone protein Rab3 interacting molecule 1 alpha in the regulation of norepinephrine release, response to novelty, and sleep. *Neuroscience* 154 (2), 821-831 (2008).

M. Machida, R. A. Britten, S. Mitchell, A. M. Johnson, S. J. Singletary-Britten, L. D. Sanford, G. Lonart. X-ray induced spatial memory impairment is associated with perturbation in noradrenergic transmission in the hippocampus (submitted to *Radiation Research* in April 2009).

M. Machida, G. Lonart, R. A. Britten. Effect of HZE particles on the rat hippocampal glutamatergic neurotransmission (in preparation).

M. Machida, L. D. Sanford, G. Lonart. A role of RIM1α in fear acquisition and extinction (in preparation).

Awards:

2005	First Prize, Research Day Graduate Student Poster Presentation, Eastern Virginia Medical School
2004	Outstanding Student in Biochemistry, Department of Chemistry and Biochemistry, Old Dominion University

Presentations:

2007	**M. Machida**, G. Lonart. Why are they fearless? – Behavioral and neurochemical analysis of the *Rim1α* knockout mice. Poster presented at Research Day, EVMS
2006	**M. Machida**, G. Lonart. Effect of guanfacine, a "non-stimulant" ADHD medication, on norepinephrine release from mouse synaptosome. Poster presented at Research Day, EVMS
2005	**M. Machida**, G. Lonart. Active zone protein RIM1α regulates noradrenaline release in the amygdala. Poster presented at Society for Neuroscience Meeting, Washington, D. C.
2005	**M. Machida,** G. Lonart. Neurochemical analysis of norepinephrine release from mouse amygdala. Poster presented at Research Day, EVMS.